

MUSCLE

M-POS-F1 THE MECHANISM OF β -ADRENERGIC INDUCED RELAXATION OF SMOOTH MUSCLE. C.R. Scheid*, T.W. Honeyman*, and F.S. Fay, U.Mass.Med. School, Worcester, Mass.

Possible ionic mechanism(s) underlying relaxation of smooth muscle in response to the β -adrenergic drug isoproterenol (ISO) was studied. Isolated smooth muscle cells were prepared by enzymatic digestion of the stomach muscle of Bufo marinus. Ion contents and unidirectional fluxes were measured in suspensions of cells and the effect of ISO on Na^+ and K^+ movements was assessed. While ISO produced only small changes in ion contents, it had a large effect on ion fluxes. Within 1 min, ISO stimulated ^{42}K influx > 7 fold but had little effect on efflux during this interval; dibutyryl cyclic AMP mimicked these effects. In contrast, ISO stimulated ^{24}Na efflux > 10 fold but had little effect on influx. These data suggest 1) that ISO stimulated Na^+/K^+ pump activity without affecting passive membrane permeability to these ions and 2) that cyclic AMP may mediate this effect. Consistent with this interpretation is the finding that "Na-dependent ATPase" activity in membrane fragments increased 2X after exposure to purified cA-dependent protein kinase. Supported by Am. Heart Assoc. (13-432-756). NIH (1F32 AMO5653, HL14523), RCDA (HL 00048).

M-POS-F2 ACTION POTENTIALS AND PASSIVE MEMBRANE PROPERTIES OF FRESHLY DISSOCIATED SINGLE SMOOTH MUSCLE CELLS. Joshua J. Singer and John V. Walsh, Jr., University of Massachusetts Medical School, Worcester MA 01605.

Membrane potentials were recorded with intracellular micropipettes from freshly isolated, single smooth muscle cells (enzymatically dissociated from Bufo marinus stomach) in order to avoid the complications of intercellular coupling and the presence of neural elements encountered in whole tissue. The steady-state current voltage relationship of the isolated cell displayed outward-going rectification, and the input resistance often exceeded 500M Ω . The cell near rest behaves as an isopotential surface as shown by calculation and verified by the single exponential decay of potential in response to a small hyperpolarizing current step. The time constant of this decay varied by about an order of magnitude as did input resistance and calculated membrane resistance, whereas the capacity calculated from photomicrographic measures of each cell's surface area varied only slightly ($C_m = 1.32 \pm 0.33 \mu\text{F}/\text{cm}^2$; mean \pm S.D.). Overshooting action potentials were as readily obtained at low external Na^+ concentrations ($< 12\text{mM}$) as at normal ($\approx 100\text{mM}$) levels, suggesting that there is an inward Ca^{++} current. NIH HL 14523 and Mass. Heart Assoc. 13-512-756.

M-POS-F3 CONTRACTILE PROTEIN CONTENTS IN FIRST TO THIRD ORDER BRANCHES OF THE UTERINE VASCULATURE. D.M. Cohen* and R.A. Murphy, Dept. of Physiology, University of Virginia School of Medicine, Charlottesville, Va. 22901

We have shown that large conduit arteries have higher thin filament protein contents than most large veins and many other types of smooth muscle. To determine if vessel size was associated with differences in contractile protein (CP) contents, 4 uterine arteries (UA) and 4 veins (UV) ranging from 4 to 0.15 mm external diameter (main through tertiary branches) were examined. Myosin (M), actin (A), and tropomyosin (T) contents were quantified by densitometry of sodium dodecyl sulfate (SDS) polyacrylamide gels after electrophoresis of SDS-treated vessel homogenates. All UA had similar M (8.6 ± 0.4 mg/g tissue wet wt. \pm SEM, N=4), A (28.0 ± 2.0), and T (8.0 ± 0.1) contents. UV M contents (8.1 ± 0.2) were the same as those of UA; however, A (15.9 ± 0.7) and T (4.8 ± 0.2) contents were less than those of UA ($p < 0.05$). UA A/M ratios (3.2 ± 0.2) were higher than those of UV (2.0 ± 0.2), and A/T ratios were the same for both groups (3.5 ± 0.3). Our results confirm the major distinction between arterial and venous smooth muscle CP contents, which was unaffected by vessel size. [Supported by NIH Grant HL 19242.]

M-POS-F4 OBSERVATION OF THE T-SYSTEM OF RAT SKELETAL MUSCLE FIBERS IN THREE DIMENSIONS USING HIGH VOLTAGE ELECTRON MICROSCOPY AND THE GOLGI STAIN. L. D. Peachey and C. Franzini-Armstrong, Philadelphia, Penna. 19104.

Using the Golgi black reaction after glutaraldehyde fixation (osmium-dichromate and silver nitrate) to stain the T-system, we have examined thick (1-5 μm) slices of muscle fibers of rat skeletal muscles by high voltage electron microscopy. Bundles of fibers from the red and the white portions of sternomastoideus muscles were studied in stereoscopic pairs of micrographs. T-system helioids, as observed earlier in frog muscles (Peachey and Eisenberg, Biophys. J. 15, 253a, 1975), were commonly found. These were double helioids, in that a pair of T-tubule networks in one sarcomere ran helically into a pair of T-tubule networks in the next sarcomere. Quantitative estimates of the extent of T-tubules in the two muscle fiber types were made and compared.

Supported by grants from NIH (Penna. Muscle Institute, HL-15835) and the Muscular Dystrophy Associations of America.

M-POS-F5 IMAGE ANALYSIS OF SARCOMERE MOTION DURING SPONTANEOUS CONTRACTIONS IN DISSOCIATED HEART CELLS.

G. Rieser*, R. Sabbadini, P. Paolini, Dept. of Biology, San Diego State University, San Diego, CA 92182, M. Fry* and G. Inesi, Dept. of Physiology, University of the Pacific, San Francisco, CA 94115.

Isolated cardiac cells were prepared by perfusion of adult rabbit hearts with saline containing collagenase and hyaluronidase, followed by 0.3mM EGTA saline. Myocytes were detected by a computer-interfaced vidicon camera mounted on a phase contrast microscope; camera output was stored on a VTR for computer analysis employing image enhancement techniques to evaluate the length of each sarcomere in the cell image. Automaticity was exhibited by these cells at rates of 40-120 beats/min. for a $[\text{Ca}^{++}]$ range of 10^{-5} - 10^{-4}M : higher concentrations rapidly induced a degenerative supercontraction, as did 10^{-3}M caffeine. Myocytes undergoing phasic contraction showed sequential sarcomere shortening (3.5 μs), with a wave of activation beginning at one cell end and propagating longitudinally with a constant velocity ($[\text{Ca}^{++}]$ -dependent) of $111 \pm 13 \mu\text{s}$ at 10^{-5}M and 22°C . These observations are consistent with a regenerative mechanism of Ca^{++} induced Ca^{++} release. (USPHS Grant HL 16607-04.)

M-POS-F6 DIFFERENT CROSS-BRIDGE REPEATS IN LONG AND SHORT LIMULUS THICK FILAMENTS. R.J.C. Levine and M.M. Dewey, The Medical College of Pennsylvania, Philadelphia Pennsylvania, 19129, and SUNY, Stony Brook, New York, 11794.

Optical transforms reveal a difference in the packing of surface myosin molecules between long and short paramyosin-containing thick filaments isolated from *Limulus* striated muscle. Long filaments ($l=4.4\mu\text{m}$, $d=23\text{nm}$) show a 145nm repeat of the cross-bridge helix, while short filaments ($l=3.2\mu\text{m}$, $d=33\text{nm}$), including those induced to shorten *in vitro*, show a 220nm repeat. Filaments of intermediate length ($3.7\mu\text{m}$) show both sets of reflections. Diffraction patterns from all filaments have both meridional reflections at 14.5^{-1}nm and layer lines at 72.5^{-1}nm . These data suggest that filament shortening occurs stepwise along each half-filament with: (1) retention of both a 14.5nm distance along the filament between adjacent cross-bridge projections and a 72.5nm distance along the filament between projections in the same plane, as well as, (2) conservation of numbers of surface myosin molecules.

Supported by USPHS grants: GM20628 and HL15835 to The Penn. Muscle Inst. R.L. has RCDA: NS70476.

M-POS-F7 ENERGETICS OF SKELETAL MUSCLE CONTRACTION IN DEUTERIUM OXIDE. Jack Rall, Department of Physiology, Ohio State University, Columbus, OH 43210.

The energetics of contraction was studied in isolated frog semitendinosus muscles incubated in 99.8% deuterium oxide Ringer (D_2O) at 50°C . Twitch force was 4% of control values whereas tetanus force was slowed in its rate of development but only slightly depressed in amplitude. With repeated tetanic contractions, the rate of force development increased but not to control values. Muscles bathed in normal Ringer displayed no posttetanic twitch potentiation but in D_2O the potentiation was large. Energy liberation (heat + work) attributed to Ca^{2+} cycling, as measured from stretched muscle preparations incubated in D_2O , was 60% of control values. This observation is consistent with the interpretation that D_2O decreases the amount of Ca^{2+} released in an isometric twitch. Despite the elevated posttetanic twitch force in D_2O the energy liberation attributed to Ca^{2+} cycling, and thus presumably the amount of Ca^{2+} reaccumulated by the sarcoplasmic reticulum, was unchanged. Energy liberated by the cross-bridges per unit isometric force developed was similar in normal and D_2O Ringer. (Supported in part by the Central Ohio Heart Chapter and MDA).

M-POS-F8 INTERFILAMENT PRESSURE OPPOSING RADIAL COMPRESSION OF RELAXED SKINNED SKELETAL MUSCLE CELLS. D.W. Maughan & R.E. Godt, Dept. Physiology & Biophysics, Univ. Vermont, Burlington, VT 05401 and Dept. Pharmacology, Mayo Foundation, Rochester, MN 55901

Changes in fiber diameter, reflecting corresponding changes in interfibrillar distance, were measured as a function of external osmotic pressure at a given sarcomere length. Osmotic compressive pressure (π) was applied using Polyvinylpyrrolidone (PVP, no. avg. MW 40,000) over the range 2×10^3 – $2 \times 10^5 \text{ N/m}^2$ (2–20% PVP in relaxing solution: pH 7, 22°C). Both diameter (θ) and sarcomere length (S) were measured from light micrographs (at $1430\times$) at the same point along the fiber. At a given S (2.20–3.50 μm , 7 fibers), θ varied logarithmically with π according to the relation $\theta/\theta_0 = 1 - 0.08 \ln \pi/\pi_0$, where θ_0 is the observed θ at $\pi_0 = 7.93 \times 10^3 \text{ N/m}^2$ (4% PVP relaxing solution). The average θ of fibers ($S=2.4 \mu\text{m}$) freshly skinned in mineral oil was $0.92\theta_0$, corresponding to $\pi = 2 \times 10^4 \text{ N/m}^2$. In PVP-free relaxing solution, fibers swelled to $1.23\theta_0$, corresponding to $\pi = 4 \times 10^2 \text{ N/m}^2$. These results demonstrate the existence of substantial radial expansive forces between myofilaments in relaxed muscle fibers. (Supported by VHA 547, BRS 5-S07, & AM 17828)

M-POS-F9 CHLORIDE AND HYPOSMOTIC CONTRACTURES IN SKINNED MUSCLE FIBERS. B. A. Mobley, Dept. of Physiology, Wayne State University School of Medicine, Detroit, MI 48201

Contractures were elicited in segments of skinned muscle fibers when segments were loaded with calcium and then moved from relaxing solution to a solution which differed from relaxing solution as indicated: (1) Cl had been substituted, 1:1, for some of the methanesulfonate (MS). (2) Cl had been substituted for some of the MS, and choline had been substituted for some of the K so that the product, $[\text{K}][\text{Cl}]$, was the same as in the relaxing solution. (3) The solution was hyposmotic in that the $[\text{KMS}]$ was lower. (4) A combination of methods (2) & (3). Two outer segments from each fiber contracted in 120 mM $[\text{Cl}]$, method (1), and the results served as a control for the test contracture in a central segment of the same fiber. The maximum tension and the area of the test contracture were divided by the corresponding means of the two controls in each fiber. Contractures were graded with $[\text{Cl}]$, (1) & (2), or decrease in $[\text{KMS}]$, (3). The contractures elicited by (2) were significantly smaller than those elicited by (1) for a given $[\text{Cl}]$. It was found that some contractures elicited by method (1) could be reproduced quantitatively by method (4).

M-POS-F10 INOTROPIC ACTIONS OF DIACETYL MONOXIME-A NEW MODE OF "Ca ANTAGONISM". J. Wiggins, J. Reiser*, D. Fitzpatrick*, and J. Bergey*. Dept. of Pharmacology, Univ. So. Fla. Med. Ctr., Tampa, FL 33612

Diacetyl monoxime (DAM), a nucleophilic agent, has verapamil (V)-like actions in cardiac Purkinje fibers. V and La^{3+} reduce contraction force and markedly alter the force-frequency relation (FFR) in cardiac muscle, but do so by clearly different mechanisms. We examined the inotropic actions of DAM in isometric contractions of cat papillary muscle, especially with respect to FFR. 20 mM DAM rapidly and reversibly abolishes contraction without markedly altering the action potential. Lower concentrations (0.5–5 mM) have a concentration-dependent negative inotropic effect, reducing force, df/dt , and time to peak force. In contrast to V and to La^{3+} , FFR is unchanged by DAM, as is paired pulse stimulation. The inotropic response to 3x Ca or to 500 nM epinephrine is enhanced in the presence of DAM. 20 mM DAM reduces phosphorylation of isolated cardiac microsomes, but does not affect Ca uptake. These results suggest that DAM reduces Ca current and force in cardiac muscle by nucleophilic dephosphorylation of specific membrane sites. Thus, the mechanism and action of DAM is unlike that of V or La^{3+} .

M-POS-F11 TWITCH POTENTIATION DURING RAPID TEMPERATURE JUMPS OF FROG MYOCARDIUM. M.D. Tufts, Dept. of Physiol., Case Western Reserve Univ., Cleveland, Ohio 44106

Isometric (fixed end) twitches and action potentials were measured simultaneously on single isolated atrial trabeculae at various steady temperatures and with shifts in T during the twitch. Resting sarcomere spacing was maintained at 2.3 μm with the aid of a HeNe laser diffraction pattern. Changes in T were accomplished either by rapid flush (10 – 15° change in 200 – 400 ms) or by microwave heating (1.5° in 20 ms). In the range 5° – 20° upon raising the steady T of the trabeculae there were: 20–80% decrease in peak tension, 100–500% increase in rate of rise, and 200–400% increase in rate of relaxation. In contrast, there was potentiation of 10–25% above the cold twitch if the T was rapidly increased during a critical period of 100–300 ms after stimulation. T-jump before the critical period produced a characteristic warm twitch; after the critical period, a characteristic relaxation superimposable regardless of time of the T-jump. The critical period coincided with the first third of the action potential plateau, and the extent of potentiation increased with decreasing external Ca.

Supported by USPHS Grant HL 19848 to B.D. Lindley.

M-POS-F12 KINETICS OF THE SYNCHRONIZATION PROCESS OF CHICK EMBRYONIC HEART CELLS. D. Clapham*, D. Ypey*, L. J. DeFelice & R. L. DeHaan, Anatomy Dept., Emory Univ., Atlanta, GA 30322

The time sequence of the synchronization of newly apposed pairs of spontaneously beating embryonic chick ventricular cell aggregates was recorded simultaneously with intracellular electrodes and extracellular suction electrodes. The course of coupling can be divided into four distinct phases: adhesion without rate interaction, partial synchrony, synchrony and minimal latency. At the beginning of synchrony a phase delay of 30-80ms exists between extracellular voltage spikes of the apposed aggregates. During the synchronous phase, the latency decreases according to a single simple exponential process. The contact area can be experimentally varied by micromanipulation from a single 10 μ strand to 160 μ . Contact area is shown to determine both the latency and the fidelity of synchronization. The use of cytochalasin B to disrupt microfilaments did not slow the time course of coupling. Repeated coupling and decoupling of the same pairs of aggregates produced no change in time to synchrony. An electrical model based on the formation of gap junctions between cells of the two aggregates is developed. Sponsored in part by NIH HL16567.

M-POS-F13 EFFECTS OF REDUCED SODIUM CONDUCTANCE ON CARDIAC ACTION POTENTIALS: COMPUTED AND EXPERIMENTAL.

A. Shrier and R. L. DeHaan, Anatomy Dept., Emory Univ., Atlanta GA 30322. (Supp. by Canadian Hrt. Fndn. & NIH HL 16567).

Spherical heart-cell aggregates approach nearly ideal voltage homogeneity and approximate the relation $I = CV$. We compared the effect of reduced sodium conductance (g_{Na}) on the electrical activity of reaggregates exposed to 10^{-6} M to that predicted by the McAllister, Noble & Tsien (MNT, 1975) Purkinje fiber model. Reducing g_{Na} in aggregates caused both a decrease in \dot{V}_{max} and a depolarizing shift in pacemaker potential. In both simulated and experimental action potentials (AP), reduced g_{Na} caused a depolarized threshold level, leading to a decrease in beat rate in the MNT model but an experimental increase. The model predicts that the sodium current (I_{Na}) and \dot{V}_{max} of the second and subsequent APs of a repetitive series are at least 50% smaller than the first AP. This change in \dot{V}_{max} from 1st to 3rd AP apparently results from a shift in the I_{Na} inactivation variable (h) in the MNT model. We saw no decline in \dot{V}_{max} in trains of APs recorded from aggregates, suggesting that the observed behavior of h in the aggregate system does not conform to the model. The relationship between \dot{V}_{max} or \dot{V}_{Na} and g_{Na} for the first computed AP was nearly linear, but not for the second and subsequent APs.

M-POS-F14 ULTRASTRUCTURE CHANGES IN DIBUTYRYL CYCLIC AMP INDUCED CARDIAC LESIONS. J. C. Lee and S. E. Downing*, Yale University, Department of Pathology, New Haven CT 06510

The purpose of this study was to assess the myocardial changes produced by administration of DB-cAMP. Rabbits (N=12) were given 10^{-2} M dibutyryl 3'-5'-cyclic AMP (A) 2.5 mg/kg/min i.v. for 90 min. They were sacrificed 7 and 14 days after infusion. Both left and right ventricular papillary muscles (PM) were examined. The main alterations were: myofibrillar degeneration with hypercontraction and lysis; mitochondrial translocation, swelling and degradation; deep scalloping of sarcolemma; and fragmentation and distortion of intercalated discs. The SR and T system also showed varying degrees of dilatation. However, in guinea pigs, 7 days after A (1 mg/kg, i.p., N=3) myofibrillar lesions with formation of hypercontraction bands were found only in the right, but not in left ventricular PM. These data suggest a common pathogenetic mechanism for myocardial damage by a variety of stimuli involving excessive stimulation of the cyclic system.

M-POS-F15 DYE ABSORPTION CHANGES IN SINGLE MUSCLE FIBERS. S. Nakajima and A. Gilai*, Purdue U., West Lafayette, Indiana 47907

Ross et al. (1977) and Grinvald et al. (1976) reported that the absorption signals with WW375 and NK2367 were always an absorption decrease upon depolarization in the squid axon. In muscle, however, the absorption change induced by action potential was an increase between 620 to 740 nm with WW375 (between 600 to 700 nm, with NK2367), but was a decrease outside this range. When the absorption was measured at an edge of the fiber, or when the fiber was stained for a short time to obtain more signal from the surface membrane, the wave-length dependency was not markedly different from that obtained from the entire width of fiber stained for a long time. These results suggest that the difference in the absorption spectrum between the squid axon and amphibian muscle is not attributable to the presence of T-system. By analyzing the time course of absorption change we calculated the radial conduction velocity of action potential in the T-system. The value was 6.0 cm/s (24°C) using Merocyanine 540, in agreement with González-Serratos (1971). (Supported by NIH Grant NS-08601)

M-POS-F16 THE EFFECTS OF INHIBITION OF THE SODIUM PUMP ON THE LANTHANUM-RESISTANT FRACTION OF CALCIUM IN THE INCUBATED RAT TAIL ARTERY. V. Palatý, Dept. of Anatomy, The Univ. of Brit. Columbia, Vancouver, B.C. V6T 1W5.

The La-resistant fraction of Ca in the title tissue consists of two components that differ in the rates at which they exchange with external Ca^{2+} . The rapidly exchanging component (I) behaves in the manner expected from the cell Ca if translocation of Ca across the sarcolemma were the rate-limiting step in the exchange. Dissipation of the Na^+ and K^+ gradients resulting from inhibition of the Na pump with ouabain in catecholamine-depleted arteries is accompanied by a significant increase in (I), but no detectable increase in tension. The increase in (I) is not due to enhanced active accumulation of Ca by intracellular organelles such as mitochondria and sarcoplasmic reticulum. The increase in (I) may reflect an increase in $[Ca^{2+}]_i$ or, more likely, increased binding of Ca^{2+} by unspecified components of the cytoplasm.

Supported by a grant from the Medical Research Council of Canada.

M-POS-F17 SARCOMERE LENGTH-TENSION RELATIONS IN LIVING AND CALCIUM ACTIVATED MUSCLE FIBERS. R. L. Moss and F. J. Julian, Muscle Res., Boston Biomed. Res. Inst., Boston 02114

The sarcomere length (SL) dependence of steady isometric tension has been studied in chemically and mechanically skinned frog skeletal muscle fibers for SL 1.3-3.6 μ m, at 4-5°C. The length-tension relation (LT) was first measured in living, tetanically stimulated fibers at SL < 2.20 μ m. The fibers were then skinned and the LT measured in segments (0.8-1.7 mm long) activated in solutions of pCa 5.76 or 6.09. The entire segment was observed and photographed through a microscope. Confirming and extending earlier work, the LT at SL < 2.20 μ m was found to agree well with the results on the living fibers. At SL > 2.20 μ m, steady tension was found to decrease as SL was extended to 3.6 μ m. However, the LT at SL > 2.20 μ m was usually found to be elevated relative to the LT in living fibers. These results indicate that the form of the LT is mainly determined by the amount of filament overlap. Deviations from this simple theory can probably be accounted for by failure to maintain uniform striation spacing during activation. The results eliminate any theory to explain the form of the LT based on variation of calcium level along the length of each sarcomere. (Supported by USPHS HL-16606, AHA 77-616 and MDA.)

M-POS-F18 ABSTRACT WITHDRAWN

DNA-LIGAND INTERACTIONS

M-POS-F19 FORCE TRANSMISSION AMONG HEART CELLS. T. F. Robinson and S. Winegrad, Dept. Physiology, Sch. Med., Univ. Pennsylvania, Philadelphia, PA 19104.

The heart depends upon contractile properties and inter-connections of cardiac cells for production of pressure and shape changes. Although transmission of tension among cells has usually been attributed to intercalated discs, it can occur in their absence. When isolated bundles of mammalian heart cells are exposed to EGTA, two changes occur: surface membranes become permeable to small molecules and the intercalated discs open. Ca activation of these bundles generates at least as much tension as electrical stimulation of intact tissue; therefore, there must be a system for intercellular force transmission other than intercalated discs. Ultrastructural investigation has revealed a highly organized network of connections between basement membranes of adjacent cells and collagen fibers. These connections may be linked to an intracellular network. Intercellular structures have the appearance of a major force-bearing structure and are probably the primary pathway for force transmission.

(Work supported by USPHS grant HL 18900.)

M-POS-G1 COMPARATIVE BINDING STUDIES OF CIS AND TRANS-DICHLORODIAMINE $^{195}\text{Pt}(\text{II})$ (DDP) TO DNA, Neil P. Johnson,[†] James D. Hoeschele,* and Ronald O. Rahn, Biology Division and Health and Safety Division, Oak Ridge National Laboratory,[†] Oak Ridge, TN 37830.

cis-DDP is a potent antitumor drug which is believed to act by covalently binding to nuclear DNA; *trans*-DDP shows no antitumor activity. We have used radioactive DDP to study its binding to DNA *in vitro*. Competition studies indicate that the reaction is irreversible. In 5 mM NaClO₄, *cis*-DDP binds to a small extent to thymine in poly(dT). 5-8% of either isomer binds to DNA in the presence of Cl⁻ at nuclear concentrations (0.15 M) after 24 hr at 37°C, which may explain low levels of DDP observed bound to DNA *in vivo*. In 5 mM NaClO₄, both isomers react with similar rates ($E_A = 11.3$ kcal/mole) and to the same extent. A variety of salts and buffers (>0.01 M) depress the reaction rate, and high pH reversibly inhibits the reaction ($pK = 7.3$) for both isomers. The different biological effectiveness of these two compounds is most likely caused by other factors than the stoichiometry of binding to DNA.

[†]American Cancer Society Postdoctoral Fellow.

*Operated by the Union Carbide Corp. for DOE.

M-POS-F20 TRANSLATIONAL MOTION OF HEAVY MEROMYOSIN IN THE PRESENCE OF ACTIN AND ATP. J. Borejdo* (Intr. by J. Duke). Cardiovascular Research Institute, University of California, San Francisco, Ca. 94143.

The rate of the translational motion of heavy meromyosin (HMM) was measured during its actin-activated ATPase reaction by the method of fluorescence correlation spectroscopy. This technique monitors the random fluctuations in the concentration of fluorescent molecules in an open volume which result from the translational diffusion of molecular species under observation. The statistical behaviour of the fluctuations is represented in the form of the autocorrelation function which is related to the translational diffusion coefficient of the fluorescent molecules. The translational motion of fluorescently labelled HMM was progressively slowed down after addition of the increasing amounts of actin in the presence of excess MgATP. The extent of this retardation was related to the apparent association constant of HMM and actin in the presence of MgATP. In 0.1 M KCl and at 20°C the apparent association constant was determined as $K = 9.5 \times 10^4 \text{ M}^{-1}$. These results are interpreted to indicate that the significant portion of the energy of hydrolysis of ATP cannot be directly converted into the translational motion of HMM.

M-POS-G2 THEORETICAL CALCULATION OF BINDING CURVES FOR DNA BIS-INTERCALATION. R. H. Shafer, University of California, San Francisco, CA. 94143.

Statistical mechanical calculations of the interaction of bis-intercalators with DNA are presented. The model considers binding of a bis-intercalator *via* intercalation of one or both chromophores. The grand partition function for the ligand-DNA system is calculated by the Sequence Generating Function method of Lifson, treating the DNA as an infinite, linear lattice of binding sites. Nearest neighbor, next to nearest neighbor, etc., interactions are considered. Bis-intercalation with none, one or two unoccupied binding sites separating the bound chromophores is described. The generalization to an arbitrary number of unoccupied sites separating the bound chromophores of one ligand is straightforward. Negative cooperativity arising from nearest neighbor exclusion forces and positive cooperativity due to the high local concentration of free chromophore when a ligand binds by attachment of only one of its chromophores are observed. Comparison with experiment for several DNA bis-intercalators is presented. (Supported by the Petroleum Research Fund.)

M-POS-G3 CONFORMATIONAL FEATURES OF DISTAMYCIN-DNA AND NETROPSIN-DNA COMPLEXES BY RAMAN SPECTROSCOPY. J. Martin, R. Wartell and D. C. O'Shea, School of Physics, Georgia Institute of Technology, Atlanta, Georgia 30332.

The binding of the antibiotics distamycin A and netropsin to DNA was studied by non-resonance Raman Spectroscopy. Spectra of the drugs in solution were similar. Assignments of observed Raman bands to the motion of atomic groups were made by a combination of methods. Empirical correlations were made between the Raman spectra of molecular subunits of the drugs and the drug spectra. Normal coordinate analysis of the central portion of the drugs was performed. The Raman spectra of drug-DNA complexes were obtained. Changes between the bound and unbound drug spectra were noted in bands assigned to pyrrole ring stretching modes. Prominent bands assigned to methyl groups remained unchanged. Changes were observed in bands associated with peptide linkages. The results indicate a binding mode in which the methyl groups are directed away from the DNA. Model building and conformational calculations produced several models of the drug-DNA complexes consistent with available data.

Supported by Res. Corp. and N.I.H.

M-POS-G4 ION EFFECTS ON BIOPOLYELECTROLYTE INTERACTIONS. C.F. Anderson*, P.L. deHaseth, T.M. Lohman, M.T. Record; Dept. of Chemistry, U. of Wisconsin, Madison, WI 53706.

Biopolyelectrolyte interactions such as reversible complexation can be strongly affected by changing the concentration of supporting electrolyte. This effect results mainly from a change in the extent of association of small ions with the interacting macroions [Record et al (1978) Quart.Rev.Biophysics]. A complete thermodynamic description of the salt-dependence of such interactions requires a model for the association of small ions with each macroion. The analysis of equilibria involving nucleic acids can be especially simple and physically informative because small ion association with rod-like polyanions conforms to the condensation model [Manning (1972) Biopolymers 11, 937]. The salt-dependence of protein-nucleic acid binding constants provides quantitative information about the extent to which such complexes are stabilized by the formation of ionic interactions [Record et al., J. Mol. Biol. (1976) 107, 145]. This analysis depends upon a model for the association of small ions with a nucleic acid segment containing an isolated bound protein. Using recent advances in the theory of condensation, this model can be clarified and extended.

M-POS-G5 COOPERATIVE DISSOCIATION OF GENE 32 PROTEIN FROM ITS COMPLEX WITH fd DNA. C.-W. Wu and B.F. Peterman* (Intr. by F.Y.-H. Wu) Albert Einstein Col. of Med., Bx., NY 10461

Gene 32 protein of bacteriophage T4 interacts very weakly with double-stranded DNA, but binds cooperatively to single-stranded DNA with high affinity. We have performed equilibrium and kinetic studies of the interaction of gene 32 protein with single-stranded fd DNA monitoring the changes in protein fluorescence. At saturating concentrations of fd DNA, approximately 50% of the protein fluorescence was quenched. From the fluorescence titration curve, it was estimated that a monomer of gene 32 protein covers 6 nucleotide bases on the DNA and the lower limit for the apparent K_A is $1.9 \times 10^8 M^{-1}$ in 0.1 M Tris-Cl, pH 7, at 25°C. Taking an average value of $2 \times 10^5 M^{-1}$ for the apparent K_A of gene 32 protein binding to various dinucleotides, a lower limit for the cooperativity parameter of 10^3 was obtained. When an ionic strength jump was applied to the fd DNA-gene 32 protein complex using a stopped-flow apparatus, the complex underwent dissociation into individual components accompanied by an increase in protein fluorescence. The kinetic data obtained can be analyzed in terms of a mechanism in which the protein molecules dissociate cooperatively from the DNA in a manner close to an all-or-none transition.

M-POS-G6 Effect of Metal Ions on the Luminescence of Acridine Dyes Bound to DNA.* H. C. BRENNER, T. PRUSIK, M.J. MORELLI, and C. TOBIASZ, New York U.--The fluorescence and phosphorescence of three acridine dyes intercalated in DNA are studied as a function of the concurrent binding of metal ions to specific sites in DNA, in an effort to deduce specific site interactions of the dyes. It is found that the luminescence yield of the dyes is determined by a delicate interplay of the quenching ability of the DNA itself and the quenching of the bound metal ions. For example at room temperature the fluorescence of DNA-bound acridine orange is decreased when silver is bound, while the fluorescence of proflavine (PF) is increased. Since silver binds to sites in DNA which quench PF fluorescence, it ostensibly "turns off" the quenching by DNA at these sites, and this effect is greater than the quenching ability of the silver ion. These results are altered at 77°K where it appears that the quenching power of specific base-pair sites in DNA is radically altered relative to room temperature. In agreement with previous studies of DNA base phosphorescence, the 77°K phosphorescence of the bound dyes is markedly enhanced by concurrent binding of Ag⁺ and Hg²⁺.

*Supported in part by NIH BRSG Grant RR07062

CHROMATIN I

M-POS-H1 ELECTROOPTICAL MEASUREMENTS OF H1 AND H4 HISTONES COMPLEXED WITH DNA. A. Mozo*, and J. Palau* (Intr. by G. Katz) (Inst. Biologia Fundamental, U. Autònoma de Barcelona and H.H.Merritt Clin. Res. Ct. Columbia U. New York 10032

Electrooptical measurements on the interaction of nucleosomal histone H4 with DNA and non-nucleosomal histone H1 with DNA, were carried out at low ionic strength. The induced dipole character of DNA was not affected by H4, but H1 increased both induced and permanent dipole moments throughout the range 0-1.0 (w/w) of H1/DNA ratios analyzed. Intrinsic birefringence and dichroism of H4/DNA and H1/DNA complexes did change in a manner suggesting that H4 induces localized conformational changes and H1 has a generalized effect on DNA conformation. Changes in the fluorescence spectra upon complexing, suggest an energy transfer mechanism from the tryptophan residues to the bases of DNA. These results indicate that the H1/DNA interaction is a cooperative dipole-dipole coupling, in which part of the histone tightly binds to DNA, while another part is responsible for the aggregation of the complexes. H4 binds to DNA in localized regions of both molecules, by both electrostatic and hydrophobic forces, inducing bendings in the nucleic acid which can be related to its nucleosomal configuration. (Dr.Mozo MDA Fellow).

M-POS-H2 HETEROGENEITY IN CONFORMATION AND COMPOSITION OF ISOLATED NUCLEOSOMES. W.O. Weischat* and K.E. Van Holde, Oregon State University, Corvallis, OR 97331.

We present a model describing the action of micrococcal nuclease on chromatin from higher eukaryotes. It is based on simple, generalized ideas concerning the differential susceptibility of regions of DNA interacting with either the histone core (~160 bp), or H1 (~20 bp), or other proteins (~20 bp). It takes into account the progressive and discontinuous processing of both DNA ends of chromatin fragments. Consequently, the following hypotheses arise: oligomeric nucleosomes after digestion consist of a contiguous sequence of core-particles or they contain short spacers which are effectively protected by their interaction with H1. This produces some quantization of the DNA lengths associated with oligomers. Clipping of both DNA ends leads to parallel pathways in processing of fragments yielding various relative arrangements of DNA and histones with the same total DNA length; e.g., 160 bp-monomers comprise structures containing H1 and being clipped into the core at the other DNA end, as well as H1-deficient core-particles with two complete turns. 140 bp-monomers, devoid of H1, consist of core-particles showing both a symmetrical or asymmetrical position of the DNA ends with respect to the histone core.

M-POS-H3 INFLUENCE OF THE BUFFER SYSTEM ON THE DIGESTION OF NUCLEAR CHROMATIN. C. Sahasrabudhe and G. Saunders, University of Texas System Cancer Center, Houston, Texas 77030.

Using micrococcal nuclease the effect of two different buffer systems (phosphate and tris) on the digestion of chromatin was investigated. A simple rapid method for preparation of clean intact nuclei from human placental tissue was developed. The digestibility of the native chromatin in nuclei was followed by measuring the kinetics of release of acid soluble material. The relative distribution of the nucleosomal and oligonucleosomal DNA at several levels of digestion was estimated by acrylamide gel electrophoresis. We find that at pH 7.2 the nuclear chromatin is digested to nucleosomes and oligonucleosomes at a 50% faster rate in Tris-HCl buffer than in phosphate buffer. Also there is no detectable effect of slight variation of ionic strength on this differential digestibility. These results indicate that the choice of the buffer system may be important during structural studies of chromatin.

M-POS-H4 CONFORMATIONAL CHANGES OF THE CHROMATIN SUBUNIT V. C. Gordon*, C. M. Knobler*, D. E. Olins† and V. N. Schumaker*, *Dept. of Chem. and MBI, UCLA, L. A., CA 90024, VCG, CMK and VNS, USPHS Research Grant GM13914, †U. of Tenn.-Oakridge Grad. Sch. of Biomed. Sci., Biol. Div. ORNL, Oakridge, Tn. 37830, DEO, USPHS Research Grant GM19334

Sedimentation and diffusion coefficients and circular dichroic spectra of the chromatin monomer subunit were measured as a function of ionic strength and pH. Two extremely sharp conformational transitions were identified. The first of these occurred between 0.4mM and 1mM ionic strength and the second was found between 5mM and 10mM ionic strength. These transitions were fully reversible. Both transitions were suppressed by crosslinking with either formaldehyde or dimethylsuberimide at 10mM ionic strength. The characteristic properties of the subunit were unchanged from pH 5.2 to pH 9.2. Below pH 5.0, the salt dependent transitions were no longer observed.

M-POS-H5 NUCLEOSOME CONFORMATIONS: pH AND ORGANIC SOLVENT EFFECTS. M. Zama*, D. E. Olins, U. Tenn.-Oak Ridge Grad. Sch. Biomed. Sci., Biol. Div., ORNL, Oak Ridge, TN 37830, E. Prescott*, G. J. Thomas, Jr., Southeastern Mass. U., North Dartmouth, MA 02747.

Monomer nucleosomes (v_1) from chicken RBC nuclei were examined in aqueous buffers (pH 3 to 10) and in water/organic solvent mixtures (i.e., ethanol, ethylene glycol, dioxane, DMSO and MPD). Circular dichroism and laser-Raman spectroscopy detected conformational transitions in histone and DNA 2° structure. Solvent-dependent fluorometric changes were observed with v_1 covalently labeled with N-pyrenemaleimide on the thiol groups of H3 histone. pH studies: pH > 5, negligible conformational changes; pH 5-4, sharp and simultaneous changes in CD (i.e., increased "B" character of DNA) and fluorescence (i.e., loss of "excimer"); pH < 4, protonation of DNA bases C and A. Organic solvent studies: sharp transitions that variously involved loss of α -helix, increase in B character of DNA, and loss of excimer. Different solvents required different vol % concentrations. Laser-Raman and CD furnish complementary data; certain solvents are better studied by one or the other technique. †Operated by Union Carbide Corp. Research sponsored by DOE and NIH grants GM19334 (DEO), AI11855 (GJT).

M-POS-H6 SALT AND pH INDUCED STRUCTURAL CHANGES IN THE INNER HISTONES. A. P. Butler*, D. E. Olins, U. Tenn.-Oak Ridge Grad. Sch. Biomed. Sci., Biol. Div., ORNL, Oak Ridge, TN. 37830; R. E. Harrington, Dept. Chem., U. of Nev., Reno, NV. 89507; W. E. Hill, Dept. Chem., U. Mont., Missoula, MT. 59801.

The inner histone complex from chicken RBC, extracted in 2 M NaCl, 10 mM Tris, 10 mM DTT, 0.1 mM PMSF, pH 7.2, has been studied as a function of ionic strength and pH. As isolated, $S^{20}_w = 3.7$ and the molecular weight is about 54,000 consistent with a tetramer containing equimolar quantities of H2a, H2b, H3, and H4. In 4 M NaCl, $S^{20}_w = 4.2$ and the apparent molecular weight is 106,000, suggesting a salt-dependent conversion of tetramer to octamer. At ≤ 1 M NaCl, S^{20}_w decreases; chemical cross-linking studies show dissociation of the inner histone tetramer; and circular dichroism indicates loss of α -helix. pH studies: decrease of pH from 6-4.5 results in gradual loss of α -helix. CD at 278 nm and intrinsic fluorescence show sharp changes of histone tyrosines between pH 4-4.5. †Operated by Union Carbide Corporation. Research supported by DOE and NIH grants GM19334 (DEO), and GM17436 (WEH).

M-POS-H7 PROPERTIES OF INNER HISTONE-DNA COMPLEXES. P. N. Bryan*, E. B. Wright*, M. H. Hsieh*, A. L. Olins, and D. E. Olins, U. Tenn.-Oak Ridge Grad. Sch. Biomed. Sci., Biol. Div., ORNL, Oak Ridge, TN 37830.

Chicken RBC inner histone tetramer has been complexed with several natural and synthetic DNA-duplexes by salt-gradient dialysis at various protein/DNA. The resulting complexes, in low ionic strength buffer, have been examined by electron microscopy, circular dichroism, and thermal denaturation. EM revealed v bodies randomly arranged along DNA fibers, including poly (dA-dT)·poly (dA-dT), poly (dI-dC)·poly (dI-dC), but not poly (dA)·poly (dT). CD studies showed prominent histone α -helix and "suppression" of nucleic acid ellipticity ($\lambda > 240$ nm). Thermal denaturation experiments revealed T_m behavior comparable to H1 (or H5)-depleted chromatin. T_m III and T_m IV increased linearly with GC % (natural DNAs), but were virtually independent of the histone/DNA ratio. Therefore, the melting of v bodies along a DNA chain is insensitive to adjacent "spacer" DNA lengths, suggesting that T_m III and T_m IV arise from the melting of different domains of DNA associated with the core v body. †Operated by Union Carbide Corp. Research sponsored by DOE and grants, NIH GM19334 (DEO) and NSF PCM01490 (ALO).

M-POS-H8 BINDING OF BENZO(a)PYRENE DIOL EPOXIDE TO CHROMATIN. A. Kootstra*, T.J. Slaga*, and D.E. Oling, U. of Tenn.-Oak Ridge Grad. Sch. Biomed. Sci., Biol. Div., ORNL†, Oak Ridge, TN. 37830.

Chicken RBC DNA, chromatin and nucleosomes (v_1) were reacted with the "ultimate" carcinogen (+)-trans-7 β ,8 α -dihydroxy-9 α ,10 α -epoxy 7,8,9,10-tetrahydrobenzo(a)pyrene (14 C). Relative binding of labeled epoxide (normalized to the same amount of DNA) was: DNA, 100%; chromatin, 45%; v_1 , 40%. Over 90% of the reacted epoxide, in chromatin or v_1 , appears bound to the DNA. Chromatin, reacted with labeled epoxide, was redigested with micrococcal nuclease to yield v_1 and multimers. Analysis of epoxide distribution revealed that binding (per unit DNA) to v_1 v_2 < chromatin; suggesting that the "spacer" region between nucleosomes bound 3-4 X more epoxide than v_1 . Other studies on the nature of the epoxide reaction with susceptible nucleophiles indicated that: (1) binding is proportional to DNA concentration; (2) a competing nucleophile (e.g., cysteine) can inhibit the reaction with DNA. †Operated by Union Carbide Corp. Research supported jointly by DOE and NIH grants CA20076 (TJS) and GM19334 (DEO).

M-POS-H9 HIGHER ORDER STRUCTURE IN METAPHASE CHROMOSOMES. J.B. Rattner* and B.A. Hamkalo, University of California, Irvine, California 92717

Deduction of the organization of chromatin in nuclei and metaphase chromosomes requires a fundamental understanding of the packing arrangement of nucleosome subunits and the factors which govern their interactions. Our approach to these questions involves ultrastructural analysis of partially dispersed mouse metaphase chromosomes in the presence of EGTA and mono- or divalent cations. Electron microscopy of these preparations shows that the bulk of the chromosome remains condensed but peripheral chromatin is dispersed and appears as regular fibers 250-300 Å in diameter. Heavy metal shadowing of preparations emphasizes the helical nature of the fiber and negative staining provides preparations in which individual nucleosomes are distinguishable. We propose that these fibers result from helical coiling of the basic 100 Å nucleohistone fiber into a solenoid-like structure which has a period repeat of 100-120 Å and five to six nucleosomes per turn.

Research supported by NIH GM23241.

M-POS-H11 THE H2A SPECIFIC PROTEASE: PARTIAL PURIFICATION AND CHARACTERIZATION. D.K. Watson* & E.N. Moudrianakis. The Johns Hopkins University, Baltimore, Maryland 21218 (Introduced by M.A. Tiefert).

A proteolytic enzyme which cleaves histone H2A at a single site has been found complexed with isolated calf thymus chromatin (Cell 9, 785, 1976). This H2A specific protease present among the proteins extracted from chromatin by 2.0 M NaCl is now partially purified by chromatography on G100 and CM-Sephadex columns. Based on its mobility in SDS-acrylamide gels, G100 columns, and sucrose gradients, it appears to have a molecular weight of approximately 14,000. From the effect of various inhibitors, the enzyme can be defined as a serine-type protease. The requirement of high ionic strength for cleavage and maintenance of enzymatic stability, the tissue and species specific distribution, and chromatin localization will be discussed briefly in light of the possible *in vivo* function of the H2A specific protease.

BIOENERGETICS III

M-POS-H10 RECONSTITUTION OF HISTONES AND SUPERHELICAL DNA. S. C. Rall,* R. T. Okinaka,* and G. F. Strniste, Cellular and Molecular Biology Group, Los Alamos Scientific Laboratory, University of California, Los Alamos, New Mexico 87545

Salt-extracted calf thymus histones (no H1) and PM2 DNA (form I) were reconstituted and subjected to sedimentation analysis in 0.5 M NaCl. The reconstituted particles have S values which increase with increasing histone:DNA, reaching a plateau value of 120-130S at H:DNA of 5 to 7:1. These complexes have also been visualized by electron microscopy in varying concentrations of NaCl or ammonium acetate. Micrococcal DNase-treated complexes give distribution patterns reminiscent of native chromatin when analyzed on isokinetic sucrose gradients or when the DNA is analyzed on polyacrylamide gels. Whether the reconstitution is done by direct mixing of calf thymus histones with PM2 DNA in 2 M NaCl, followed by immediate reduction to 0.25 M NaCl, or by sequential step-wise reduction from 2 M to 0.25 M NaCl, the results of sedimentation analysis, electron microscopy, and micrococcal DNase treatment of the complexes show many similarities between the two methods of reconstitution. (This work was performed under the auspices of the U. S. Energy Research and Development Administration.)

M-POS-II ORIENTATION STUDIES OF CHROMOPHORES IN PLANAR ARRAYS. J.C. Smith†, L.S. Powers† and P. Claddis†

†Johnson Res.Fdn., U. of Pa., Phila., PA, †Murray Hill, NJ
The problem of the orientation of a chromophore in a planar array for the case in which a limited range of orientations exist about some most probable orientation angle has been explored theoretically. Expressions have been derived for the orientation of the projection of the oscillator onto the matrix plane as well as the tilt angle that it makes relative to that plane for a gaussian distribution of the orientation angles. The theoretical treatment has been extended to the case in which the oscillator has a single component out of the matrix plane but is "infinitely degenerate" in the plane. The expressions were tested using liquid crystals formed from MBBA. The most probable in-plane angle obtained from a curve fitting procedure coincided satisfactorily with the angle with which the alignment direction of the sample was mounted in the sample holder, and the spread in the distribution of this angle agreed closely with that obtained from NMR studies. The expressions were applied to a series of voltage-sensitive oxonol dyes doped into a lipid multilayer. A model for the orientation of these dyes in the lipid bilayer has been developed. Work at the Univ. of Pa was supported by NINCDS Grant No. 10939.

M-POS-12 NUCLEAR MODULATION STUDIES OF PROTON-DEUTERON EXCHANGE IN FERREDOXINS AND HIGH POTENTIAL IRON-SULFUR PROTEINS. N. Orme-Johnson,*W. H. Orme-Johnson,*W. B. Mims, and J. Peisach, University of Wisconsin, Madison, Wisconsin, Bell Laboratories, Murray Hill, N.J., and Albert Einstein College of Medicine, Bronx, N.Y.

The nuclear modulation effect in EPR has been used to study the interaction of protons and deuterons with the paramagnetic centers in 2- and 4-Fe ferredoxins and in high potential iron-sulfur proteins (HIPPI) (Peisach *et al.* (1977) *J. Biol. Chem.* 252, 5643). For the ferredoxins, close lying protons readily exchange with deuterons from D₂O. We have found that for adrenodoxin and *B. Polymyxa* ferredoxin, more protons are exchanged if the protein is equilibrated with D₂O prior to reduction than if the protein is first reduced and then exchanged with D₂O. Since the change of redox potential with respect to pH for many ferredoxins does not obey the Nernst equation (Stombaugh *et al.* (1976) *Biochemistry* 15, 2633), it is unlikely that the reduction of these ferredoxins requires the concomitant acquisition of a proton. For the HIPPI's which either have been exchanged in D₂O and subsequently oxidized or have been oxidized and subsequently exchanged in D₂O, little or no replacement of protons by deuterons can be observed. Only by partial unfolding of the HIPPI holoprotein or reconstitution of the apoprotein in D₂O can exchange with deuterium be demonstrated.

M-POS-13 PROTEIN INFLUENCES ON PORPHYRIN STRUCTURE.

D. L. Rousseau, J. A. Shelnutt,* and J. M. Friedman, Bell Laboratories, Murray Hill, New Jersey 07974

Although the amino acid sequences of many cytochrome c type proteins have been determined and the number of invariant residues have been found to be minimal, there are only a few reports of influence of the protein environment on the porphyrin ring and no changes in nuclear symmetry have been found. Resonance Raman scattering offers the opportunity to sensitively probe nuclear structural variations in such systems by analysis of the vibrational frequencies. We have developed a technique in which two spectra may be simultaneously obtained and frequency differences determined. This technique is very sensitive to small frequency shifts and is therefore an ideal probe of protein influences on porphyrin structure. We will report on results obtained from horse heart cytochrome c, yeast iso 1 cytochrome c and *Rhodospirillum rubrum* cytochrome c₂. In these systems we have found changes in the Raman spectra that we may interpret in terms of changes in the nuclear structure of the heme as a function of amino acid composition.

M-POS-14 ELECTRON TUNNELING IN THE CYTOCHROME c CYTOCHROME OXIDASE REACTION, B. Chance & A. Waring Johnson Res. Fdn., Univ. of Penna., Phila., PA 19104

The mechanism by which electrons are transferred between macromolecular assemblies of electron transfer units in the mitochondrial membrane requires reevaluation because of the large distance between donor and acceptor (~35Å) (1-4), making contact or outer sphere electron transfer reactions extremely unlikely. Electron tunneling in the photobiological system ("Chromatium experiment") (1-5) may also occur in the cytochrome oxidase reaction. Electron transfer between cytochrome c and Compound B "peroxycytochrome oxidase" occurs below -50°. Above -50° cytochrome c accepts electrons from cytochrome c. Tunneling distances from cytochrome c to a₃ and a may be about equal. The specificity and control may be due to nuclear tunneling parameters followed by electron tunneling. Thus tunneling may be a generalized mechanism in biological systems (6). 1. Vanderkooi, J. *et al* (1977) *Eur. J. Biochem.* (in press). 2. Vanderkooi, J. *et al* these abstracts. 3. Tiede, D.M. *et al.* these abstracts. 4. DeVault, D. and Chance, B. (1966) *Biophys. J.* 6:825. 5. Hopfield, J.J. (1974) *PNAS, US* 71:3640. 6. Frauenfelder, H. *et al.* Tunneling in Biol. Reac., Johnson Res. Fdn., Nov. 2-5, 1977, Academic Press (in prep.) Support GM 12202; GM 23652-01; PCM770826

M-POS-15 LOW TEMPERATURE KINETICS OF CYTOCHROME c - CYTOCHROME OXIDASE IN BEEF HEART MITOCHONDRIA. A. Waring Johnson Research Foundation G 4, Dept. Biochem. and Biophysics, University of Penn., Philadelphia, PA 19104.

The oxidation of cytochrome c - cytochrome oxidase has been studied using single turnover (reduced to oxidized) kinetics at low temperature. Substrate reduced-CO complexed mitochondria were photolyzed in the presence of 300μM O₂ and the course of oxidation of the electron transport chain components was followed in a Johnson Foundation time sharing photospectrometer at low temperature¹. Oxidation of cytochrome c followed at 550-540nm had a polyphasic kinetic character from -37° to -80°C. In contrast a + a₃ (608-630nm) showed an initial rapid absorbance decrease due to compound B formation, followed by a slower absorbance change indicating a biphasic kinetic character in the temperature range of -37° to -50°C. At -60° to -80°C the fast initial absorbance change at 608-630nm was still apparent, however the slower absorbance change was not observed. Perturbation of these responses is discussed.

1. B. Chance, N. Graham, and V. Legallais. 1975. *Anal. Biochem.* 67:552-579

M-POS-16 CONTROL OF ELECTRON FLOW BY PROTON GRADIENTS IN MITOCHONDRIA? D. Zorov,* (Intr. by C. Owen), Johnson Res. Fdn., Univ. of Penna., Philadelphia, PA 19104

The role of hydrogen ion gradients in respiratory control is a topic of considerable interest in the chemiosmotic hypothesis and a further investigation of the possible shift of cross-over points from proton to electron carriers only would be possible in state 4 mitochondria supplemented with nigericin or ammonia. Rat liver mitochondria (RLM) were chosen for this study because of their 10-fold respiratory control and their large cross-over responses. RLM were suspended in 75 mM sucrose, 225 mM mannitol, 50 mM MOPS medium, pH 7.4 and 4 mM succinate as substrate causing large reduction of cytochrome b. The mitochondria showed characteristic oxidation of cytochrome b on addition of an uncoupler (3.3 μM PCP) and nigericin plus valinomycin, 0.33 μg/ml and 6.6 mM K⁺. The extent of cytochrome b oxidation was nearly equal for the two cases and is termed 100%. Ammonia additions in the range 3-30 mM caused a linear response (slope 1% per 0.2 μg/ml) yet nigericin gives a larger effect together with valinomycin than does ammonia. Conclusions are: 1) the control of electron flow is not due to the proton carriers but due to the electron carriers; 2) a different type of control mechanism exists in the respiratory chain.

M-POS-17 CYTOCHROME c₂ OXIDATION AND REDUCTION *in vivo*: INTERACTIONS WITH REACTION CENTER AND REDUCTASE. C.L. Bashford, R.C. Prince*, K. Takamiya* and P.L. Dutton Johnson Foundation, U. of Pennsylvania, Phila., PA 19104.

The reaction centers (RC) of *Rhodospseudomonas sphaeroides* each possess 2 tightly associated cytochromes c, whose oxidation by the RC is complete within 1 ms. On a functional timescale, the c is not mobile between RC. The reductant of c (Z) is membrane bound, and requires 2e⁻ and 2H⁺ for its redox reaction (pH 5-11), with E_m'=150 mV (Fed. Proc. 36, 726). Surprisingly, ferri-c reduction has second order characteristics, depending on both [ferri-c] and [ZH₂]. With [ZH₂] constant, the half-time of c reduction varies with ferri-c, and, characteristic of a second order reaction, has a maximum when the two reactants are equimolar. This allows an estimation of both the ratio of Z to RC, and of the apparent second order rate constant. In five different preparations, Z:RC=0.8±0.25 and k=8.3x10⁶/M.s. There are 30-60 Z per chromatophore, and although the ratio of Z:RC is close to 1, the kinetics of ferri-c reduction suggest the rapid interaction of at least 4ZH₂ with each cytochrome-reaction center complex.

Supported by US PHS GM 12202.

M-POS-18 POSITION OF CYTOCHROME P-450 HEME IN ADRENAL MITOCHONDRIAL MEMBRANE. H. Blum*, J.C. Salerno, T. Ohnishi and J.S. Leigh, Johnson Foundation, Dept. of Biochemistry and Biophysics, University of Pennsylvania, Phila., PA 19104.

Oriented multilayers prepared from adrenal cortex sub-mitochondrial particles display orientation dependent EPR signals arising from cytochrome P-450. The z axis of the g tensor, corresponding to the normal to the heme plane, coincides with the normal to the plane of the membrane stack. Cytochrome a in cytochrome oxidase, on the other hand, has been shown to have the heme normal perpendicular to the membrane normal. The EPR signal of cytochrome P-450 in adrenal SMP is readily quenched by addition of small amounts of paramagnetic ions such as dysprosium EDTA, also in contrast to cytochrome oxidase a heme. The heme in P-450 thus lies near or on the membrane surface, and the plane of the heme is parallel to the membrane plane.

M-POS-19 PROTON TRANSLOCATION ASSOCIATED WITH ANAEROBIC GLYCEROL 3-PHOSPHATE (G3P) DEHYDROGENATION-FUMARATE REDUCTION IN ESCHERICHIA COLI. K. Miki and T. H. Wilson*, Depts. of Microbiol. and Mol. Genetics and Physiology, Harvard Medical School, Boston, Mass. 02115

Anaerobic electron (or hydrogen) transfer from G3P to fumarate as the final electron acceptor in *E. coli* results in ATP formation. With whole cells, proton extrusion was seen on the addition of fumarate, in the presence of endogenous G3P. This proton extrusion was sensitive to the uncoupler, CCCP. The stoichiometry was near 2 H⁺ extruded per mole of dihydroxyacetone phosphate formed. Inverted membrane vesicles take up H⁺ in the presence of added G3P and fumarate. This H⁺ accumulation was sensitive to CCCP and 2-heptyl-4-hydroxyquinoline-N-oxide which is a potent inhibitor for the coupling of anaerobic G3P dehydrogenase to fumarate reductase.

Supported by NIH Grants GM 22906 and AM-0-5736.

M-POS-110 N-ETHYLMALIMIDE LABELED PROTEINS AND THE MITOCHONDRIAL PHOSPHATE CARRIER. H. Wohlrab and J. Greaney, Jr*, Boston Biomedical Research Institute, Boston, MA 02114

Mitochondria (M) from the flight muscle of the adult blowfly are highly specialized towards oxidative phosphorylation and thus contain only monocarboxylate, adenine nucleotide, and phosphate carriers (PC). Many labeled proteins can be identified when the PC is inhibited with (3H)N-ethylmaleimide (NEM), the labeled M are solubilized with SDS, and the proteins separated on 20cm SDS polyacrylamide gels, with all or only the > 25K dalton proteins on the gel. If, however, sonic submitochondrial particles are prepared from the labeled M and are electrophoresed, only seven labeled proteins (73K, 71.5K, 67K, 48K, 34.5K, 32K, and about 10K daltons) can be identified with 0.15, 0.19, 0.35, 0.45, 0.87, 0.10, and 0.17 nmol (3H)NEM/nmol cytochrome a, respectively, at 90% inhibition. Coty and Pedersen (JBC 1975 250 3515) found five NEM labeled proteins in their search for the PC NEM binding protein (PCNP) in rat liver M using their p-mercuribenzoate sensitization method. Among the labeled proteins only the 48K and 32K are common to both types of M and one of these is very likely the PCNP. Supported by NIH AG 00100 and an EI from the AHA.

M-POS-111 A PARAMAGNETIC PROBE OF pH GRADIENTS IN CHLOROPLASTS. R. Mehlhorn and A. Quintanilha, Membrane Bioenergetics Group, Lawrence Berkeley Laboratory, University of California, Berkeley, California 94720.

A spin labeled primary amine, 4-amino-2,2,6,6-tetramethyl piperidinoxy (TEMPAMINE) and a tertiary amine 4-dimethylamino-2,2,6,6-tetramethyl piperidinoxy were shown to accumulate within spinach chloroplast thylakoids upon illumination. Spin label uptake occurred at the same rate as the pH change measured in the bulk aqueous phase. The spin signal arising from the thylakoid interior was observed directly by quenching the remaining signal with the impermeable paramagnetic broadening agent ferricyanide and was used to infer the water volume within unbroken thylakoids. Direct measurements of spin label concentrations yielded light-driven pH gradients of about 3 units. A permanently charged analogue of TEMPAMINE, 4-trimethyl ammonium-2,2,6,6-tetramethyl piperidinoxy did not accumulate within the thylakoids. (Research supported by Department of Energy).

M-POS-112 THE RELATIONSHIP BETWEEN CYTOCHROME REDOX LEVELS AND ACTIVE POTASSIUM TRANSPORT IN INSECT MIDGUT. J.T. Blankemeyer and G.W. Kidder III, Dept. of Physiology, Univ. of Md. Schl. of Dentistry, Baltimore, Md. 21201

The larval midgut of fifth instar lepidopteran insects (*H. cecropia*, *M. sexta*) actively transports potassium from the hemolymph-side to the lumen-side when chamber mounted. Mandel et al. (1975, BBA 408:123), using *cecropia* midgut, suggested that cyt. b₅ linked oxidative metabolism and active transport of potassium. In the present study, using midgut from *M. sexta* and a multiple wavelength, dual beam spectrophotometer (Kidder and Blankemeyer, 1978), we have shown that the relative amount of b₅ is small, that b₅ does not track active K transport, and that the cytochrome redox levels are not significantly changed by removing K from the bathing solutions. We conclude that there is no direct cytochrome link between K active transport and oxid. metabolism in insect midgut.

M-POS-113 ION FLUXES AND MEMBRANE POTENTIAL IN ASCITES TUMOR CELLS. T. Bakker-Grunwald and M.C. Neville, Dept. Physiol. Univ. Colo Med Center, Denver, Colo 80262.

The membrane potential of ascites cells has been estimated using a new method based on the rate of increase of sodium, J_{Na}, in ouabain-poisoned cells. J_{Na} is a function of the membrane potential, V, and the Na permeability, P_{Na}. Valinomycin brings V close to or at the potassium equilibrium potential, V_K, without changing P_{Na}. By varying the external K concentration, J_{Na} was determined as a function of V_K in the presence of valinomycin; from this curve, and J_{Na} in the absence of valinomycin, it was estimated that V has a value of -35 mV in ouabain-poisoned cells with normal Na and K concentrations. Under conditions where exchange diffusion was blocked, ouabain had no effect on the rate of efflux of either Rb or Tl. This indicates that any electrogenic pump contribution to V under steady-state conditions is small (≤ 5 mV). These findings suggest that the membrane potential of ascites cells has a value between -35 and -40 mV. (Supported by NIH grant AM 15807).

M-POS-114 TOPOGRAPHICAL STUDY OF ACTIVE SITE OF HORSE-RADISH PEROXIDASE USING SPIN-LABELED BENZHYDROXAMIC ACID G. Rakhit and C. F. Chignell, NIH, Bethesda, Maryland 20014.

The electron spin resonance measurements indicated that the nitroxide function of the spin-labeled analog of benzhydroxamic acid [N-(1-oxy-2,2,5,5-tetramethylpyrroline-3-carboxyl)-p-aminobenzhydroxamic acid] (I) became strongly immobilized when this label bound to ferric or manganic horseradish peroxidase (HRP). The titration of HRP with I revealed a single binding site with dissociation constant $K_d = 2 \mu\text{M}$. The binding of I to HRP was inhibited upon equimolar addition of NaF, KCN or H_2O_2 . At alkaline pH, HRP did not bind I and from the measurements of both free and bound spin-labeled intensity with variation of pH, the pK value of acid-alkali transition of HRP was determined to be 10.5. The $2T_{1\rho}$ value of the bound spin label varied inversely with temperature, reaching a value of 68.25 G at 0°C and 46.5 G at 52°C. From the dipolar interaction between iron atom and spin label I bound to HRP the distance between the two spins and hence the depth of the heme pocket of HRP was estimated to be at least 14Å.

M-POS-115 COMPLEX FORMATION BETWEEN VALINOMYCIN AND FCCP IN THE PRESENCE OF POTASSIUM. Thomas A. O'Brien, David Nieva-Gomez*, and Robert B. Gennis. Department of Chemistry, University of Illinois, Urbana, Illinois 61801.

Spectral evidence is presented which indicates that the uncoupler carbonyl cyanide p-trifluoromethoxyphenylhydrazone (FCCP) and the peptide antibiotic valinomycin form a complex in the presence of potassium both in aqueous and nonaqueous media. In aqueous solution, the absorption spectrum of FCCP is significantly perturbed in the presence of valinomycin and K^+ , and there is also a large induced circular dichroism signal. In addition, the previously characterized complex which forms between valinomycin, K^+ , and the fluorescent probe 1-anilino-8-naphthalene sulfonate (ANS) in aqueous solution is apparently disrupted by the addition of FCCP. In a non-polar solvent the absorption spectrum of FCCP is also perturbed by valinomycin in the presence of K^+ , again indicating the formation of a complex. It is likely that the valinomycin- K^+ cation is complexed with the FCCP anion. These data point to the importance of considering the role of a valinomycin- K^+ -uncoupler complex in interpreting physiological or ion transport data in which these substances have been used together.

M-POS-116 PHOTOLYSIS OF BACTERIORHODOPSIN PHOTOTRANSIENTS. M. Ottolenghi* and R.H. Lozier. Dept. of Physical Chemistry, Hebrew University and Cardiovascular Research Institute and Dept. of Biochemistry and Biophysics, University of California, San Francisco 94143

Long-lived transients in the photocycles of light-adapted (LA) and dark-adapted (DA) bacteriorhodopsin (BR) have been studied by laser photolysis methods. Double pulse experiments allow the detection of effects due to light-induced depletion of such transients. In the BR^{LA} system the (unprotonated) M_{410} species appears to be equilibrated with the two (protonated) intermediates N_{530} and O_{640} . The 610 intermediate in the BR^{DA} photocycle is a precursor of the DA \rightarrow LA (13-cis \rightarrow trans) isomerization process. No detectable proton pumping activity is associated with the BR^{DA} photocycle. Molecular mechanisms accounting for the optical changes in the two cycles and for the proton pump will be discussed.

M-POS-117 pH TITRATION AND TYROSINE MODIFICATION OF BACTERIORHODOPSIN. T. Konishi* and L. Packer. Membrane Bioenergetics Group, University of California, Berkeley, CA 94720.

The 412 nm intermediate of the photoreaction cycle of bacteriorhodopsin reflects uptake and release of a proton from the protein moiety to the chromophore Schiff base. Flash photolysis showed that decay of the 412 nm species was highly pH dependent. There was a close correlation between increased $t_{1/2}$ of 412 nm decay and changes in tyrosine absorbance between pH 9-11.5. At pH > 11.5 $t_{1/2}$ became infinite and bacteriorhodopsin was irreversibly damaged.

Iodination of tyrosine caused a shift of both chromophore absorption and pKa of tyrosine. The pH dependency of the 412 nm decay was also shifted concomitant with this pKa shift; hence tyrosine residues may mediate movement of protons between the protein and chromophore Schiff base. A tight packing of hydrophobic residues in the chromophore region appears essential for photoreaction.

(Research supported by the Department of Energy.)

M-POS-118 MICROCALORIMETERS FOR INDIVIDUAL INSECT THERMOGRAMS. C. Wensman* and R. Lovrien, Biochemistry; T. Kurtti* and M. Brooks (Sponsor: I. Rubinstein), Entomology; University of Minnesota, St. Paul, MN 55108

Four instruments have been constructed for obtaining the detailed power outputs as a function of time for single insects. The main features are: (i) Figure of merit, 7 $\mu\text{W}/\mu\text{V}$. (ii) Twin, or differential operation: Sample vs. a reference. (iii) Continuous exchange of air and humidity, with CO_2 exhaust. (iv) Metered exposure to attractants, repellants, pheromones, and toxic compounds. (v) Easily removable and sterilizable vessels, made of Pyrex. The insect after the run may be recovered, intact. (vi) Rapid (20-40 min) recovery from the thermal shock of loading or unloading. (vii) Electronic (Peltier pumped) thermal barriers. (viii) Little skill needed to run the instruments. (ix) Long term stability; runs of several days on 2 to 4 mg. insects (e.g. a single mosquito) are practical, drift $1.5 \pm 0.5 \mu\text{V}/\text{day}$. Several classes of experiments have been carried out, involving chronobiologic phenomena, basal metabolic rates, (BMR) bacterial and gut protozoa infection, morphogenesis, hydrocarbon vapor toxicity, aging, diet, and male-female (pheromone) attractants. Thermograms have a steady (BMR) heat component, plus transient heats, dependent on the state of the insect.

M-POS-119 CAN LITHIUM ACTIVATE THE INSIDE SODIUM SITES OF THE (Na+K)ATPase? L. Beaugé, Dept. of Biophysics, Univ. of Md., Baltimore, Md. 21201

Purified pig kidney ATPase and broken human red cell membranes were incubated in 3 mM MgCl_2 , 3 mM ATP (Boehringer), 30-160 mM TrisCl, pH (37°C) 7.4 and variable monovalent cation composition (in Na-free solutions the [Na] was less than 30 μM). In purified enzyme the total ATPase activities ($\mu\text{mole Pi}/\text{mg.min}$) were: Max. (Na+K) 13.7 ± 0.02 ; 160 mM TrisCl 0.12 ± 0.01 ; 130 mM NaCl 0.52 ± 0.02 ; 130 mM LiCl 0.83 ± 0.02 . The LiCl activation did not show any sign of saturation up to 130 mM. The addition of 10^{-4} M ouabain brought all the activities to the TrisCl levels. In the absence of Na and with 110 mM LiCl the ATPase activity as a function of [KCl] showed an initial activation (Maximal at 0.2 mM) followed by inhibition; the inhibition was half maximal at 5 mM KCl and at 25 mM there was no ouabain sensitive activity left. In red cell membranes the ouabain sensitive activities ($\mu\text{mole Pi}/1\text{h}$) were: Max (Na+K) 1.86 ± 0.04 ; 160 mM TrisCl 0.03 ± 0.02 and 130 mM LiCl 0.25 ± 0.02 .

TRANSPORT SYSTEMS II

M-POS-J1 DIFFUSION CONSTANT OF XENON IN WATER. Gerald L. Pollack and David C. Fleckenstein,* Physics Department, Michigan State University, East Lansing, Michigan 48824

The radioactive isotope Xe-133 (half-life 5.3 days) is widely used in nuclear medicine to study pulmonary function and cerebral blood flow. In the latter application the Xe-133 is initially inhaled as a gas or dissolved in saline solution and injected. It gets distributed in the body by blood flow and diffusion, concentrates briefly in fatty tissues, and is then washed out of the tissues and eliminated through the lungs. We have measured the diffusion constant (D , molar flux per unit concentration gradient) of Xe-133 through water; the result is $D(20^\circ\text{C}) = 1.3 \times 10^{-6} \text{ cm}^2/\text{sec}$. The method used is a direct application of the definition. The diffusion path is a horizontal cylindrical water column. Various lengths around 1 cm and various diameters of a few mm were used. Xenon-133 concentrations are measured on the source and sink sides by monitoring the emitted gamma rays. The experiments can be extended to study: (a) transport across the liquid-gas interface and (b) the application of the Stokes-Einstein Law, $D = kT/6\pi\eta R_B$ (k , Boltzmann's constant; η , solute viscosity; R_B , radius of diffusing particle), to diffusion of small molecules.

Supported by E.R.D.A. Grant EY-76-S-02-1574.

M-POS-J2 METHOD FOR DETERMINING THE OXYGEN PERMEABILITY OF THE RED CELL MEMBRANE. V.H. Huxley and H. Kutchai, University of Virginia, Charlottesville, Virginia 22901

The measured diffusion resistance to oxygen uptake by human red blood cells (RBCs) is the sum of the O_2 diffusion resistance of the unstirred layer external to the membrane plus the true O_2 resistance of the plasma membrane. We have devised a method to determine the true O_2 permeability of RBC ghost membranes and the effect of the unstirred layer external to the plasma membrane. The ghosts are loaded with an O_2 -consuming enzyme system (Glucose oxidase, catalase and glucose). As O_2 is consumed by the cells at 35°C , oxygen enters the chamber through an O_2 permeable membrane. The PO_2 of the suspension is monitored with an O_2 electrode until a steady state is established. From the extracellular steady-state PO_2 and the kinetic properties of the trapped enzyme system, the apparent membrane permeability is computed. Diffusion is assumed to vary inversely with viscosity in the unstirred layer. Quantification of the effect of unstirred layers in this system is obtained by altering the viscosity of the extracellular fluid by addition of high molecular weight Dextrans. (supported by HL 17967)

M-POS-J3 STRUCTURE-ACTIVITY RELATIONSHIP OF AROMATIC SULFONIC ACIDS AS INHIBITORS OF THE ANION TRANSPORT SYSTEM OF HUMAN RBC. M. Barzilay,* S. Ship,* Z.I. Cabantchik (Intr. by M. B. Burg), NIH, Bethesda, Md. 20014

The inhibitory effects of aromatic sulfonic acids on sulfate exchange were studied. Two series of compounds were tested: benzene sulfonic (BS) and 2,2'-disulfonic stilbene (DS) derivatives. As judged by kinetic criteria the compounds acted at the sulfate transport site. Potency of inhibition (ID_{50}) varied over 10^4 fold ($2-50,000 \mu\text{M}$). The degree of inhibition depended principally on two chemical characteristics of the substituents: 1) Lipophilicity (for chloro derivatives of BS and for acetamido and benzoamido derivatives of DS) and 2) electron donor-acceptor capacity (for nitro, azido and amino derivatives of BS and DS). Based on these results, we suggest that the microenvironment of substrate recognition sites of the anion transport system bears positive charges and possesses functional groups with electron donor capacity, embedded in a hydrophobic area. These chemical properties may define the susceptibility of the anion transport system not only to specific probes such as DS and BS but also to diverse agents such as diuretics, anesthetics and sedatives.

M-POS-J4 INFLUENCE OF SITS ON $\text{HCO}_3^-/\text{Cl}^-$ EXCHANGE IN HUMAN RED CELLS. A. L. Obaid*, E. D. Crandall and R. E. Forster. University of Pennsylvania, Philadelphia, PA.

Using a stopped flow rapid reaction apparatus, changes in extracellular pH (pH_0) in red cell suspensions were monitored under conditions where dpH_0/dt was determined by the rate of $\text{HCO}_3^-/\text{Cl}^-$ exchange flux across the membrane. These conditions were obtained by mixing equal volumes of a 20% hematocrit erythrocyte suspension containing NaHCO_3 and extracellular carbonic anhydrase at pH 7.7 with an equal volume of phosphate-buffered saline preadjusted to $5.0 < \text{pH} < 6.8$. Experiments were performed at $50 < T < 37^\circ\text{C}$ using either untreated cells or cells exposed to 0.11 mM SITS (4-acetamido-4'-isothiocyanostilbene-2,2'-disulfonic acid). Both untreated and SITS-treated cells showed similar transition temperature (17°C) and activation energies (19.6 kcal/mole below and 11.7 kcal/mole above 17°C) for $5.4 < \text{pH}_0 < 6.8$, although bicarbonate flux was reduced by 90% due to SITS exposure. These findings, similar to those reported for Cl^-/Cl^- self-exchange using another inhibitor, suggest that the mechanisms for $\text{HCO}_3^-/\text{Cl}^-$ exchange above and below the transition temperature are unchanged by exposure to SITS, but that the number of sites available for transport is reduced. (Supp. by HL19737, AHA 75-992 and RCDA HL00134.)

M-POS-J5 ANION EXCHANGE: EVIDENCE FOR A SEQUENTIAL REACTION MECHANISM AND A SINGLE TRANSPORT SITE. R.B. Gunn and O. Fröhlich* Dept. Pharm. & Physiol. Sci., U. Chicago Chicago, IL 60637

We have measured the stimulation of Cl^- efflux from human red cells through the anion exchange mechanism into acetate solutions by external Br. The initial Cl^- efflux was nearly all in exchange for external Br since the efflux into acetate alone was very much slower (Gunn et al. J.G.P. 65:731,1975). The double reciprocal plot of efflux vs external Br was a straight line when $\text{Br} = 1.5-15 \text{ mM}$. The maximum flux (V_{max}) was $330 \text{ mM}/(\text{kg cell solids} \cdot \text{min})$ and the Br concentration at which the flux was half maximum ($K_{1/2}$) was 10 mM when $\text{Cl}_i = 118 \text{ mM}$. Above 30 mM Br the flux decreased as does the self-exchange of halides. When cell Cl^- was reduced by substitution with acetate the Br stimulated efflux was reduced and both V_{max} and $K_{1/2}$ decreased as expected if the molecular mechanism is a sequential reaction of a single site with alternating access to the inner and outer solutions as proposed in the titratable carrier model. These findings are inconsistent with a simple simultaneous heteroexchange of chloride and bromide. (Supported in part by USPHS grants HL-20365 and 5K04-HL-00208 and a DFG fellowship.)

M-POS-J6 Cl EFFLUX STIMULATED BY cAMP; BLOCKED BY SITS OR FUROSEMIDE. J.M. Russell and M.S. Brodwick, Dept. of Physiology and Biophysics, UTMB, Galveston, TX 77550

Cl efflux from internally dialyzed barnacle giant muscle fibers was reversibly stimulated by cyclic AMP (cAMP). When cAMP (10^{-6} - 10^{-7} M) was presented intracellularly via the dialysis fluid Cl efflux increased from 55 to 220 pmoles/cm²·sec (p/c.s). Upon removal of cAMP, the efflux declined to 63 p/c.s. The extracellular application of 0.5 mM SITS during cAMP treatment caused the average efflux to fall to about 24 p/c.s. Thus, all the cAMP-stimulated efflux was blocked as well as more than half the resting efflux. The effects of 0.6 mM furosemide were studied since it has been reported to inhibit adenylate cyclase (Naunyn-Schmied. Arch. Pharmacol. 281:301, 1974). Resting Cl efflux was inhibited 60% by this agent. When Cl efflux was stimulated by cAMP, furosemide treatment inhibited all the cAMP-induced efflux, as well as about 30 p/c.s of the resting efflux. These data demonstrate a clear effect of cAMP on Cl efflux and suggest that cAMP might play a role in resting Cl efflux. (Supported by NIH grant NS-11946).

M-POS-J7 NUMBER OF WATER MOLECULES (n) COUPLED TO THE TRANSPORT OF K⁺ AND Na⁺ VIA NONACTIN AND GRAMICIDIN. D.G. Levitt, S.R. Elias,* and J.M. Hautman,* Dept. of Physiology, Univ. of Minn., Mpls., Mn. 55455.

The value of n was determined directly from the volume flux per ion when a current was passed and indirectly (using Onsager's relation) from the open circuit potential produced by an applied osmotic pressure difference. Monoolein-decane membranes were formed on the end of a P.E. tube. For gramicidin: n=12 for 0.15 M/L and n=6 for 3.0 M/L for both KCl and NaCl; and n=0 for .01N HCl. For nonactin: n=4 for both 0.15 and 3.0 M/L K⁺ and Na⁺. It can be shown that the n of 12 for gramicidin with the .15 M salts indicates that the channel can hold at least 12 water molecules. This places an important constraint on models of channel structure. The n of 0 for HCl is consistent with a process in which protons jump along a continuous row of water molecules. The n of 4 for nonactin (and valinomycin) indicates that 4 water molecules are associated with the carrier cation complex--probably in the interstices between the carrier and the disordered lipid.

M-POS-J8 MEASUREMENT OF MEMBRANE POTENTIALS BY H⁺ DISTRIBUTION. R. Macey, J. Adorante*, and F. Orme*, Dept. of Physiology-Anatomy, Univ. of California, Berkeley.

Changes in membrane potential in red cells suspended in unbuffered solutions can be measured by following changes in external pH. Rapid equilibration of H⁺ can be assured by the addition of the H⁺ carriers TCS and CCCP. Under these conditions, internal pH is constant, and changes in membrane potential equal changes in voltage V measured by an external glass electrode. Validity of the method is established by showing: (1) plotting changes in V vs log (Cl) yields a straight line with a 59 mV slope, (2) in cells with high K⁺ permeability (induced by Gardos effect) and low Cl⁻ permeability (inhibited by DIDS), a linear plot of V vs log (K) has a 59 mV slope. Measurements of V during anion substitution give important information about both conductive and exchange pathways for anions transport. The peak jump in V obtained when an anion is substituted for (Cl) is used to calculate relative conductive permeabilities. The subsequent decay in V is used to recover the kinetics of the exchange process. Supported by NIH Grant GM 18819.

M-POS-J9 CAGED-ATP, A PHOTOLABILE SOURCE OF ATP. J.H. Kaplan,* B. Forbush* and J.F. Hoffman, Department of Physiology, Yale School of Med., New Haven, CT. 06510.

Caged-ATP, P³-1-(2-nitro)phenylethyl-ATP, has been synthesized from 1-(2-nitro)phenylethyl phosphate and ADP. Irradiation at 340 nm of aqueous solutions of caged-ATP results in the release of ATP in high yield (70%) in under 30 secs. Caged-ATP is not a substrate for purified Na,K-ATPase from pig kidney. Following photolysis, enzymatic hydrolysis of the photo-released substrate, ATP, can be followed. Addition of glutathione or bisulfite to the caged ATP solution prior to photolysis in the presence of enzyme completely eliminates a partial photo-dependent inhibition of enzymatic activity without affecting the rate of release of ATP. Caged-ATP incorporated into resealed red cell ghosts prepared from energy depleted red cells did not support Na pump activity; photolysis of the ghost suspension resulted in Na pump activation by the photo-released ATP as shown by measurements of ouabain-sensitive Na efflux. Caged-ATP is thus a stable source of intracellular ATP which can be liberated rapidly by photolytic irradiation. (Supported by NIH Grants AM-17433 and HL-09906 and NIH Fellowship F22-AM-02262 to B.F.)

M-POS-J10 SIDE-SPECIFIC INTERACTIONS OF Na⁺ AND K⁺ WITH Na-ATPASE OF INSIDE-OUT MEMBRANE VESICLES OF HK AND LK SHEEP RED CELLS. P. Drapeau,* and R. Blostein (Intr. by T.M.S. Chang), Royal Victoria Hosp., Montreal, Canada.

Na-ATPase of high-K⁺ (HK) and low-K⁺ (LK) sheep red cells was studied, particularly the sidedness of Na⁺ and K⁺ effects, using inside-out membrane vesicles. Short reaction periods (45 min) were used to minimize changes in ionic composition and low [Y-32P]-ATP (≤0.2 μM) to minimize non-specific ATP hydrolysis and to optimize sensitivity to K⁺. At 0.02 μM ATP, Na⁺ in the medium (Na_{ext} at the cytoplasmic surface, Na_{cyt}) caused a hyperbolic activation in HK and a sigmoidal activation in LK vesicles. Both types are further stimulated by intravesicular Na⁺ (Na_{int} at the originally external surface, Na_{ext}); stimulation in LK, though greater than HK, is more sensitive to K⁺-competition. Intravesicular K⁺ (K_{ext}) activates Na-ATPase in HK but not in LK vesicles and extravesicular K⁺ (K_{cyt}) inhibits LK but not HK vesicles. Thus, the genetic difference between the two is expressed as differences in affinities for both Na⁺ and K⁺ and for the relative Na⁺/K⁺ affinities at both surfaces. (Supported by the MRC of Canada and a Quebec DGES Scholarship to P.D.).

M-POS-J11 CHOLESTEROL DEPLETION AND K⁺ FLUXES IN HUMAN AND SHEEP ERYTHROCYTES, AND THE EFFECT OF ANTI-L. J.E. Grey* & P.K. Lauf, Dept. Physiology, Duke University, Durham, N.C.

Giraud et al. (Nature 264:1976,646) proposed that cholesterol behaves as inhibitor of the pump's turnover and activator of its apparent affinity for cellular Na⁺ ions. We have tested this concept on high and low potassium (HK & LK) sheep red cells (SRC) which have different turnover rates and Na⁺ affinities of the pump. Particularly, we were interested if cholesterol depletion would alter: a) K⁺ pump and leak fluxes in HK and LK SRC, b) the effect of anti-Lp on the pump and c) of anti-L1 on K⁺ leak flux in LK SRC. Cholesterol depletion by the "preincubated serum method" led to only 20% loss of cholesterol in HK and LK SRC as compared to 50% in human red cells (HRC). In both HK and LK SRC, active and passive K⁺ influxes were not altered by cholesterol depletion, and anti-Lp and anti-L1 exerted their full effects. In contrast to the finding of Giraud et al. we did not see a severalfold stimulation of pump turnover in HRC. Hence the cholesterol removed (by the serum method) is not involved in modulation of K⁺ pump and leak fluxes in human and sheep red cells nor is it required for the effects of anti-Lp and anti-L1 on the LK pump and leak systems (Supported by USPHS HL 12157).

M-POS-J12 CYCLING HYPER/HYPOOSMOTIC DIALYSATES INCREASE PERMEABILITY OF THE PERITONEAL MEMBRANE. P.J. Whittam*, R.H. Parsons, D. Gisser*, A. Zelman, Rensselaer Polytechnic Institute, Troy, New York 12181

Hyperosmotic peritoneal dialysate induces an alteration of the peritoneal membrane which increases its hydraulic conductivity and solute permeabilities. The use of hyperosmotic solutions also increases dialysis efficiency, but adversely invokes excessive ultrafiltration which leads to patient dehydration. Our studies indicate that the controlled alternation of dialysate osmolalities in programmed hyper/hypoosmotic cycles effectively induces the described alteration of the membrane while also permitting a controlled ultrafiltration by the intermittent reversal of volume flow. The direction of this flow is determined by dialysate osmolality. Convective transport resulting from repeated hyperosmotic cycles appears to have a small value compared to diffusive transport. Diffusive transport is greatly augmented by a factor of two (2) by the cycling of hyper/hypoosmotic dialysates. Histological studies of the membrane show no gross changes related to the use of this technique. The membrane's alteration appears to occur at the molecular or submicroscopic level.

PURPLE MEMBRANES I

M-POS-J13 CEREBROVASCULAR PERMEABILITY TO WATER-SOLUBLE NONELECTROLYTES. K. Ohno*, K.D. Pettigrew* and S.I. Rapoport. NIMH, Bethesda, Md. 20014

^{14}C tracers of inulin, sucrose, mannitol and glycerol were injected i.v. in conscious rats. Arterial plasma concentration, C_t , dpm/ml, was followed until a rat was killed 3 min to 2 hr later. Radioactivity in different brain regions, C_b , dpm/g, was found after correction for intravascular tracer. As $C_t \gg C_b$ up to the time of death, tracer flux into brain equaled $dC_b/dt = PAC$, (P = permeability, A = capillary surface area). Integration of this equation gives $PAC = C_b / \int C_t dt$. For $A = 240 \text{ cm}^2/\text{g}$, P was found to be $1.4 \times 10^{-7} \text{ cm/sec}$ for inulin, $2.5 \times 10^{-6} \text{ cm/sec}$ for sucrose, $1.5 \times 10^{-7} \text{ cm/sec}$ for mannitol and $2.3 \times 10^{-6} \text{ cm/sec}$ for glycerol. Nonelectrolyte permeability at the cerebral vasculature does not vary among brain regions with a blood-brain barrier, and is as low as at plasma membranes and aporous, bimolecular lipid membranes. This low permeability and a linear relation between $PM^{1/2}$ (M = mol wt) and lipid solubility suggest that nonelectrolytes cross cerebral vessels by a nonporous mechanism. Neither interendothelial tight junctions nor vesicular transport normally contributes to significant nonelectrolyte transfer at the vasculature.

M-POS-K1 PHOTISOIMERIZATION OF BACTERIORHODOPSIN (BR). N.A. Dencher, K.D. Kohl*, Ch.N. Rafferty*, and W. Sperling*, Institut für Neurobiologie, KFA, D-517 Jülich, Germany.

The ratio of trans BR ($\lambda_{\text{max}} = 568 \text{ nm}$) and 13-cis BR ($\lambda_{\text{max}} = 548 \text{ nm}$) in the purple membrane depends on the light intensity. The difference in the photochemistry of 13-cis and trans BR was used to determine the ratio of these isomers in various preparations of purple membrane and in living bacteria (1). In the dark-adapted state the ratio of trans to 13-cis BR is one. Under conditions of moderate light intensities (10 mW/cm^2 , corresponding to a sunny day) nearly 100 % trans BR are present (2). Using very high light intensities, part of the trans BR is photoconverted to 13-cis BR, and a mixture of 20 % 13-cis and 80 % trans BR could be obtained. The pathway of this reaction will be discussed.

1) Dencher, N.A., Rafferty, Ch.N., and Sperling, W. *Berichte der Kernforschungsanlage Jülich*, Jül-1374 (1976).

2) Sperling, W., Carl, P., Rafferty, Ch.N., and Dencher, N.A. *Biophys. Struct. Mechanism* 3, 79 (1977).

M-POS-K2 NEUTRON DIFFRACTION STUDIES ON THE LOCALIZATION OF THE CHROMOPHORE OF BACTERIORHODOPSIN. G.I. King, P. Mowery, and W. Stoeckenius, Cardiovascular Res. Inst. and Dept. Biochemistry and Biophysics, University of California, San Francisco, Ca. 94143. H. Crespi, Argonne National Laboratory, Argonne, Ill. 60439. B. P. Schoenborn, Dept. Biology, Brookhaven National Laboratory, Upton, New York 11973.

Analyses of the in-plane neutron diffraction data obtained from bleached purple membrane samples regenerated with deuterated and protonated retinals, respectively, have been performed in order to locate the chromophore in the plane of the membrane. The analysis was done with the use of Patterson difference functions between the two substituted samples, thus giving the set of retinal autocorrelation peaks in the membrane lattice. These Patterson maps show the existence of two different sites for the exogenously added retinals in the samples. One of these sites is the one described in these abstracts last year (King, et al, *Biophys. J.* 17, 97a, 1977), which shows an interesting time dependent behaviour; the other site does not show this peculiarity. The possible interpretations of these results will be presented.

M-POS-K3 ORIENTATION OF THE PURPLE MEMBRANE WITH RESPECT TO THE *HALOBACTERIUM HALOBIVM* CELL. S.B. Hayward,* (Intr. by H.J. Burki), Graduate Group in Biophysics and Donner Laboratory, University of California, Berkeley, CA 94720

The structure of the purple membrane (PM) as determined by electron microscopy has not yet been related to the inside and outside of the *H. halobium* cell. PM adsorbs to polylysine at pH 7.4 preferentially with the cytoplasmic side to the polylysine. However, the glucose-embedding technique has been found to be unsuitable for hydrophilic support films, making electron diffraction of PM adsorbed to polylysine-coated EM grids impossible using glucose-embedding. A new technique for making frozen-hydrated EM specimens has been applied to this problem. Grids coated with polylysine were held on a plastic coverslip by the formvar support film. PM were applied, and the coverslip was passed through a stearate film at an air-water interface. The grids were then frozen in LN and used for selected area diffraction on a LN-cooled stage in a JEM-100B. Diffraction patterns extending to 4.5\AA showed preferential orientation with respect to the grids. High resolution imaging is being used to relate this orientation to the projected potential of the membrane.

M-POS-K4 INFRARED DICHOISM OF ORIENTED PURPLE MEMBRANE K.J. Rothschild and N.A. Clark*, Intr. by H.E. Stanley Boston University School of Medicine 02118 and University of Colorado at Boulder 80309

Polarized Fourier transform infrared spectroscopy has been used to study the structure of purple membrane from *Halobacterium halobium*. Membranes were oriented by drying a suspension of membrane fragments onto Irtan-4 slides. Dichroism measurements of the amide I, II and A peaks were used to find the average spatial orientation of the bacteriorhodopsin α -helices. By deriving a function which relates the observed dichroism to the orientational order parameters for the peptide groups, helical axis distribution and mosaic spread of the membranes, the average orientation of the α -helices is found to lie in a range less than 26° away from the membrane normal in agreement with electron microscopic measurements. The frequency of the amide I and A peaks is at least 10 cm^{-1} higher than values found for most α -helical polypeptides and proteins. This indicates along with X-ray data that bacteriorhodopsin may contain distorted α -helical conformations.

M-POS-K5 PLATINUM LABELLING OF BACTERIORHODOPSIN, M. Dumont* and J.W. Wiggins, Jenkins Department of Biophysics, The Johns Hopkins University, Baltimore, Md. 21218

Amino acid-specific heavy atom labels are being prepared for use in structural studies of bacteriorhodopsin. This protein forms a two dimensional hexagonal lattice in purple membrane from *Halobacterium halobium*. Its structure has previously been solved to 7\AA resolution using combined electron microscopy and electron diffraction.¹ Electron diffraction is being used to find the sites of heavy atom binding in the unit cell of the lattice. A complex of platinum with the dipeptide glycyl-L-methionine binds to three or four sites per protein molecule. This binding causes a change in the intensities of reflections in circularly averaged electron diffraction patterns of multiple membrane patches. Patterson difference maps are being prepared from diffraction patterns of single patches of the protein. Since purple membrane lacks cysteines, the platinum probably binds to methionine residues. The labelling process causes no noticeable degradation of the purple membrane.

1) Unwin, P.N.T. and Henderson, R. *J. Mol. Bio.* 94, 425 (1975).

SYMPOSIUM

PRIMARY REACTIONS IN PHOTOSYNTHESIS

TU-AM-15 DYNAMIC STRUCTURAL ORGANIZATION OF PIGMENT-PROTEIN COMPLEXES IN CHLOROPLAST MEMBRANES. Charles J. Arntzen, USDA/ARS, Dept. of Botany, University of Illinois, Urbana, Illinois 61801

Most, if not all, chlorophyll in chloroplast membranes is organized in pigment-protein complexes. Three classes of these complexes can be isolated from chloroplast membranes by mild detergent techniques: 1) a photosystem I reaction center (P700) complex containing light-harvesting chlorophyll a, 2) a photosystem II reaction center complex also containing light-harvesting chlorophyll a, and 3) a photochemically inactive complex containing light-harvesting chlorophylls a and b. Electron microscopic analysis (using the freeze-fracture technique) of intact chloroplast membranes and detergent-derived pigment-protein complexes suggests that each complex exists as a discrete membrane subunit that can be released from the lipid matrix of the membrane by mild non-ionic detergents. More extensive dissociation of the proteins and pigments within each complex can be achieved by use of ionic detergents such as sodium dodecyl sulfate (SDS). Membrane subunits within chloroplast membranes exhibit lateral mobility within the lipid phase of the membrane. The membrane subunits corresponding to the PS II complex and the light-harvesting complex (LHC) can be observed to become uniformly distributed along unstacked chloroplast membranes prepared in solutions of low cation concentrations. If cations are added to these membranes, the membrane subunits redistribute such that a higher density of particles occurs in the regions of cation-induced membrane appression (grana stacks). Evidence will be presented defining the role of the LHC in mediating the cation-mediated regulation of stacking and particle mobility. Cations are known to influence the characteristics of chlorophyll fluorescence and activities of photosystem I and II partial reactions. These changes are usually interpreted as alterations in excitation energy distribution between the pigment beds of the two photosystems. Evidence will be provided to indicate that the LHC mediates cation-induced effects on excitation energy distribution. A model will be presented which emphasizes that the cation-induced formation of grana can result in a relative immobilization of certain populations of pigment-protein complexes within the membrane and the creation of a shared pigment bed between photosystem II-LHC complexes across two membranes. These structural alterations are suggested to account for cation-induced energy distribution changes within the functional pigment-protein complexes.

TU-AM-25 EXCITON DYNAMICS IN LIGHT-HARVESTING CHLOROPHYLL SYSTEMS. R. S. Knox, University of Rochester, Rochester, New York 14627

A review of several topics relating to the optical production of excitons and their motion in the photosynthetic unit, largely in the non-saturating intensity regime, will be presented. Emphasis will be on the theory of excitation transfer, fluorescence depolarization, and localization and delocalization of excitation. Recent fluorescence studies of certain chlorophyll-protein complexes will also be reviewed, along with an assessment of their implications for the process of energy transfer in photosynthetic systems.

TU-AM-3S THE PRIMARY ELECTRON TRANSFER REACTION IN BACTERIAL PHOTOSYNTHESIS. W. Parson,*

University of Washington, Seattle, Washington 98195

The photochemical reaction of bacterial photosynthesis has been studied with picosecond and nanosecond spectrophotometric techniques, in preparations of photosynthetic reaction centers isolated from *Rhodospseudomonas sphaeroides* and *Rhodospseudomonas viridis*. Reaction center preparations contain four molecules of bacteriochlorophyll, two molecules of bacterioopheophytin (bacteriochlorophyll with two H's replacing Mg), one or two quinones, and three polypeptides. The arrangement of the chromophores in the complex is not well understood, but two of the bacteriochlorophylls appear to interact with each other particularly strongly. When these are excited with light, they transfer an electron to an acceptor which appears to be one of the bacterioopheophytins interacting strongly with another bacteriochlorophyll. This occurs in about 10 ps. The electron then moves to one of the quinones in about 200 ps. If the second step is blocked, reverse electron transfer reactions occur in about 10 ns. Electron spin rephasing can occur in the initial radical pair, so that the reverse reaction places the bacteriochlorophyll in a triplet state. One can trap the system in other transient states, such as the initial excited singlet state, by suitable adjustment of the conditions prior to the excitation. One of the puzzling questions that remain is, not how the forward electron transfer reactions can be as fast as they are, but how the reverse reaction can be so slow. Model photochemical reactions of bacterioopheophytin in solution have much faster reversals. The reaction center must prevent the back reaction in order for the photosynthetic apparatus to work as efficiently as it does, but how it manages this is not clear. Another puzzle concerns the interpretation of a set of very fast (20-40 ps) absorbance transients that do not seem to correlate well with any of the events mentioned above.

My collaborators have been R.E. Blankenship, R.K. Clayton, R.J. Cogdell, J.D. Holtz, T.G. Monger, J.P. Thornber, and M.W. Windsor.

TU-AM-4S CHLOROPHYLL LASERS AND THE PRIMARY EVENTS IN PHOTOSYNTHESIS.[†] J. J. Katz, M. R. Wasielewski,* and J. C. Hindman, Argonne National Laboratory, Argonne, Illinois 60439

The observation that chlorophylls and their derivatives can be induced to emit laser light (Proc. Natl. Acad. Sci. USA 74, 5-9 (1977)) has some interesting implications for the nature of excited chlorophyll states. The production of high populations of chlorophyll excited states results in the shortening of fluorescence lifetimes and narrowing of the fluorescence band widths. These *in vitro* effects appear to be remarkably similar to the shortening of fluorescence lifetimes observed in pico-second experiments on "in vivo" photosynthetic systems. We have explored the effects of photon flux on the fluorescence yield and life-times of *in vitro* chlorophyll systems to provide an experimental basis for the interpretation of photochemical experiments on *in vivo* chlorophyll systems in which high concentrations of excited states are generated. These studies include an examination of the lasing properties of open and folded linked chlorophyll dimers (Wasielewski, et al., Proc. Natl. Acad. Sci. USA 73, 4282-86 (1977)). While both the open and the folded configurations are approximately equally fluorescent, only the folded configuration seems capable of stimulated emission. The fate of excited chlorophyll states, it is clear, depends on more than intermolecular distances. The implication of these findings for the interpretation photochemical experiments on photosynthetic systems will be discussed.

[†]Work performed under the auspices of the Division of Basic Energy Sciences of the Department of Energy.

MINISYMPOSIUM

MOVEMENT OF MOLECULES ON CELL SURFACES

TU-AM-IMMOBILITY, MOTILITY AND IMMOBILIZATION ON THE CELL MEMBRANE. W. W. Webb, Cornell Univ., Ithaca, N.Y. 14853.

Molecular movement in cell surface membranes is essential in the development of cellular architecture and in response to many external stimuli. Nevertheless it is only recently that new methods have made possible systematic measurements of lateral mobility of various membrane components. Recent mobility experiments using fluorescence photobleaching recovery methods have revealed a substantial diversity of mobility in mammalian cell membranes. Lipid-probe molecules appear completely mobile with diffusion coefficients $D \sim 10^{-8} \text{ cm}^2/\text{sec}$; "typical" unselected membrane proteins have $D \sim 10^{-10} \text{ cm}^2/\text{sec}$ but only about half are mobile, and some proteins like the "cell surface protein" CSP or LETS are virtually immobile. Available results will be summarized and compared with properties of model membranes. The capability and limitations of the experimental methods most suitable for cell studies, particularly the fluorescence photobleaching recovery method including recent developments for study of cooperative motions such as driven convection of the membrane and motile processes will be discussed.

Some current research involving molecular motions on cell surfaces is illustrated by the accompanying three lectures of this symposium for which this lecture provides some of the background. Of current concern are the more complex movements involved in the response of membrane bound receptors to particular hormones and antigens, coupling to the cytoskeleton and in phagocytosis.

TU-AM-2M DYNAMICS OF RECEPTOR INTERACTIONS ON CELL MEMBRANE. Joseph Schlessinger, Immunology Branch, NCI, National Institutes of Health, Bethesda, Maryland 20014

The plasma membrane is not only a barrier which isolates the interior of the cell from the exterior, but also a dynamic structure which participates in the mechanism of cell growth, differentiation, motion and communication with other cells. Some of these biological events are followed by changes in the distribution of cell surface molecules.

In this talk I will analyze the possible relationship between the motion of identified cell surface receptors and their biological function. Quantitative diffusion coefficients of membrane receptors were measured by the fluorescence photobleaching recovery (FPR) method. Qualitative observations of long range motions and receptor aggregation were visualized by image intensified video fluorescence microscopy.

Employing biologically active fluorescent derivatives of insulin and epidermal growth factor (EGF) which were bound to 3T3 fibroblasts, we draw the following conclusions: Insulin and EGF receptors are mobile on the cell membrane with similar diffusion coefficients $D \sim (3-4) \times 10^{-10} \text{ cm}^2/\text{sec}$ at 23°C . Increasing the temperature to 37°C yields pronounced receptor immobilization. When the cells were labeled at 37°C with either the fluorescent insulin or the fluorescent EGF derivatives the receptor hormone complexes rapidly aggregate into patches on the cell surface and soon thereafter appeared in endocytic vesicles within the cell. The receptor immobilization is presumably the consequence of receptor aggregation, internalization or both.

The talk will also include an analysis of the possible relationship between the mobility of IgE: Fc receptor complexes on rat peritoneal mast cells and the early events which lead to mast cells degranulation (1).

(1). J. Schlessinger, W.W. Webb, E.L. Elson and H. Metzger, Nature 264, 550 (1976).

TU-AM-3M CYTOSKELETAL COUPLING TO MEMBRANE COMPONENTS. S. J. Singer, J. F. Ash, L. Y. W. Bourguignon, M. Heggeness, and D. Louvard, Department of Biology, University of California at San Diego, La Jolla, California 92093.

We have demonstrated directly that the intracellular (cytoskeletal) proteins actin and myosin play important roles in three membrane-related phenomena: 1) the apparent immobility of surface components on normal fibroblasts and other flattened cells grown in monolayer culture; 2) the capping of surface components on lymphocytes and other cells in suspension; and 3) the arrangement of external surface proteins such as LETS. These observations were made with double immunofluorescence and other specific staining methods, by which a particular surface component and either actin or myosin were stained on the same cell. Staining of intracellular tubulin was also carried out, but no correlations between surface component and microtubule distributions were observed. In phenomenon 1), several different membrane integral proteins were found initially to be mobile on the cell surface, but upon being clustered into patches by their respective lectins or antibodies, became lined up directly over intracellular stress fibers containing actin and myosin. In other words, the immobility of surface components was induced by the reagents used to detect them. In 2), the same lectin- or antibody-induced clustering of surface components in these round cells (lacking stress fibers) produced patches and subsequently caps. Under the patches or caps of any of a wide range of surface components there was always found a juxtaposed patch or cap containing actin and myosin under the membrane. In 3) the paucidisperse fibrous surface distribution of LETS protein was found to be superimposed over the stress fibers. The three phenomena indicate that under appropriate circumstances most surface components can become physically linked across the membrane to cytoskeletal proteins inside the cell. The molecular mechanisms of such linkages are under investigation.

TU-AM-4M SURFACE ORGANIZATION: MICROFILAMENTS, MICROTUBULES AND PHAGOCYTOSIS.
R. Berlin, University of Connecticut Health Center, Farmington, Conn. 06032

PROTEINS AND POLYPEPTIDES I

TU-AM-A1X-RAY STRUCTURE OF [LEU⁵]ENKEPHALIN, Jane F. Griffin,* G. David Smith* (Intr. by W. L. Duax), Medical Foundation of Buffalo, Buffalo, NY 14203

Enkephalin, an endogenous morphine like substance, Tyr-Gly-Gly-Phe-X, where X may be Leu or Met, binds to the opiate receptor in brain, spinal cord and gut. Hydrated [Leu⁵]enkephalin, C₂₈H₃₇O₇N₅·H₂O, crystallizes in space group C2, cell constants a=31.871(6), b=8.535(2), c=12.467(2)Å, β=96.53(2)° and Z=4. The observed conformation possesses a β-bend stabilized by antiparallel hydrogen bonding between Tyr and Phe. The phenyl groups of Phe and Tyr are nearly coplanar; the Leu side chain is directed away from the plane of the molecule. All peptide linkages are *trans*; both Gly residues adopt a conformation which is forbidden to L-amino acids while the other three residues are in an extended conformation. Five structural features observed in enkephalin provide a starting point for explaining the structure-activity relationships for opiate agonists and antagonists: (1) hydrophilic bonding through the phenoxy side chain of Tyr; (2) the protonated amino group of Tyr; (3) hydrophobic bonding through the side chain of Phe; (4) hydrophilic interactions of the carboxylate group of Leu; and (5) hydrophobic binding of the Leu side chain.

TU-AM-A2 MOLECULAR ORBITAL CALCULATION STUDIES ON MIF: Pro-Leu-Gly-NH₂, G. Butt,* M. E. Druyan,* and R. Walter, Dept. Physiol. Biophys., Univ. Ill. Med. Ctr., Chicago, IL 60612 and Dept. Biochem., Loyola Univ. Sch. Dent., Maywood, IL 60153

Molecular orbital calculations in the framework of the Complete Neglect of Differential Overlap (CNDO/2) hypothesis were performed on low energy conformations (PANS, 71, 1142, 1974) of the melanocyte-stimulating hormone inhibitory factor (MIF). In vacuo the lowest energy conformation was found to contain two hydrogen bonds, one between the N-H group of Pro and the other between the carboxamide proton of Gly and the C=O group of Leu. The 10-membered β-turn structure originally proposed for MIF in DMSO (Proc. Third Amer. Peptide Symp., 1972) and also found by crystallographic studies, which features one hydrogen bond between the C=O of Pro and the terminal amide, had the highest dipole moment. Our results indicate that rather than having a rigid conformation due to Pro and Leu sidechain interactions (PNAS 73, 1203, 1976), the structure is heavily influenced by hydrogen bonding in vacuo and that the β-turn structure is stabilized by solvent interactions. (Supported in part by AM 13399).

TU-AM-A3 SINGLE PROTON HYDROGEN EXCHANGE KINETICS IN BPTI BY NMR. B. Hilton*, and C. Woodward, Univ. of Minnesota, St. Paul, MN 55108

The pH and temperature dependence of the deuterium-hydrogen exchange of 10 resonances assigned to amide protons in the low field NMR region of BPTI have been measured from pH 1.5 to 7 and 55 to 70°C. The pH-rate profiles are similar for all the resonances, showing very shallow rate minima from pH 3 to 3.5 where the exchange rates are about 0.06 hr⁻¹ at 67°C, and showing non-first order dependence on either the bulk solvent [H⁺] or [OH⁻] far away from the pH minima. The exchange rates are described by $k_{ex} = k_H [H^+]^X + k_{OH} [OH^-]^X$ where X is 0.3-0.5. Model polypeptides show exchange rate minima from pH 3-3.5 and X = 1. The data are not consistent with a model proposing free exposure of the amide to bulk solvent during exchange. Apparent activation energies are 55-70 Kcal/mole.

TU-AM-A4 CARBON-13 NMR PROPERTIES OF ANGIOTENSIN-II. J.A. Ferretti and G.R. Marshall, N.I.H., Bethesda, MD. 20014 and Washington University, St. Louis, MO 63130

Carbon-13 longitudinal relaxation times (T₁) and nuclear Overhauser enhancement factors have been determined at 25.2 MHz and 67.9 MHz for the aliphatic carbon atoms of angiotensin-II (Asp-Arg-Val-Tyr-Ile-His-Pro-Phe) in aqueous solution at pH 4.3. From these data, it was possible to evaluate the effective correlation times for both the overall motion of the molecule (τ_R) and for the internal motion of each peptide residue (τ_{CI}). Using the Woessner formulation, it was found that τ_R is ca. 6 × 10⁻⁹ sec., whereas the τ_{CI} range from 6 × 10⁻¹¹ sec. for the α-carbon of the terminal Asp residue to 2 × 10⁻¹⁰ sec. for that of the interior Tyr residue. The temperature dependence of the T₁'s at 67.9 MHz was also determined. These data, together with other thermodynamic properties, are used to specify the nature of the molecular association of angiotensin-II in aqueous solution.

(Supported in part by NIH Grant HL 14509).

TU-AM-A5 CIS IMIDE BONDS AND SALT INDUCED ISOMERIZATION OF THE POLY(IMINO ACIDS). D. S. Clark, J. J. Dechter,* and L. Mandelkern, Dept. of Chem., Inst. Molec. Biophys., Florida State U., Tallahassee, FL 32306.

P(Pro) and P(Hyp) possess a small, but significant, concentration of *cis* imide bonds in aqueous solution. Both polymers have essentially the same measured characteristic ratios. The consequences of these observations will be discussed. Despite the fact that they exhibit a positive maximum in their CD the spectra do not represent ordered structures as is demonstrated by the CR's. Certain classes of salts alter the CD spectra in a similar way. ¹H nmr has shown that P(Pro) undergoes an isomerization of some of its imide bonds under these conditions. We have found from ¹³C nmr studies that P(Hyp) under similar conditions also undergoes chain isomerization. The salt induced isomerization is random, rather than block. A comparison between this isomerization and the changes in the CD for the salts studied reveals that there is not a one to one correlation. The energetics for the salt induced isomerization for both polymers will be discussed. Similar spectral results that are obtained with other polypeptides can not be explained on the basis of isomerization.

TU-AM-A6 CONFORMATION OF COPOLYPEPTIDES OF L-LYSINE WITH L-LEUCINE, L-ALANINE, AND L-ORNITHINE IN SODIUM DODECYL SULFATE SOLUTION. K. Shirahama,* K. Ikeda,* and J. T. Yang, CVRI, Univ. California, San Francisco, CA 94143.

The unordered form of (Lys)_n at neutral pH is known to adopt the β -form in NaDodSO₄ solution, but (Orn)_n with one less -CH₂- group in the side chain to become helical. Leu and Ala are helix-formers. We synthesized a series of copolypeptides and measured their circular dichroism (CD) in NaDodSO₄ solution. On a molar (residue) basis, (Lys^x, Leu^y)_n is helical up to about 80% Lys, (Lys^x, Ala^y)_n up to about 75%, and (Lys^x, Orn^y)_n at about one half, above which the β -form dominates. In the transition region based on the x/y ratio, the initial CD of the copolymer in NaDodSO₄ solution indicates a helix, which is then converted to the β -form. The kinetics depends on the nature of the residue, the polymer concentration, and the x/y ratio. The order of helical stability of the 3 residues in the copolymers is: Leu > Ala > Orn. The results may be related to the enhancement of helicity for some proteins in NaDodSO₄ solution, although the surfactant seems to cause no helix-to- β transition of these proteins (Supported by USPHS grants HL-06285 (Program Project) and GM-10880.)

TU-AM-A7 THE BROWNIAN MOTION OF HIGHLY CHARGED POLY (L-LYSINE). S.-C. Lin and J. Michael Schurr, Dept. of Chem., Univ. of Wash., Seattle, WA 98195.

Dynamic light scattering studies of solutions of highly charged polylysine ((Lys), n=955) have revealed some remarkable phenomena at low salt (NaBr) concentrations. In the ordinary range from 1.0 M down to 0.01 M [NaBr] the observed diffusion coefficient D_{app} increased linearly with both [(Lys)_n] and [NaBr]⁻¹ in partial agreement with the simple linearized coupled mode theory developed previously. However, the value of D_{app} extrapolated to zero polyanion concentration (at fixed salt) declined catastrophically below 10⁻² M salt to values well below the hydrodynamic lower limit for a fully extended rod-like chain! This may imply a large contribution of ion-atmosphere or dielectric relaxation to the retarding force on a moving polyanion. A prominent feature of the low-salt behavior is the transition to an extraordinary phase that scatters very little light and exhibits only very slow apparent diffusion with D_{app} ≈ 10⁻⁸ cm²/sec. At the salt concentration where the transition takes place a fast component τ ≈ 10 μ sec is observed in the correlation functions at all angles, which may be a manifestation of a kinetic process involved in the transition.

TU-AM-A8 CALCIUM BINDING AND CALCIFICATION OF ELASTIN REPEAT PEPTIDES, M.M. Long, D.W. Urry, R.S. Rapaka* and W.D. Thompson*, Laboratory of Molecular Biophysics and the Cardiovascular Research and Training Center, Univ. of Alabama in Birmingham, Birmingham, Alabama, 35294

Arterial wall mineralization occurs because of elastin calcium binding and subsequent calcification. The repeat peptides of elastin, VPGVG and VAPGVG, both as monomers (5,6) and as high polymers (5n,6n) interact with divalent cations (Sr,Ca,Mg) selectively over monovalents (Na, K) and compete effectively with water for the divalents. The ratios of water to peptide carbonyls at the midpoint of the water titration of the peptide-ion complex are: 5:215 for Ca, 53 for Mg; 5n:350 for Ca, 97 for Mg; 6:270 for Ca, 66 for Mg; 6n:535 for Ca, 167 for Mg, indicating that the 6n interacts with calcium the best. However calcification studies with bovine serum show that the X-linked 6n calcifies poorly relative to the X-linked 5n, suggesting variability of calcifiability within portions of the elastin molecule. The serum incubation medium also introduced variability for bovine serum supports calcification of X-linked 5n under conditions where human serum does not.

TU-AM-A9 NOE DEMONSTRATION OF HYDROPHOBIC SIDE-CHAIN ASSOCIATION IN REPEAT PEPTIDES OF TROPOLASTIN, M.A. Khaled*, V. Renugopalakrishnan, R.S. Rapaka*, K. Okamoto* and D.W. Urry, Laboratory of Molecular Biophysics, Univ. of Alabama Medical Center, Birmingham, Alabama 35294

On raising the temperature, the polytetrapeptide (-L-Val¹-L-Pro²-Gly³-Gly⁴)_n and polypentapeptide (-L-Val¹-L-Pro²-Gly³-L-Val⁴-Gly⁵)_n of tropoelastin coacervate in aqueous solution. This phenomenon includes the hydrophobic association of side-chains of Val¹ and Pro² residues of the polytetra- and polypentapeptides. An increased nuclear Overhauser enhancement (NOE) of Val¹ γ -CH₃ protons on irradiation of Pro² δ -CH₂ protons on elevating the temperature has been used to show the increased proximity of the side-chains of the Val¹ and Pro² residues. As controls non-coacervatable derivatives with Ala replacing Val¹ were synthesized and found to show the more common situation of decreased NOE with increased temperature. Conformational energy calculations also show that the Val¹ γ -CH₃ - Pro² δ -CH₂ distances, ranging from 2.2 Å to 2.8 Å, fall well within the low energy basin for the preferred conformation. This combined approach thus provides direct evidence of hydrophobic side-chain association in repeat peptides of tropoelastin.

TU-AM-A10 QUANTIZATION OF SOLVENT EFFECT ON ADSORPTION OF POLY- γ -BENZYL-L-GLUTAMATE. C.M. Balik, and A.J. Hopfinger, Case Western Reserve University, Cleveland, Ohio 44106.

The isothermal adsorption of poly- γ -benzyl-L-glutamate (PBLG) onto alkali-halide [100] surfaces has been studied with special consideration given to the role of solvent. The solvent effect was empirically quantized using a two-dimensional (polar/non-polar) solubility parameter. The non-polar component (δ_d) has been correlated with PBLG solubility. The polar component (δ_a) was correlated with the state of aggregation of PBLG in solution, as well as with the adsorption behavior of PBLG onto alkali-halides. PBLG having $M_v \approx 300,000$ was found to be soluble in solvents and solvent mixtures having δ_d in the range 8.0 - 9.3 (cal/cm³)^{1/2}, and simultaneously having δ_a in the range 1.0 - 8.7 (cal/cm³)^{1/2}. Pure solvents with low δ_a values (e.g. $\delta_a \approx 1.0$) allow formation of liquid crystalline phases of PBLG; while PBLG is completely unaggregated in solvents with $\delta_a \geq 5.2$. The amount of adsorption of PBLG onto alkali-halides decreases with increasing δ_a of the solvent.

TU-AM-A11 Conformational Aspects of Synthetic Polypeptides via Excimer Fluorescence. J.T. CHAPIN, S.J. HUANG and E.T. SAMULSKI, University of Connecticut. -- Excimer fluorescence of aromatic chromophores is used to probe the secondary structure of synthetic polypeptides. A series of phenyl alkyl and naphthyl alkyl esters of L-glutamic acid have been polymerized. In the α -helical conformation, a superhelical array of the aromatic side-chains can be constructed on the periphery of the rigid helical core of the polypeptide backbone. The fluorescence studies permit the characterization of the nature of this sidechain secondary structure in terms of interchromophore distances and relative orientations.

ENERGY COUPLING AND MEMBRANES

TU-AM-B1 LIGHT/DARK LABELLING PATTERNS OF CF_0 COMPONENTS. James L. Ellenson, D. J. Pheasant* and R. P. Levine*. The Biological Laboratories, Harvard University, Cambridge, MA 02138.

We have investigated the light/dark labeling pattern of chloroplast thylakoid membranes using the fluorogenic reagent fluorecamine. Membrane polypeptides labeled with fluorecamine are detected by scanning high resolution SDS polyacrylamide gradient slab gels at 470 nm. Three polypeptides show a decrease of labeling intensity when chloroplast membrane are labeled in the light compared to when they are labeled in the dark. The three polypeptides have apparent molecular weights of 32, 18 and 15 kdal, and they may correspond to polypeptides thought to comprise part of the CF_0 membrane sector of the DCCD sensitive ATPase.

The light-induced difference in the level of labeling of these polypeptides is dependent upon the presence of a pH gradient; this difference may arise from conformational changes that occur during the course of proton translocation.

TU-AM-B2 MEGADALTON GLYCOLYTIC ENZYME COMPLEX IN HUMAN RED CELLS. E.T. Fossel and A.K. Solomon, Biophysical Laboratory, Harvard Medical School, Boston, MA 02115.

^{31}P NMR resonance shifts of 2,3-diphosphoglycerate (2,3-DPG) are observed when 2,3-DPG is added to the outside surface of human red cell inside out vesicles (IOVS) in the presence of phosphoglycerate kinase (PGK) and monophosphoglycerate mutase. We have added sequentially the glycolytic enzymes from aldolase to pyruvate kinase and found resonance shifts indicating direct communication between all these enzymes. A multi-enzyme complex of 1 to 2 x 10^6 daltons has been separated from broken red cell ghosts by gel filtration; this complex exhibits aldolase, glyceraldehyde 3-phosphate dehydrogenase, and PGK activity. The glycolytic multi-enzyme complex interacts with the outer face of IOVS prepared from human red cells and the interaction is suppressed by application of 10⁻⁶ M ouabain to the inner face of these vesicles. These studies show that the conformation of the enzymes comprising the megadalton complex in the cell are responsive to the application of ouabain to the outer membrane surface. [Supported by AHA grant-in-aid 76-900 and NIH grant GM 15692]

TU-AM-B3 INHIBITION OF THE PURPLE MEMBRANE PROTON PUMP BY REACTION WITH CARBODIIMIDE. R. Renthal and G. Harris*, Univ. of Texas at San Antonio, San Antonio, Texas 78285

The difference in proton binding to isolated sheets of purple membrane (PM) from *H. halobium* between darkness and continuous illumination (Δh) has been used as a simple measure of proton pump activity. Reaction of PM with 1-ethyl-3(3-dimethylaminopropyl)-carbodiimide (EDC) at 0°, pH 8, for 5 hours slows proton uptake. For both unreacted PM and for PM reacted with EDC in the presence of nucleophile, Δh is less than 30 meq/mol, while for both PM in 3M NaCl and for EDC-PM, Δh = 80 meq/mol (at pH 10 and 3.5 x 10⁴ ergs/cm²/sec of 560 nm light). EDC also slows light-induced proton release at acid pH. The altered properties of EDC-PM are not reversible by mild alkaline or acid hydrolysis, and are not due to intermolecular covalent cross-links. Polyacrylamide gel electrophoresis in dodecyl sulfate shows virtually no bacteriorhodopsin (BR) dimers after reaction with EDC. Dissociation of EDC-PM into BR monomers with 0.4% Triton X-100 gives Δh = 130 meq/mol at pH 9.4, nearly identical to unreacted PM in Triton. Thus, EDC may affect a cooperative interaction between BR monomers by intramolecular crosslinking. (supported by a grant from Research Corporation)

TU-AM-B4 KINETIC PROPERTIES OF THE PHOSPHORYLATED INTERMEDIATE OF Ca^{2+} -DEPENDENT ATPase OF SARCOPLASMIC RETICULUM FORMED IN THE ABSENCE OF ALKALI METAL SALTS. M. Shigekawa*, J.P. Dougherty*, and A.M. Katz, Dept of Medicine, Univ. of Conn. Health Center, Farmington, CT 06032

The phosphoenzyme formed at the steady state in a partially purified ATPase preparation of sarcoplasmic reticulum in high Mg^{2+} (~2 mM) and low Ca^{2+} (~20 μM) and in the absence of added alkali metal salts (EP), was ADP-insensitive. Thus, EP decomposition was not accelerated by added ADP, in contrast to the phosphoenzyme formed in high KCl. Variation of ATP from 2 to 226 μM , and pH from 6.8 to 9.1 in the phosphorylation medium did not allow EP to react with ADP. Hydrolysis of EP was accelerated by $MgATP$, Mg^{2+} , Ca^{2+} or KCl. Stimulation of EP hydrolysis by $MgATP$, Mg^{2+} or Ca^{2+} was similar to that for steady state ATP hydrolysis. However, the KCl-dependence of EP hydrolysis differed significantly from that predicted from the rate of ATP hydrolysis and phosphoenzyme level at the steady state. These findings are consistent with the view that phosphoenzymes formed in the presence and absence of alkali metal salts differ kinetically. (Supported by HL-22135, HL-21812, and Conn. Heart Assoc.)

TU-AM-B5 KINETICS OF ^{28}Mg FLUX INTO RAT LIVER MITOCHONDRIA. Joyce Johnson Diwan and David Aronson*, Biology Department, Rensselaer Polytechnic Institute, Troy, New York 12181

Initial rates of ^{28}Mg flux into isolated rat liver mitochondria have been determined in the presence of the substrate, succinate. Lineweaver-Burk plots show a linear relationship between the reciprocal of the unidirectional Mg^{++} influx rate and $1/(Mg^{++}$ concentration). The apparent K_m for Mg^{++} is about 0.6 mM. A change in external pH from 7 to 8 has little effect on the apparent K_m for Mg^{++} , but the average V_{max} is higher at pH 8. N-ethyl maleimide (NEM) increases the pH-dependence of the V_{max} of Mg^{++} influx. Rates of unidirectional Mg^{++} influx and efflux are decreased when respiration is blocked. Mitochondrial K^+ flux exhibits a comparable energy-dependence, pH-dependence and sensitivity to NEM (Diwan & Tedeschi, FEBS Lett., 60: 176, 1975; Diwan & Lehrer, Membr. Biochem., in press). La^{++} , at concentrations which inhibit Ca^{++} -stimulated respiration, does not affect influx of Mg^{++} or K^+ . However, the K^+ analog, Tl^+ inhibits Mg^{++} influx. Thus similar mechanism(s) appear to mediate mitochondrial Mg^{++} and K^+ fluxes. Supported by NIGMS Grant GM-20726.

TU-AM-B6 FURTHER STUDIES WITH GIANT MITOCHONDRIA USING MICROELECTRODES. Charles L. Bowman*, Bruce L. Maloff and Henry Tedeschi, Dept. of Biological Sciences, The University at Albany, Albany, N.Y. 12222.

New studies have been carried out on the electrical properties of giant mitochondria prepared from the liver of mice fed a diet containing cuprizone. (a) A number of impalements were carried out in the presence and in the absence of valinomycin using microelectrodes filled with 2M NaCl, rather than 2M KCl. The membrane potentials and resistances were approximately the same as those reported previously (Maloff et al, Science, 195, 898 (1977) and Maloff et al in press). Together with previously reported validations these experiments rule out the alternative that the K^+ dependence of the potentials in the presence of valinomycin is an artifact involving the K^+ of the microelectrode. (b) New assays of biochemical viability using myofibrils were developed in which a single mitochondrion is separated out from a suspension by micromanipulation and placed in close proximity to a myofibril. ADP is then released next to the mitochondrion using a micropipette. The assays demonstrate that impaled mitochondria phosphorylate. Aided by grant PCM76-23747 A01 of the NSF.

TU-AM-B7 PROTON STOICHIOMETRY IN MITOCHONDRIAL ELECTRON TRANSPORT AND ATP HYDROLYSIS. A. L. Lehninger, B. Reynafarje*, and A. Alexandre*, Johns Hopkins Univ. School of Medicine, Baltimore, Maryland 21205

With three different methods (anion uptake, steady-state rate, and a modified oxygen pulse procedure), having different types of errors, we have established that the average H^+ /site ratio of mitochondrial electron transport is close to 4.0, with either K^+ + valinomycin or Ca^{2+} as permeant cation to exchange with the ejected H^+ , thus transforming $\Delta\mu_{H^+}$ entirely into ΔpH . The observed H^+ /site ratio was close to 4.0 with 3-site, 2-site, and 1-site substrates. A newly developed steady-state rate method for determination of the H^+ /ATP_{hyd} ratio, with either K^+ or Ca^{2+} as permeant cation, yielded values close to 3.0. Of the 4 H^+ equivalents transported per site, 3 are used to make ATP_{in} from ADP_{in} and P_{in} and the remaining H^+ is used for the transport work. The span succinate + $Fe(CN)_6^{3-}$ shows H^+ /site = 4 and the span $Fe(CN)_6^{3-} \rightarrow O_2$ H^+ /site = 3+. Models to account for the proton stoichiometry have been developed. Supported by NIH (GM05919), NSF (PCM75-21923) and NCI Contract (N01-CP-45610).

TU-AM-B8 RATES OF PARTIAL REACTIONS IN SARCOPLASMIC RETICULUM ATPase. S. Verjovski-Almeida*, M. Kurzmack*, and G. Inesi, Laboratory of Physiology and Biophysics, University of the Pacific, San Francisco, CA 94115.

Forward and reverse time constants for partial reactions of SR ATPase were determined by rapid kinetic methods. Rate constants for phosphoenzyme formation were found to be 85 sec⁻¹ in the presence of ATP, and 21 sec⁻¹ in the presence of ITP. Turnover numbers for Pi production were 5-8 sec⁻¹ with ATP and 2-3 sec⁻¹ with ITP as substrate. In all cases, measurements of Ca^{2+} transport within the first 300 milliseconds were consistent with these time constants, assuming two moles of calcium transport for each enzyme cycle. The rate constant for reversal of the phosphoenzyme formation measured in the presence of ATP was comparable to the forward rate. In addition, the reversal of the Pi production step, namely the formation of phosphoenzyme from Pi, was measured in vesicles that had a Ca^{2+} gradient across the membrane. This time constant is smaller and comparable to the turnover numbers obtained in the forward direction. Supported by NIH and Muscular Dystrophy Association. Dr. Almeida holds a postdoctoral fellowship from MDA.

TU-AM-B9 PROTECTION AND LOCATION OF SH GROUPS IN Ca-Mg ATPase. W. F. Tivol and A. E. Shamoo, University of Rochester School of Med. & Dent., Rochester, N.Y. 14642.

Sarcoplasmic reticulum, Ca-Mg ATPase and specifically cleaved Ca-Mg ATPase were exposed to NEM in the presence and absence of ATP and Ca^{++} . Remaining SH groups were determined by titration with CH_3HgCl . Those groups protected by ATP or Ca^{++} were determined by difference. NEM-modified, specifically cleaved Ca-Mg ATPase was exposed to $CH_3^{203}HgCl$ and autoradiograms were made to determine the locations of the remaining SH groups. Results indicate protection by 5 mM ATP and de-protection by 5 mM Ca^{++} . Ca^{++} de-protection could be explained by a conformational change in Ca-Mg ATPase or by an effect on the membrane. Further experiments are in progress to clarify this point.

*This paper is based on work performed under contract with the U.S. Department of Energy at the University of Rochester Department of Radiation Biology and Biophysics and has been assigned Report No. UR-3490-1284.

NERVES AND AXONS II

TU-AM-C1 LARGER FLUORESCENCE AND BIREFRINGENCE SIGNALS FOR OPTICAL MONITORING OF MEMBRANE POTENTIAL.

A. Grinvald*, K. Kamino*, S. Leshner, L.B. Cohen, C.H. Wang* and A.S. Waggoner, Marine Biological Lab., Woods Hole, Mass. 02543.

In birefringence measurements on squid axons we obtained signals as large as the largest absorption signal by using incident light filters with higher transmittance. Since wavelengths outside the absorption band are measured, dye bleaching and photodynamic damage were eliminated. Two fluorescent dyes, a pentamethine oxonol with [1,3 dibutyl barbituric acid (5)] and [1,(p-sulfonyl)3-methyl, 5-pyrazolone (4)] groups and a quinolinium styryl dye, gave large fractional changes ($1-2 \times 10^{-3}/50$ mv). The photodynamic damage obtained with these dyes was 30-200 times less than that obtained with dye I. We hoped that the reduced photodynamic damage would allow the use of a higher intensity, laser light-source. After using a Pockell's cell to reduce fluctuations in beam intensity, a signal-to-noise ratio of 10 was found with the oxonol dye. Larger signals would be obtained if the spatial inhomogeneity in the laser noise were eliminated. In addition, we found two pairs of dyes with identical chromophores which give large signals but have localized charges of opposite sign.

TU-AM-C2 "RECOGNITION PROTEINS" REGULATING IONIC PERMEABILITY IN NERVE HIGHLY SENSITIVE TO EXTERNAL IONS AROUND RESTING LEVELS. A. Strickholm, Physiol. Sect., Med. Sci. Prog., Indiana Univ., Bloomington, IN 47401

Passive ionic permeabilities of K, Na, and Cl for crayfish giant axons (*Procambarus clarkii*) were determined as a function of external K_0 , Ca_0 , and pH around normal resting values ($K_0=5.4$ mM, $Ca_0=13.5$ mM, pH=7-7.5, $V_m=-86$ mV) (Biophys. J. 19:29). Passive ionic permeabilities were found relatively insensitive to changes in resting membrane potential. Na permeability was maximum for resting nerve and decreased with (+) changes in K_0 and became zero at $K_0=10$ mM. K permeability increases with increasing K_0 with a maximum slope (dP_K/dK_0) at resting values. Cl permeability slowly increases from $K_0=2$ to 6 mM and then rapidly increases. Ca_0 effects were unique in that membrane permeability regulating components have a conformational change around resting Ca_0 levels. At $Ca_0=13.5$ mM, Na and Cl permeabilities are maximum and approach zero with increased or decreased Ca_0 . The results show that passive ionic permeabilities are not constant, are most sensitive to external ion changes at resting levels, and depend on conformational states of membrane protein which regulate ionic permeabilities.

TU-AM-C3 TETANIC HYPERPOLARIZATION OF SINGLE MEDULLATED NERVE FIBERS. G. M. Schoepfle, Department of Physiology and Biophysics, University of Alabama in Birmingham, Birmingham, Alabama 35294

Repetitive stimulation of a single medullated nerve fiber of *Xenopus* yields a succession of postspike voltage-time curves which are nearly coincident prior to time of attainment of a voltage that corresponds to the maximum associated with the normal postspike undershoot. From this time onward the direction of voltage change is frequency dependent. At high rates of stimulation hyperpolarization continues to develop, whereas at lower rates the voltage returns to a low but constant level of hyperpolarization. In any event, the postspike time dependent changes are confined to an interval which does not exceed that of the normal postspike undershoot and subsequent return to a resting level. This tetanic hyperpolarization, attributable to electrogenic sodium pumping, is reversibly depressed by cyanide but is unaffected by ouabain or neomycin. NIH support.

TU-AM-C4 VOLTAGE-CLAMP STUDIES OF CHEMICAL DRIVING FORCES OF Na^+ AND K^+ IONS IN SQUID GIANT AXON. D. C. Chang, Rice University and Baylor College of Medicine, Houston, TX 77001.

A physical model of the nerve axon based on an adsorption concept has been extended to explain ionic currents under voltage-clamp conditions. Unlike the ionic theory which attributes the excitation current solely to a change of membrane permeabilities, it is proposed in this model that attached to the membrane is a layer of axoplasm (axon cortex) which can undergo conformational changes and, hence, can modulate the selectivity for mobile ions. To test these two models, we have used a two-step voltage-clamp method to study the chemical driving force of Na^+ ions and K^+ ions in the squid giant axon. The experimental results showed that the chemical potential of Na^+ ions varied as a function of time during excitation. It changed reversibly as the axon was depolarized and repolarized. These observations appear to agree with the physical model but not with the ionic theory. (Supported by NIH grant GM-20154 and ONR Contract N00014-76-C-0100 and N0014-77-C-0025.)

TU-AM-C5 VOLTAGE CLAMP EXPERIMENTS ON SINGLE MYELINATED MAMMALIAN NERVE FIBERS: A COMPARISON WITH FROG KINETICS. S.Y. Chiu*, R.B. Rogart*, and D. Staggs*, Dept. Pharmac., Yale Univ., New Haven, CT 06510 (Intr. by S. Leshner).

Single myelinated fibers from sciatic nerve of rabbits and frogs were voltage-clamped at 13°C. Resting potential was defined as the potential at which inactivation was 0.75. Nodal ionic currents in rabbit consisted of an inward sodium current superimposed on an outward current which, in contrast to frog, was non-rectifying and was TEA insensitive and hence, appears to be mainly leak rather than potassium current. The sodium current after leak subtraction was well fitted by m^2h kinetics. $h_{\infty}(V)$ for rabbit was S-shaped and was slightly steeper than frog. $\tau_{1h}(V)$ was comparable to frog. $\tau_{1h}(V)$ was 2-3 times faster than frog around -50 mV and was much less voltage dependent. The peak permeability for sodium current was reached at an earlier potential of about 15 mV in the hyperpolarizing direction, with respect to frog. Despite the lack of potassium current in rabbit, the action potential at 22°C repolarizes faster and has a duration half that of frog. This probably reflects the more rapid inactivation of inward sodium currents in rabbit.

Supported by USPHS Grant NS-12327.

TU-AM-C6 INWARD RECTIFICATION IN APLYSIA NEURONS.

Eaton, D. C., Brodwick, M. S., and Ifshin, M. S., (Intr. by F. H. Rudenberq). University of Texas Medical Branch, Galveston, Texas 77550.

Giant neurons of *Aplysia* display inward rectification for potentials more negative than -50 mV. The inward rectification is strongly dependent upon temperature with a Q_{10} greater than 3 in the range 15°C to 25°C. The rectifying conductance depends upon the square root of the external K^+ concentration and does not depend upon internal K^+ in the range 50 mM to 180 mM. Cs^+ and Rb^+ are poor substitutes for K^+ . Low concentrations of Cs^+ (1 mM) added to K^+ solutions, produce time independent blockage of rectification. Similar concentrations of Ba^{++} produce time dependent blockages of rectification. The dose response curve for Ba^{++} blockage suggests that Barium is interacting with three sites. The forward rate constant for Barium interaction is voltage dependent while the off rate constant is voltage independent.

Supported by NIH grant NS-11963.

TU-AM-C7 FREQUENCY ENTRAINMENT OF SQUID AXON MEMBRANE. R. Guttman and L. Feldman*, Brooklyn College of the City University of New York, Brooklyn, N.Y. 11210 and University of Texas Medical Branch, Galveston, Texas 77550.

Frequency and intensity of sinusoidal stimulation of space-clamped squid giant axons were varied and the repetitive response expressed in terms of the ratio (R) of the frequency of spikes to the frequency of spikes plus subthreshold responses. Under steady-state conditions, R never exceeded one (probably because of hyperpolarization by sucrose) but otherwise agreed with (HH) calculations. If the steady-state regions are displayed on a contour plot in which frequency and intensity of stimulation are varied, then narrow intermediate regions between the steady-state regions can be demonstrated where R 's are irrational numbers and no stable periodic patterns nor phase-locking are present. Signals from a small patch of squid axon membrane, stimulated periodically, are periodic and their frequency depends upon the frequency and intensity of the input. This first step in excitation may be a model for what occurs at a pacemaker cell. Aided by NIH grant 5 R01 NS12272.

TU-AM-C8 Effects of a Transient Longitudinal Current Gradient on Action Potential Transport in the Hodgkin-Huxley Axon. Howard E. Brandt, Harry Diamond Laboratories, Adelphi, Md.---Perturbations of the action potential of the Hodgkin-Huxley axon by a transient longitudinal current gradient are calculated. Explicit integration of the forced nonlinear diffusion equation is employed using a space-time grid of $1 \mu s \times 0.5 \text{ mm}$. Transient longitudinal current gradients ranging from -50 to $+50 \mu A/cm$, initiated 1.4 ms following nerve pulse initiation, and lasting 0.1 ms are considered. Transient perturbations, abolition, and effective acceleration of the action potential are calculated at various points along the axon.

TU-AM-C9 CELL SHAPE CAN AFFECT EXCITATION AND PROPAGATION IN NEURONS. R. M. Westerfield and J. W. Moore, Dept. of Physiol., Duke University, Durham, NC 27710, USA. We have examined the separate contributions of membrane characteristics and cell shapes to excitation and propagation of impulses in neurons by experiments and computer simulations.

Squid axons were used as the experimental preparation. An increase in the electrical diameter (a lower longitudinal internal resistance) was achieved by insertion of a low surface resistance axial wire. Computer simulations of the experimental system used the Hodgkin-Huxley equations to describe uniform membrane segments in a set of difference equations describing a cable.

In both experiments and simulations, action potentials in the larger diameter ("soma") region were similar to those seen in motor neurons under antidromic invasion, showing more than one inflection point or peak.

Similar to the lower threshold observed in the axon hillock of neurons, both the current and voltage threshold were lower in the normal squid axon adjacent to that region with the wire. Under certain conditions, impulse initiation occurred in this region when current was injected into the "soma".

TU-AM-C10 Theory for Threshold Excitations in Myelinated Axons. E. MADSEN, Univ. of Wisconsin -- An experiment was reported in 1952 by Hodler, Stämpfli, and Tasaki in which threshold excitations of a single frog's myelinated axon were measured. In this experiment the axon was passed through an aperture in a thin insulating barrier, the whole system being immersed in Ringer's solution; the barrier was at distances x from the nearest excitable node. Rectangular voltage pulses, $v(x, \tau)$, of duration τ were applied across the barrier, and excitation thresholds, $V(x, \tau)$, found. Thus, three variables are involved: V , x , and τ . Two of these are independent. Results are reported only for $\tau \geq 50 \mu\text{sec}$. An empirical relation, called the "Weiss formula", has evolved; viz, $V(x, \tau)/b(x) = 1 + \sigma(x)/\tau$ where $b(x) = 1/b_0 \exp(-a_1 x + a_2 x^2)/\tau^{b_0}$ is called the "chronaxie".

Using recently measured values of the electrical properties for this type of axon, a theoretical expression corresponding to this experiment was developed and evaluated via computer. The results occur in functional forms very similar to those in the experiment but differ in order of magnitude. The ranges of τ and x covered are 10 to 10^{-4} sec , and $.4$ to 1.2 mm . Excellent fitting is obtained using $V(x, \tau)/b(x) = \exp(-(a_1 + a_2 x^2)/\tau^{b_0}) + \sigma(x)/\tau$ where a_0 , a_1 , and a_2 are constants.

TU-AM-C11 EXPO-EXPONENTIAL KINETICS OF NERVE EXCITATION Dexter M. Easton, (Intro. by L. M. Beidler), Department of Biological Science, The Florida State University, Tallahassee, Florida, 32306.

The general function $dy/dx = +yR$ (Eq. 1) describes biological growth or decay, when the rate "constant" R changes exponentially with x , i.e. $R = R_0 \exp + kx$. This expo-exponential expression also models other rate processes. Membrane conductance, $g(t)$ of squid axon under voltage clamp, is an example of a sigmoid rate process. In the Hodgkin-Huxley model, it is constructed by raising to an arbitrary power, a simple exponential decay function. From expo-exponential kinetics, it may be generated in simpler fashion, by integration of Eq. 1, or of the differential equation $dy/dt = yk \ln(y/y_0)$, arising from Eq. 1. The H-H model of the squid axon includes empirical relationships between rate constants and membrane potential, and requires nearly two dozen constants, empirically specified. In contrast, with the assumption of exponential change of rate "constants" with respect to time and membrane potential, about half as many parameters, phenomenologically defined, will suffice (Easton, D. M., *Biophys. J.*, in press) (support in part by Psychobiology Program and Computer Center, FSU).

TU-AM-C12 MEMBRANE NOISE MAY BE ESSENTIAL TO MEMBRANE EXCITABILITY. F. F. Offner, Evanston, Illinois 60201.

The fractional change in conductivity of a channel due to a gate opened by an energy ΔG (units of kT) is less than $1/(1 + \exp(\Delta G))$, due to thermal motion. The energy available for shifting the gates will be increased by the electric field shift on gate opening (or closing) due to ionic redistribution (time constants τ_d and τ_n). The final change in energy is limited by the total (Nernst) membrane potential, rather than the applied step. The Markov process is given by the equations

$$dn/dg = ((1 - \tau_d \exp(-G_c)) \cdot n + \tau_d \exp(g - G_o) \cdot C) / (G_m - g)$$

$$dc/dg = (-\tau_n \exp(-G_c) \cdot n + (\tau_n \exp(g - G_o) - 1) \cdot C) / g$$

n and C are the fractions of the gates open and closed, g the shift in depolarizing energy due to ionic redistribution, G_m its maximum value, and G_o and G_c the activation energies for opening and closing the gates when $g=0$. Solution of the equations shows that gates may be "flipped" by small applied voltages, and that membrane "noise" may play an essential role in membrane function. Calculation of noise spectrum and amplitude should be possible. Supported by USPHS Grant NS08137.

TU-AM-C13 ON THE DIFFERENTIATION OF CHANNEL MODELS BY NOISE ANALYSIS. Yi-der Chen, Laboratory of Molecular Biology, NIH, Bethesda, Maryland 20014

Recently noise measurements in biological systems have attracted considerable attention. A question frequently asked is: How much information on the kinetic properties of the system can one get from noise analysis? In general, if a sufficient number of simultaneous independent measurements (such as conductance, optical absorbance, etc.) are available, the measured noise power spectrum matrix of the system can be used to evaluate the rate parameters of the reactions comprising the kinetic system. On the other hand, even with a limited number of independent measurements (such as conductance fluctuations alone), noise data can still be used to differentiate between rival kinetic models. In this communication we present a simple method to distinguish between an equilibrium system and a nonequilibrium steady-state using the "auto" noise power spectrum and the "cross" time correlation function of the system. Specifically, the "peaking" or the "sharpening" in the auto noise power spectrum is shown to be a useful indicator in identifying a nonequilibrium kinetic mechanism. Applications to nerve axon membranes will be discussed.

TU-AM-C14 EFFECT OF TEMPERATURE ON GATING CURRENTS.

F. Bezanilla and R. E. Taylor, Dept. of Physiology UCLA Los Angeles, CA, NINCDS, Bethesda, MD and MBL, Woods Hole, MA.

The time courses of gating currents, $I_g(t)$, and non-linear charge movement, $q(t) = \int_0^t I_g(z) dz$, were measured in internally perfused, voltage clamped squid axons, during potential steps from a holding potential of -70 mV to values from -130 to +70 mV at temperatures from 30°C to 26°C. The total charge moved in 2.5 msec between saturation regions (e.g., -100 mV to +50 mV) showed an apparent increase of 13%±5% for a 10°C rise in temperature. Time expansion, by an arbitrary factor α , of $q_1(t)$ recorded at high temperature, T_1 , did not superimpose on $q_0(t)$ recorded at low temperature, T_0 . When $T_1 = T_0 + 10^\circ\text{C}$, superposition was fair for short times when α was in the neighborhood of 1.6 and for long times when α was about 2.3. These results suggest that dipoles or charges confined to the membrane move in a small number of discrete steps rather than continuously.

(We thank Drs. C. M. Armstrong and M. Cahalan for providing space and equipment. Supported in part by USPHS Grant No. NS08951.)

MUSCLE PHYSIOLOGY II

TU-AM-C15 WHY AND HOW THE "INDEPENDENCE PRINCIPLE" FAILS. AN ANALYSIS OF AN APLYSIA CHANNEL. J. L. Schwartz, University of Connecticut, Storrs, CT. 06268.

Hodgkin and Huxley's independence principle fails in several ionic channels. It has been assumed that this is due to phenomena with which thermodynamic electrodiffusion theory cannot cope. This assumption is studied in a cholinergic K channel in *Aplysia californica*. The current through the voltage clamped channel at 20mM external K is predicted by the independence principle from currents at 10mM K. Comparison of predicted and measured currents at 20mM K shows the principle to be only approximately correct. Although apparently formulated on other grounds, this principle actually contains the supposition that permeability is independent of permeant ion concentration. Generalized diffusion theory shows this supposition to be usually incorrect. Calculation of this *Aplysia* channel's permeability confirms this prediction experimentally; the permeability is actually weakly dependent on K. The independence principle's erroneous assumption in this regard, demonstrated by diffusion theory, is responsible for its failure. Phenomena beyond the scope of diffusion theory need not be invoked. (Supported in part by PHS NS 08444, EMBO, DGRST in France, and UConn. Res. Found.)

TU-AM-D1 AN INFLEXION ON THE TENSION RESPONSE OF AMPHIBIAN SKELETAL MUSCLE DURING AN IMPOSED LENGTH CHANGE. Bernard H. Bressler, Department of Anatomy, The University of British Columbia, Vancouver, Canada.

Toad (*Bufo bufo*) and frog (*Rana pipiens*) sartorii were given constant velocity releases of varying speed from the plateau of isometric tetani. With relatively slow release (< 100 mm/sec), an inflexion was seen on the tension record. The tension at which this inflexion occurred, expressed as P_i/P_0 , was directly related to the speed of release, approaching 1 during length changes < 2 mm/sec. With considerably faster releases (> 120 mm/sec), the inflexion could not be detected, as the tension response remained linear during approximately the entire length change. The observed shift in slope of the tension response during the slower releases was believed to represent the recovery of the muscle to the T_2 tension level as described by Huxley and Simmons (Nature, 233: 533, 1971).

(Supported by the Medical Research Council of Canada).

TU-AM-C16 RESTING POTENTIALS OF AXON SYSTEMS.

V. S. Vaidyanathan, SUNYAB, Buffalo, New York.

Electric potential difference across membranes are evidently determined by boundary concentrations of ions, fluxes as determined by membrane resistance. Computed potentials from first principles, are shown as -60 mV, for lobster, -43 for crayfish, -77 for *Loligo Pealii* axon systems, the observed values, -75, -87 and -60 respectively. Use of $\Delta\phi$, observed, yield values for a parameter $R = \sum G_j r_0/kT$, 13.9, 0.3, -3.19 m/cm⁴, for lobster, *Loligo Forbesii* and crayfish membranes, when $ZR = \sum G_j R_j = 0$. These results coupled with condition of zero electric current yield fluxes of 10^{-14} mole/cm² sec, with directions not in agreement with that prescribed by concentration difference. Basic equation is $(8\pi kTRd/c) = \phi'(d)^2 - \phi'(0)^2$, distinct from Maxwell's osmotic balance eqn. $\phi'(x) + (4\pi e/c) ZR = (1 + \eta^2 \lambda^2) \phi''(x)$ plus negligible terms. $\phi''(d) = \phi''(0) = 0$, $\lambda^2 = -8.33 \times 10^{-14}$ cm².

TU-AM-D2 BASIS OF EXTRA TENSION FOLLOWING STRETCH OF MUSCLE FIBERS CONTRACTING AT LONG LENGTHS. D.L. Morgan and F.J. Julian, Dept. Muscle Res., Boston Biomed. Res. Inst., Boston, Mass. 02114.

We have been investigating the long lasting extra tension which follows the stretch of a muscle during fixed end contraction at sarcomere lengths beyond the plateau region. In our experiments with single twitch fibers from the anterior tibial muscle of frogs, the extra tension is associated with several other effects likely to provide insight into its causes. The tension during relaxation is increased in a complex manner and the "shoulder," or point of give, often occurs at a later time. Using the spot follower apparatus to monitor the length of a central region, it is seen that the increase in length during the stretch is not uniformly distributed along the fiber, the central region being stretched more than the ends. Furthermore, the "creep" of a contracting fiber, as shown by the spot follower, is sharply reduced by a stretch during contraction. These experiments suggest that the extra tension after stretch and the creep phase of tension rise which is seen during contraction at these long lengths may involve common mechanisms. (Supported by USPHS HL-16606, AHA 77-616 and MDA.)

TU-AM-D3 STIFFNESS MEASUREMENTS ON FROG SKINNED MUSCLE FIBERS AT VARYING INTERFILAMENTARY SEPARATION.

Y.E. Goldman* and R.M. Simmons*, (Intr. by R.E. Forster), Dept. of Physiol., Univ. College London, London, England.

We have previously observed that the ratio of stiffness to active isometric tension in mechanically skinned muscle fibers is about 1/2 that of intact fibers during maximal activation and in rigor. Since the lattice spacing is increased in skinned fibers we have used polyvinylpyrrolidone and bovine serum albumin to restore the original dimensions. A reversible increase in the rapid stiffness was observed with shrinking in the relaxed, maximally activated and rigor states, with only a small decrease in the active isometric tension. The increased stiffness in relaxed fibers is similar to the short range elastic element of resting intact fibers, but is larger in magnitude. It was considerably reduced in the presence of 10mM Mg tripoly phosphate. Stiffness in both the fully activated and rigor states was increased by a factor of about 1.5 at reduced diameter. Data obtained for the rigor state at different sarcomere lengths are consistent with an effect of shrinking on the stiffness of the overlap zone. The results suggest that the stiffness of attached X-bridges in skinned fibers may depend on interfilamentary separation.

TU-AM-D4 INFLUENCE OF IONIC STRENGTH AND SARCOMERE LENGTH UNIFORMITY ON THE FORCE-VELOCITY RELATION IN CALCIUM ACTIVATED MUSCLE FIBERS. R.L. Moss and F.J. Julian Dept. Muscle Res., Boston Biomed. Res. Inst., Boston, 02114

The ionic strength (IS) dependence of the force-velocity (F-V) relation was studied in segments (0.8-1.7 mm) from chemically skinned frog skeletal muscle fibers. The segments were mounted between a force transducer and motor, and were viewed and photographed through a microscope. IS was varied by setting [KCl] to 50, 100 or 140mM. Relaxed segments were transferred to activating solutions of similar IS, at 8°C and pCa 6.32 or 6.09. Steady isometric tension (P_0) developed at about SL 2.3 μ m, and force was stepped to values less than P_0 . Shortening was stopped at SL > 2.05 μ m. Micrographs encompassing end-to-end views of the segment were taken just before and after each measurement. F-V at each pCa was found to be unaltered by changing [KCl] from 100 to 140 mM. Preliminary results at 50 mM have been inconsistent regarding changes in F-V and suggest a possible effect of striation non-uniformity. A consistent finding was that perturbations accelerated deterioration of segment uniformity, indicating again the importance of microscopic observation of skinned preparations. (Supported by USPHS 16606, AHA 77-616 and MDA.)

TU-AM-D5 TWO PROPERTIES ASSOCIATED WITH THE PARTIAL Ca^{2+} ACTIVATION OF SKINNED CARDIAC CELLS. A. Fabiato & F. Fabiato*, Medical Coll. Virginia, Richmond, Va. 23298

The length-active tension diagram of skinned cardiac cells presents a descending limb for sarcomere length (SL) > 2.3 μ m when the cells are either fully activated by Ca^{2+} or partially activated by decreasing [MgATP] or 1/2 in the absence of Ca^{2+} . In contrast, a continued increase of tension is observed during partial activation with Ca^{2+} (pCa 6.50-5.70, Schwartzbach) when SL is increased up to 2.9 μ m. These observations are possible only when the resting tension is low (frog ventricular cells) or artificially decreased by microdissection into 3-5 μ m wide bundles of myofibrils (dog ventricle).

Partial Ca^{2+} activation is also associated with the occurrence of spontaneous myofilament-generated oscillations constituted of a rapid decrease of tension (give) followed by a slow redevelopment of tension (Fed. Proc. 33: 1260, 1974). The rate of tension redevelopment is increased by increasing the [free Ca^{2+}], decreasing [free Mg^{2+}], increasing [MgATP], decreasing [ADP] and increasing temperature, is maximum for an optimal SL of 2.3-2.5 μ m and varies among animal species with both parallel elasticity and intrinsic properties of the myofilaments.

TU-AM-D6 THE INFLUENCE OF SARCOMERE LENGTH ON TENSION DEVELOPMENT IN RAT HEART MUSCLE. H.E.D.J. ter Keurs, R. Bloot*, W.H. Rijnsburger* and M.J. Nagelsmit*, Dept. of Cardiology, University of Leiden, The Netherlands.

Sarcomeres in the central region of rat cardiac trabeculae shorten 8-15% during isometric contractions. If sarcomere length (SL) is kept constant, tension (T) rises rapidly, reaching a maximum 50 msec after onset of contraction, then remains constant during 200 msec and declines gradually. SL-T relations were derived from muscle- and sarcomere isometric contractions at various external calcium concentrations ($[Ca^{++}]_0$). T was zero at SL = 1.54 μ m and maximal at SL = 2.35 μ m at all $[Ca^{++}]_0$. T increased linearly at $[Ca^{++}]_0 = 0.5$ mM, whereas it approached maximal tension exponentially at $[Ca^{++}]_0 = 2.5$ mM. Differences between sarcomere length tension relations and muscle length tension relations are explained by the presence of compliant regions, which are sensitive to calcium, near the clamps holding the specimen. Dependence of the SL-T relation on the external calcium concentration suggests that excitation contraction coupling in cardiac muscle is both determined by inotropic factors and by muscle length.

TU-AM-D7 STRETCH RESPONSES OF MAXIMALLY ACTIVATED SKINNED FIBERS. T. Iwazumi and G.H. Pollack, Univ. of Washington, Seattle, WA 98195

We have developed a method by which mechanically skinned single fibers of frog semitendinosus muscle can be brought to maximal activation without appreciable loss of uniformity of the striation pattern; thus sarcomere lengths during mechanical transients as well as in the steady state could be measured by light diffraction. Fibers under full activation were rapidly stretched by various length increments, and the tension responses were measured. Tension always rose sharply during stretch and decayed slowly to a new steady level. In preliminary experiments we have found that the steady level does not diminish at longer sarcomere lengths despite diminished overlap of thick and thin filaments. Furthermore, for the same amount of stretch the sharp increase of tension grew larger with progressively diminished overlap. Results will be interpreted in terms of various theories of contraction.

Supported by NIH 18676 and AHA 75791

TU-AM-D8 EFFECT OF pH ON OSCILLATORY WORK AND TENSION IN SKINNED RABBIT MUSCLES. M. Kawai & P.W. Brandt, Depts. of Neurol. & Anatomy, Columbia Univ. New York, N.Y. 10032

Tension response to sinusoidal length oscillations (0.25-250 Hz, ± 2 nm per half sarcomere) is studied on maximally activated, chemically skinned rabbit psoas single fiber preparations at (in mM) 2.5 CaATP, 2 MgATP, 5 ATP, 7.5 phosphate, 28 sulfate, 40 propionate, 5 imidazole (all Na salts, pCa 4) at 10°C. 3 rate processes observed for other species (crayfish and frog; Kawai, Brandt and Orentlicher, 1977) are present in all the pH range (6.5-7.5) studied. Oscillatory work (2 to 9 Hz) is minimal at pH 7.5, and it peaks at pH 6.75-7.00. The tension linearly increases with the increment of pH. These profiles of pH dependence are unaltered at higher buffer concentration (50mM imidazole), except that oscillatory work is depressed at low pH range (pH ≤ 7.0). Similar phenomena are observed in the presence of other pH buffers (BES, TES, PIPES, MOPS). Present observations can be interpreted that monobasic form of phosphate facilitates oscillatory work, and that local pH oscillation in myofilament lattice is important for maintained oscillatory work production.

Supported by NSF PCM 00441, NIH NS 11766-04, MDA.

TU-AM-D9 CORRELATION OF STRUCTURE AND FUNCTION IN MAMMALIAN SKELETAL MUSCLE. Roger McCarter,* (Intr. by J. T. Herlihy), University of Texas Health Science Center, San Antonio, Texas 78284

Mechanical properties and ultrastructure of the fast lateral omohyoideus (LOMO) muscle of 18 month old male rats were measured in vitro at 21°C. Measurement of average sarcomere spacing (SS) by optical diffraction methods indicated a non-uniform distribution of sarcomeres, with a 10% variation in SS at muscle lengths less than and greater than the resting length (L_0). Maximum isometric tension was obtained with initial SS of 2.6 - 2.8 μ m in the middle of the muscle. Measurement of dynamic SS changes during tetanic stimulation indicated consistent shortening of sarcomeres in the middle of the muscle by about 9% whereas sarcomeres at the ends of the muscles were stretched. Quick release experiments indicated an average series elasticity of 6% L_0 , consistent with the measured dynamic SS changes. Ultrastructural measurements of fixed tissue indicated SS corresponding to optimal overlap of thick and thin filaments of 2.5 μ m, again consistent with the measured active SS at optimal tension.

TU-AM-D10 TENSION INDEPENDENT HEAT, ACTIVATION AND RELAXATION. L.A. Mulleri & N.R. Alpert, U.Vermont, Burlington

Bundles of 50 to 75 fibers (frog semitendinosus) were stretched to $s=3.7$ μ m at 15°C. Initial heat was measured with a Hill-type thermopile under isometric twitch conditions (1 per min.). Tension independent heat has a latency of 7-8ms, a fast phase (A_f) lasting 14ms, and a slow phase (A_s) lasting about 140ms. At 0°C A_f duration is 360% longer and its rate of rise is 47% lower ($Q_{10}=1.5$). After an absolutely refractory period of 2ms a second shock delivered 3 to 8ms after the first prolongs A_f without increasing its rate of rise. A second A_f of reduced amplitude is evoked with 30ms intervals and a full amplitude A_f is evokable after a 150ms interval. Contraction and relaxation time at $s=2.25$ μ m are 33 and 104ms, respectively. A_s recruitment mirrors these A_f changes except for a continued rise with 8-30ms intervals and 90% recovery at 250ms. In 1mM caffeine Ringer (15°C) rate of rise of A_f is 150% and its amplitude is 120%. In 1mM caffeine plus 0.1mM Zn Ringer there is a further 90% increase in amplitude and a 60% increase in duration of A_f . Hypothesis: A_f comes from diffusion limited ($Q_{10}=1.5$) binding of Ca^{++} to troponin which is not saturated in a twitch at 15°C. A_s comes from the calcium release-uptake system which is 90% recovered 250ms after a stimulus at 15°C. Support: PHS R0117592

TU-AM-D11 EFFECTS OF HALOTHANE ON CAFFEINE-INDUCED TENSION TRANSIENTS IN MECHANICALLY DISRUPTED MYOCARDIAL CELLS. J.Y. Su, and W.G.L. Kerrick, Seattle, Wa. 98195

Effects of halothane on Ca^{2+} release from and uptake by the sarcoplasmic reticulum (SR) in functionally skinned cardiac muscle cells were studied. Papillary muscles from rabbits were homogenized. A small cell bundle was isolated and mounted on a force transducer. The cell bundles were immersed in halothane or control (C) solutions designed to load Ca^{2+} into and release Ca^{2+} (25 mM caffeine) from SR while tensions were monitored. Areas under caffeine-induced tension transients were used as a measure of Ca^{2+} sequestered in SR. Results (percent of C, mean \pm SE (n), * $p < 0.01$ compared to C) are as follows:

[Halothane] (%)	Loading and Release	Loading Only
0.5	82 \pm 8(4)*	-----
1	51 \pm 4(13)*	63 \pm 9(5)*
2	15 \pm 4(11)*	16 \pm 6(4)*
3	3 \pm 2(5)*	5 \pm 2(3)*

5 mM Azide used to block Ca^{2+} uptake by mitochondria had no inhibitory effect. We concluded that halothane may depress cardiac contractility primarily by inhibiting Ca^{2+} uptake by SR. (Supported by NIH-HL120754 & NIAMD17081, a PMA Research Starter Grant; halothane was supplied by Ayerst Laboratories, Inc.).

TU-AM-D12 MODEL CALCULATION OF MUSCLE TENSION AND ATPase ACTIVITY BASED ON BIOCHEMICAL DATA. G.J. Steiger and R.H. Abbott*, Cardiovascular Res. Lab., UCLA, Los Angeles Calif. 90024 and ARC Unit, Dept Zoology, Oxford, England

With the exception of the fastest observed transients, Abbott & Steiger (J Physiol. 226:13, 1977) explained most of the tension response to rapid length changes with a 2-state crossbridge model. A 4-state model proposed by Abbott (In "Insect Flight Muscle", North-Holland, 1977) simulates the ATPase activity and the slower tension transients. In this report the 4-state model calculations have been extended to include the effects of crossbridge movement on rate constants and crossbridge force. As proposed by Abbott (1977), stretch activation is obtained by alteration of the effective actin concentration and calcium activates by speeding up the attachment/detachment equilibrium without changing the equilibrium constant. The slower part of the fast tension recovery (Phase 2) and the delayed tension change (Phase 3) after rapid length changes are explained in essentially the same way as by Abbott & Steiger (1977). The fastest temperature insensitive tension transient (Phase 1) is due to a rapid reversible attachment/detachment equilibrium which does not involve ATP hydrolysis. (Supported by USPHS HL 11351-11).

TU-AM-D13 EQUATORIAL X-RAY INTENSITIES I_{10} AND I_{11} FROM PARTIALLY ACTIVATED MUSCLE. J. E. Hartt, L. C. Yu, and R. J. Podolsky, Laboratory of Physical Biology, NIAMDD, NIH, Bethesda, MD 20014

The equatorial reflections, I_{10} and I_{11} , were studied on isometrically contracting muscle activated by rapidly cooling a Ringer solution containing 1.25-2.0 mM caffeine, which produced forces between 0 and 100% of maximal force P_0 at 2-3°C. The ratio I_{11}/I_{10} was a monotonically increasing function of relative force (P/P_0) (Biophys. J. 17, 171a). It was concluded that the intensity ratio was a measure of cross-bridge number. We have now examined the individual intensities I_{10} and I_{11} , each normalized to the transmitted central peak (C) and to the intensities obtained at rest immediately prior to activation [$(I/C)_{active}/(I/C)_{rest}$]. Both reflections exhibited non-linearity as a function of force: I_{10} decreased quickly as force increased (to approximately 0.5 P_0) and then decreased more gradually. I_{11} increased slowly as force increased (also to about 0.5 P_0) and then increased more quickly. The reciprocal nature of the intensity change at all force levels is evidence that a mass shift from one position to another is associated with an increase in isometric force.

TU-AM-D14 THEORY OF LIGHT DIFFRACTION BY MUSCLE. Y. Yeh, R. J. Baskin, and K. Roos, Depts. of Applied Science and Zoology, University of California, Davis, CA 95616

Theory of diffraction of light by a model 3-dimensional single fiber of muscle at rest is presented. This work was prompted by the lack of agreement between the predicted intensity of first order band as calculated using the 1-dimensional diffraction grating model and some recent experimental results from single fibers. The present model uses for its basis the thick grating diffraction study previously carried out for an ultrasonic wave grating. Besides the usually observed diffraction pattern dependencies on the sarcomere length and the breadth of the incident laser beam, the intensity of the diffraction orders exhibit additional interferometric dependencies characteristic of a thick grating. The envelope function of the first order intensity vs. sarcomere length compares favorably with experimental results. In the limiting case of a grating only one myofibril thick, the results collapse to the result for an one-dimensional grating. Changing of polarizability upon overlap of the thick and thin filaments has been explicitly examined. Extension of this model to dynamic situations is discussed.

TU-AM-D15A PREDICTION OF SOME EFFECTS ON LIGHT DIFFRACTION PATTERNS OF MUSCLES PRODUCED BY AREAS WITH DIFFERENT SARCOMERE LENGTHS. D.L. Morgan, Dept. Muscle Res., Boston Biomed. Res. Inst., Boston, Mass. 02114.

Much use is being made of light diffraction patterns to monitor in fine detail the changes in sarcomere lengths of muscles during contraction. However, a muscle is not an ideal diffraction grating and it is useful to predict the effects of some possible non-idealities. A muscle has been modelled as an ensemble of several ideal gratings representing different areas. The number of sarcomeres in an area was represented by the number of lines in the grating, the sarcomere length by the line spacing, and registration of sarcomeres across the muscle by the relative phase of the light vectors from different gratings. The positions of peaks within the first order line of the resulting diffraction patterns, and the centroid of the entire line were calculated as the above parameters were varied individually and in combination. As a result, doubt is cast on the common assumption that the limits of accuracy in the determination of mean sarcomere lengths are imposed purely by the technical problem of locating the peak or centroid of the diffraction line. (Supported by USPHS HL-16606, AHA 77-616 and MDA.)

BIOLOGICAL STRUCTURES

TU-AM-D16^H AND Mg^{2+} EFFECTS ON SCALLOP SKELETAL AND RABBIT LEFT VENTRICULAR SKINNED FORCE. S.K.B. Donaldson, L. Bolles, M. Farrance, and S. Lucas. Depts. of Physiology/Biophysics & Physiological Nursing and Friday Harbor Laboratory, Univ. of Washington, Seattle, Wash. 98195.

Sarcolemmas of small bundles of scallop striated adductor fibers were chemically disrupted by Brij; cardiac fibers were chemically and mechanically disrupted. Their steady state isometric tension (T) was measured with a photodiode transducer during variations of bathing solution ionic composition. Complete Ca-T relationships were determined at pH 7.0 and 6.5 (imidazole buffer) for 1mM Mg^{2+} and at pH 7.0 for 10mM Mg^{2+} . Every solution contained: 7mM EGTA, 2mM MgATP, 70mM cation (K^+ + Na^+), 15mM Cl^- , 15 units/ml CPK, propionate (temp. = $23 \pm 1^\circ C$ and $\mu = 0.15M$). Cardiac maximum T was depressed by acidosis and unaltered by Mg^{2+} ; that of scallop was unaffected by acidosis and enhanced by Mg^{2+} . Curves of pCa-T showed great depression of Ca^{2+} -sensitivity by acidosis or excess Mg^{2+} that was similar for both fiber types. Scallop curves were much steeper than cardiac at pH 7.0, pMg 3 but decreased to that of cardiac at pH 6.5 and pMg 2.0; cardiac curves did not vary in steepness. These data suggest some nontroponin sites of H^+ and Mg^{2+} action. Supported by NIH grants HL17373, RR00374, HL07090.

TU-AM-E1 SPECIFIC HEAVY METAL LABELING OF SULFUR-CONTAINING tRNAs. D.J. Szalda*, K. Strothkamp*, F. Eckstein*, H. Sternbach*, and S.J. Lippard, Department of Chemistry, Columbia University, New York, N.Y. 10027

Metal attachment to specific sites in naturally occurring and modified tRNAs has been investigated. The 4-thiouridine residue in *E. coli* tRNA^{Val} is the target for the binding of a novel, polymetallic reagent, tetrakis-(acetoxymethylmercuri)methane (TAMM). The metal binding was observed spectrophotometrically to be in a 1:1 ratio with the tRNA, both in the presence and absence of Mg^{2+} . No intermolecular crosslinking occurred. A derivative of TAMM, prepared by adding three equivalents of N,N-di-methyl-2-aminoethanethiolate, also binds to the 4-thiouridine residue of tRNA^{Val} in the absence of Mg^{2+} . The binding is reversed by the addition of 9 mM $MgCl_2$. Sulfur binding sites were introduced into baker's yeast tRNA^{Phe} by replacing the CCA terminus with the identical sequence containing 5'-phosphorothioate linkages. Studies with [³H]chloroterpyridineplatinum(II) using ion exchange chromatography revealed quantitative binding in a 2:1 ratio of Pt:tRNA^{Phe}. We thank the National Cancer Institute for support of this research under Grant CA 15826 and Engelhard Industries for a loan of K_2PtCl_4 .

TU-AM-E2 ENDOR OF HIGH AND LOW SPIN METMYOGLOBIN AND METHEMOGLOBIN DERIVATIVES. C.F. Mulks* and C.P. Scholes, Dept. of Physics, SUNY/Albany, Albany, NY 12222

Hyperfine couplings have been seen from nuclei in the vicinity of heme by ENDOR of frozen solutions at g-values where the magnetic field is along the heme normal.

¹³C Metmyoglobin and Methemoglobin. ¹³C couplings of 28.6 ± 0.15 and 27.3 ± 0.15 MHz were seen from heme-bound ¹³CN (in 90% isotopic enrichment) in sperm whale metmyoglobin and human methemoglobin, respectively.

Nitrogen ENDOR from Azide Derivatives. This has been seen in the 1-6 MHz region. ENDOR from hemoglobin enriched in ¹⁵N-heme indicates that the observed ENDOR is primarily from heme nitrogen. We are presently looking for changes in ENDOR signals concomitant with conformational changes in carp hemoglobins.

Proton ENDOR from Aquo and Fluorometmyoglobins. In aquo metmyoglobin, but not fluoro, the ENDOR from exchangeable protons with hyperfine coupling of 6.1 ± 0.2 MHz has been seen. A simple dipolar coupling between heme iron and heme-bound water protons accounts for such a coupling. Assignments will be given for other exchangeable and non-exchangeable protons.

TU-AM-E3 QUADRUPOLE SPLITTING, OXYGEN GEOMETRY AND ELECTRONIC CONFIGURATION IN MODEL OXYHEME. G. H. Loew, and R. F. Kirchner*. Stanford Univ., Stanford, CA 94305

The electronic structure of model oxyferroporphyrin complexes with N-methylimidazole as an axial ligand have been calculated for twenty-two conformations of the di-oxygen ligands using the iterative extended Hucker method. A bent, end-on dioxygen ligand geometry with low energy off-axis displacements and a low energy barrier to rotation about the Fe-O axis possibly coupled to a large amplitude bending mode of the Fe-O-O bond is favored. The electric field gradient at the iron nucleus observed as quadrupole splitting in Mössbauer resonance was calculated for each dioxygen ligand geometry in six likely electronic ground-state configurations. A paired iron(II)-dioxygen configuration yields the large negative electric field gradient observed for oxyhemoglobin and synthesized model compounds. The observed temperature dependence may be accounted for by rotation about the Fe-O axis which are more hindered in the protein than in the model compound.

TU-AM-E4 THE STRUCTURE OF X-RAY ABSORPTION EDGES: APPLICATION TO BIOINORGANIC COMPOUNDS. S. Doniach, T. Eccles*, K. Hodgson, F. Kutzler*, D. Misemer* & R. Natoli*. Stanford University, California 94305.

Semiempirical numerical fits of data taken at Stanford Synchrotron Radiation Laboratory on a variety of Cu model compounds and on hemocyanin(Hc) allow a classification of features at the K-shell xray absorption edge in terms of bound excitation-like levels, continuum threshold, and resonance peaks in the continuum. The positions and strengths of these features correlate closely with the chemical oxidation state of the Cu ion for model compounds and allow an unambiguous assignment of Cu(I) and Cu(II) to both Cu ions in deoxy Hc and Oxy Hc respectively. The observed binding energies will be correlated with results of calculations using a multiple scattering treatment of the Schrödinger equation for small atomic clusters. Preliminary results show a dependence of binding energy on site symmetry for a cluster of given composition and oxidation state.

++Supported by the National Science Foundation in association with the Stanford Linear Accelerator Center and the U.S. Department of Energy.

+Research partly supported by NSF Grant PCM 78-17105.

TU-AM-E5 STEREOCHEMISTRY OF ANTITUMOR DRUG-NUCLEIC ACID BINDING: STRUCTURE OF ELLIPTICINE-5-IODOCYTIDYL(3'-5') GUANOSINE CRYSTALLINE COMPLEX. S. C. Jain, K. K. Bhandary and H. M. Sobell, Departments of Chemistry and Radiation Biology & Biophysics, University of Rochester, Rochester, N.Y. 14627.

Ellipticine, a plant alkaloid possessing high activity against mouse leukemia L1210, forms a crystalline complex with self complementary dinucleoside monophosphate, 5-iodocytidyl(3'-5')guanosine(iodoCpG). The crystals are monoclinic, space group $P2_1$ with cell dimensions $a=13.88$, $b=19.11$, $c=21.42$ Å and $\beta=105.43^\circ$.

We have solved the three dimensional structure of this complex by Patterson and Fourier techniques and presently it is being refined by Fourier and Least squares methods. The asymmetric unit in the structure consists of two iodoCpG, two ellipticine, 15 water and two methanol molecules, a total of 139 non-hydrogen atoms. The R factor at the present stage of refinement is 0.22. The structure demonstrates ellipticine intercalation into a miniature Watson-Crick type double helix formed by two iodoCpG molecules. As in ethidium-dinucleoside crystalline complexes, a mixed sugar puckering pattern of the type $C3'endo(3'-5')$ $C2'endo$ has been observed. Other details will be presented.

TU-AM-E6 RECONSTRUCTION OF GLUTAMINE SYNTHETASE FROM ELECTRON MICROGRAPHS BY COMPUTER AVERAGING. J. Frank*, W. Goldfarb, M. Kessel*, D. Eisenberg and T. S. Baker, Div. of Labs. & Res., NYS Dept. of Health, Albany, NY 12201 and Molecular Biology Institute, UCLA, Los Angeles, CA 90024

The structure of glutamine synthetase molecules from the bacteria *B. caldolyticus* and *E. coli* has been studied by using electron microscopy combined with computer averaging for low ($1e/\text{Å}^2$) and high ($200 e/\text{Å}^2$) electron dose and various conditions of stain. The particles which are dodecamers are found to adhere predominantly to the carbon support film by their flat faces, appearing as rosettes with six-fold symmetry. Groups of 64 individual particles are selected from micrographs and scanned into 70 by 70 arrays using the Perkin Elmer flatbed microdensitometer. For each group, an average particle is computed after orientations and translations are determined using correlation functions $/1,2/$.

/1/ Langer, R., Frank, J., Feltykowski, A., and Hoppe, W. Ber. Bunsenges. Phys. Chem. **74**, 1120 (1970).

/2/ Saxton, W. O. and Frank, J., Ultramicroscopy **2**, 219 (1977).

TU-AM-E7 DYNAMIC LASER SCATTERING STUDIES OF HUMAN AND BOVINE CERVICAL MUCUS. W.I. Lee, P. Verdugo and R.J. Blandau*. Dept. of Biological Structure and Center for Bioengineering, SM-20, University of Washington, Seattle WA, 98195.

We have proposed that the molecular arrangement of cow estrous cervical mucus and human midcycle cervical mucus is composed of an ensemble of entangled random-coiled macromolecules instead of a fibrillar crosslinked network (Bull. Amer. Phys. Soc., **22**:397, 1977). This report describes the studies of these macromolecules by laser light-scattering. Upon dissolving in a large amount of physiological saline by gentle and slow agitation with stirrer, macromolecules of bovine cervical mucus have a value of diffusion coefficient higher than that of macromolecules of human cervical mucus ($D_{\text{bovine}} = 0.56 \times 10^{-8} \text{ cm}^2/\text{s}$; $D_{\text{human}} = 0.38 \times 10^{-8} \text{ cm}^2/\text{s}$). In vitro observations of the migration of human spermatozoa in bovine and human cervical mucus suggest that the size of cervical macromolecules has definite effect on the flagellation and penetrability of spermatozoa.

This work is supported by NIH Grant HD-03752 and Contract HD-42826.

TU-AM-E8 THERMODYNAMICS OF GLYCOSYL ISOMERIZATION IN CYCLIC AMP. F. Jordan, P. R. Hemmes*, and L. Oppenheimer*, Chemistry Department, Rutgers University, Newark, New Jersey 07102

Ultrasonic relaxation measurements were performed on adenosine-3',5'-cyclicmonophosphate in water and in 7 M urea. The relaxation was attributed to the glycosyl C-N conformational equilibrium. The apparent thermodynamics and kinetic properties, calculated from the relaxation data, were different in 7 M urea than in water. A detailed analysis of the results showed that the glycosyl conformational and stacking equilibria are strongly coupled but in 7 M urea the effects of base stacking no longer intervene. The magnitude and sign of the thermodynamic quantities calculated in 7 M urea can be rationalized by a solvation model in which the ribosephosphate moiety is less solvated in the syn than in the anti conformation. The conformational equilibrium constant is ca. 4 near ambient temperatures.

TU-AM-E9 TWO DIMENSIONAL STRUCTURE ANALYSIS OF Gp32*I BY ELECTRON MICROSCOPY. Wah Chiu,* and Junko Hosoda,* (Intr. by Thomas Hayes), Donner Laboratory, University of California, Berkeley, CA 94720

Gp32*I with molecular weight of 27,000 was obtained by proteolytic removal of 8000-dalton peptide from COOH-terminal of the DNA-binding protein coded by gene 32 of bacteriophage T4. It is a stronger helix-destabilizer than the gene 32 protein. A thin crystal of gp32*I has been formed at a low salt condition with an area larger than $1\mu^2$ and a thickness between 85 and 400 Å. Low dose electron microscopy is used to study the structure of this crystal, as it is too small for conventional X-ray analysis. The structural amplitudes in projection have been obtained to 3.7 Å from the electron diffraction patterns of both unstained and stained protein crystal embedded in glucose. The space group is determined to be orthorhombic with $a = 63$ Å, and $b = 47$ Å. The structural phases of the crystal are derived directly from the electron images, which are presently recorded to ~8 Å resolution. (This work is supported by U.S. Public Health Service Grants GM-23323 for W.C., GM-16841 and 23562 for J.H. We thank Prof. R.M. Glaeser for his support.)

TU-AM-E10 STRUCTURAL STUDIES ON A LIPID-CONTAINING PHAGE OF E. COLI. S. Cadden*, C. Brown*, D. Auperin*, and J. Sands, Lehigh University, Bethlehem, Pa. 18015.

Bacteriophage PR4 contains lipid and can replicate in *E. coli* strains that carry an appropriate R plasmid. The genome of PR4 is approximately 8×10^6 daltons of ds DNA. Phospholipid accounts for about 10% of the weight of the phage, with (negatively charged) phosphatidylglycerol being the most prevalent lipid. The six structural proteins that are detectable in the virion have a total molecular weight of 226,000 daltons, accounting for ~65% of the classical coding capacity of the genome. The phage is readily inactivated and partially disassembled by incubation at 55°C. Heat-resistant phage mutants can be isolated that are not inactivated at this temperature. The lipid composition of one of these mutants is indistinguishable from the wild-type phage, but the protein composition of the mutant is detectably different. PR4 is readily inactivated and disassembled by incubation in .5% SDS or 2.5 M urea solutions. Molecular composition analyses of the viral fragments produced by these treatments form the foundation for future genetic studies on the molecular interactions involved in the replication of this lipid-containing virus. (Supported by NSF grant PCM 76-12546.)

TU-AM-E11 ELECTRON MICROSCOPY OF MYCOPLASMAVIRUS SINGLE AND DOUBLE STRANDED DNA'S. J. Maniloff, J.A. Nowak,* and J. Das, * Depts. of Microbiology and of Radiation Biology and Biophysics, Univ. of Rochester, Rochester, N.Y. 14642

Mycoplasmas, the smallest free living cells, can be infected by two groups of nonlytic viruses. Group 1 viruses are naked bullet shaped particles, about 14 nm by 80 nm, having helical symmetry. Group 2 viruses are roughly spherical enveloped particles, about 80 nm in diameter. The Group 1 viral genome is circular single stranded DNA. We have determined the genome size by measurement of the double stranded viral RF DNA by electron microscopy. The contour length is 0.71 that of coliphage M13 RF DNA used to calibrate these measurements. Therefore, the Group 1 single stranded DNA contains about 4520 nucleotides, corresponding to a molecular weight about 1.5×10^6 . Similar electron microscopic studies have shown that the Group 2 viral genome is circular double stranded DNA with a negative superhelical conformation. The contour length is 1.86 that of the M13 RF DNA. Therefore, the Group 2 double stranded DNA contains about 11,850 base pairs, corresponding to a molecular weight of 7.8×10^6 .

TU-AM-E12 THE STRUCTURE OF FILAMENTOUS BACTERIOPHAGE PF1. Lee Makowski* and D.L.D. Caspar (Intr. by S. Margossian), Rosenstiel Basic Medical Sciences Research Center, Brandeis University, Waltham, Mass. 02154

X-ray diffraction patterns have been obtained from oriented fibers of filamentous bacteriophage Pf1. X-ray intensities have been measured to 7 Å spacing by angular deconvolution to separate overlapping layer lines. Analysis of the packing density in the fibers and the semi-crystalline sampling on the equator and third layer line shows that there are 27 subunits in the 75 Å repeating unit. The equatorial diffraction data has been used to calculate the cylindrically averaged electron density distribution of the virus. This shows that the coat protein that envelops the DNA at the center of the virus is arranged in a protein 'bilayer'. This bilayer is made up of two layers of α -helix; one centered at 15 Å radius and the other at 25 Å radius. The electron density half-way between these two peaks is very low, about that of solvent, suggesting that many of the hydrophobic residues from the two layers of α -helix extend into this region. The coat protein is made up mainly of two α -helices, one in the inner and one in the outer layer, with a short length of non-helical peptide between them.

TU-AM-E13 LENGTH REGULATION OF T4 PHAGE TAIL TUBES. Terry Wagenknecht* and Victor A. Bloomfield, Dept. of Biochemistry, U. of Minn., St. Paul, MN 55108.

T4 phage tails are of remarkably constant length: about 1000 Å, with 144 copies of gp19 tail tube protein, surrounded by 144 copies of gp18 tail sheath protein, polymerized on a hexagonal baseplate. The length is determined solely by the baseplate and tube, but the mechanism of regulation is unknown. We used electron microscopy to study the effect of various treatments on the *in vitro* polymerization of purified gp19 onto purified baseplates. When gp19 and baseplates are combined over a wide range of initial concentration ratios, the most probable tube length is about 1000 Å. Longer tubes are observed if polymerization is allowed to proceed for longer than one hour, or if gp19 is present in great excess. Shorter than normal tubes are produced if baseplates are incubated with high concentrations (~1 mg/ml) of RNase at low ionic strength, which also eliminates the activity of the baseplates. These effects may be due to an unidentified protease contaminant, since they are abolished by phenylmethyl sulfonyl fluoride. SDS gel electrophoresis of RNase-treated baseplates shows that baseplate proteins, gp48 and gp54, have been removed. These may therefore be responsible for the regulation of tube length.

TU-AM-E14 SEDIMENTATION ANALYSIS OF SPO2c1 DNA. R. H. Pezzell, J. G. Freeman*, and L. L. Larcom, Depts. of Physics and Microbiology, Clemson University, Clemson, S. C. 29631

The Schumacher-Schachman technique of analytical centrifugation has been used to study DNA extracted from the *B. subtilis* phage SPO2c1, and the results have been compared with those obtained by electron microscopy. Eco RI digestion of SPO2c1 DNA yielded a mixture of fragments which could be analyzed using this technique of sedimentation analysis. Because the technique yields both number - and weight - average molecular weights, it would prove useful in studies requiring determination of the number of nicks in a double-stranded nucleic acid. The results obtained using SPO2c1 DNA indicate that for this virus the clear plaque mutation probably results from a deletion of genetic material.

TU-AM-E1 KINETICS OF VIRUS-CELL INTERACTIONS. M. Wong, M. E. Bayer, S. Litwin, and W. Ruppel, Institute for Cancer Research, Fox Chase, Philadelphia, PA.

We present a model of bacteriophage adsorption in which the phage is assumed to be in one of three states: in solution, at the cell surface, and over a DNA-injection site. The concentration of phage at the cell surface is assumed proportional to the phage arrival rate. Two possible mechanisms are evaluated as means for the phage to arrive at an injection site after having first collided with the cell surface. These are: a) diffusing in the vicinity of the cell surface while making multiple collisions with it, and b) diffusing 2-dimensionally on the cell surface. We evaluated the effect of many cells on the time taken to achieve first cell contact by Monte Carlo methods. Our model will be compared with experimental data.

TU-AM-F2 A THEORETICAL ANALYSIS OF THE RELATION BETWEEN CARDIAC ELECTRIC AND MAGNETIC FIELDS.⁺ J. P. Wikswo, Jr., Vanderbilt University, Nashville, TN 37235

The electric and magnetic fields of the heart are recorded as the electrocardiogram (ECG) and the magneto-cardiogram (MCG). For an unbounded homogeneous conductor in the quasi-static limit, the two fields could have independent sources¹, but conductivity inhomogeneities will partially couple the fields². If cardiac depolarization is represented by a moving, uniform double-layer, then both fields are determined by the configuration of the rim², but with differing spatial sensitivities. Electric and magnetic dipole equivalent sources, termed the electric and magnetic heart vectors (EHV and MHV)³, were used to quantify the ECG-MCG relationship. For a spherical conductor containing a uniform double-layer with a circular opening, an analytic expression relating the EHV and the MHV shows that a combined EHV-MHV measurement contains more information about the cardiac current source than either measurement alone.

⁺Supported in part by NSF/RANN Grant APR72-03447 and by a Bay Area Heart Research Committee Fellowship.

1. Grynspan, F., Ph.D. Diss., Univ. of Penn. (1971).
2. Rush, S., IEEE Trans. BME-22, 157 (1975).
3. Baule, G. and McFee, R., Am. Heart J. 79, 228 (1970).

THEORETICAL BIOLOGY II

TU-AM-F3 COOPERATIVE DYNAMICS, Okan Gurel, IBM Corporation, 1133 Westchester Avenue, White Plains, N. Y. 10604

Experiments show that biological systems possess a dynamics exhibiting multiple critical solutions either singular points[1], or periodic solutions[2], or both. Their variations, such as the results of peeling[3], indicate their autonomous as well as adaptive behavior under internal or external influences. Internal influences stem from changes of "parameters" while most of the external influences are artificial to systems and act as "forcing" terms. These changes may lead to "pathological" cases, and may also correspond to "normal" cases. A significant theoretical observation is the variations resulting from peeling of not a single singular solution [3], but multiple solutions collectively. This is "cooperative peeling"[4]. Any system with interacting multiple solutions at various levels from biomolecular to celestial would form an example of the phenomenon of cooperative peeling.

- [1] O. Gurel, Collective Phenome. 1(1972)1-4.
- [2] O. Gurel, International J. Neuroscience 5(1973)281
- [3] O. Gurel, Collective Phenomena 2(1975)89-97.
- [4] O. Gurel, Preprint (1977).

TU-AM-F1 DIFFUSION COEFFICIENTS AND FRICTIONAL RESISTANCE COEFFICIENTS FOR MACROMOLECULES POSSESSING A HINGE.

S. C. Harvey, Biophysics Section, Dept. of Biomathematics University of Alabama in Birmingham, Birmingham, AL 35294

The Brownian motion of a particle consisting of two rigid subunits connected by a hinge has been examined. The generalization of Stokes's law requires the introduction of the 7 x 7 frictional resistance tensor, \mathbf{R} , which accounts for the coupling between the various modes of motion. The dimensionality results from the seven degrees of freedom (three each for translation and rotation and one for bending). The corresponding diffusion tensor is derived and is analogous to Einstein's equation

$$\mathbf{D} = \frac{kT}{\eta} \mathbf{R}^{-1}$$

where \mathbf{R}^{-1} is the inverse of \mathbf{R} and the other symbols have their usual meanings. The derivation will be described, and the implications of the results for the interpretation of experimental measurements of transport properties of macromolecules will be discussed.

TU-AM-F4 The Two Component Specific Site Ising Model: A Theory for Cooperative Phenomena in Enzymes and Muscle.

JOHN S. SHINER, Medical College of Va., Richmond, Va. and R. JOHN SOLARO, Univ. of Cincinnati, Cinti., Oh.-- The quasi-chemical approximation is used to derive the thermodynamic relations for a lattice of two species of sites with nearest neighbor interactions between both like and unlike sites. Each species of site binds a different species of ligand and only that species; hence the term "specific site". The results may be applicable, for example, to enzymes with large numbers of sites for both substrate and modifier, and to the Ca^{2+} activation of mammalian skeletal muscle if the thin filament is pictured as a lattice of Ca^{2+} binding sites and sites that react with myosin. Of particular interest are the adsorption isotherms when the activity of one species of ligand is constant. In general, the "cooperativities" of the two isotherms depend on the value of the constant activity, and that of one isotherm differs from that of the other. Phase transitions or hysteresis may also be predicted. The theory is easily generalized to n components.

TU-AM-F5 EFFECT OF FLUCTUATIONS ON OSCILLATOR FREQUENCY. V. T. Kurtz and R. A. Spangler, Department of Biophysical Sciences, SUNY at Buffalo, Amherst, NY 14226

The study of limit cycle behavior in chemical reaction systems is considered to be important in the understanding of biological oscillations. Since biological systems are characteristically small, it is necessary to study the effect of fluctuations, inherent in chemical reactions, upon limit cycle behavior. Specifically, we have investigated the effect of fluctuations upon the frequency of the oscillation. To model the effect of fluctuations, the reaction system is considered to be a discrete, Markovian, stochastic process in continuous time. Using the Brusselator as a model reaction scheme, the stochastic process was simulated on a computer. The autocovariance matrix, a measure of the variability of the frequency of the stochastic oscillator, was calculated from the simulation. Using parameter sets for which the kinetic equations exhibit limit cycle solutions, we find that the frequency dispersion is a complex function of the system size, the magnitude of the oscillation, and the degree of the nonlinearities. Thus fluctuations may have an effect upon the maintenance of periodicity in biological oscillations.

TU-AM-F6 CONED MULTINEPHRON KIDNEY MODEL. R. Mejia* and J. L. Stephenson. NIH, Bethesda, Maryland 20014

A model of solute and water movement in the mammalian kidney [1] has been extended to include a distribution of cortical and juxtamedullary nephrons that reach to varying depths of the renal medulla. Given the concentration of solute in arterial blood, arterial and venous pressure, and bladder pressure, the time dependent equations for exchange of water and solutes through an interstitial space are solved to obtain the volume flow, hydrostatic pressure and solute concentrations along the length of each nephron and in the interstitium. A multi-solute central core model [2] has also been extended to include nephron coning. As before, it serves to establish limits for medullary concentration. The system of nonlinear equations describing each model is partitioned using the connectivity of the model [3] and is solved using a modified Newton-Raphson method. In both models the ratio of short to long nephrons is a significant parameter. For example, a 9:1 ratio has been found to be optimal for a concentrating kidney with passive salt transport in the inner medulla. References: [1] Stephenson, J.L., et al (1976), PNAS 73, 252-256. [2] Stephenson, J.L. (1973) Biophys. J. 13, 512-543. [3] Mejia, R., et al (1977), J. Comp. Phys. 23, 53-62.

TU-AM-F7 MICROCALORIMETRIC STUDIES OF GERMAN COCKROACH ACTIVITY RHYTHMS. B. R. Wilson*, L. Hagmann*, S. K. Chattopadhyay, and H. D. Brown. N.J.A.E.S., Rutgers University, New Brunswick, New Jersey 08903.

The German cockroach, *Blattella germanica* has been the subject of investigations using a Calvet-type microcalorimeter. Thermograms of male roaches show distinct activity rhythm patterns observed as heat changes resulting from biochemical and physiological activities. There are two kinds of rhythms, one free running and the other entrained. The roach is a nocturnal insect and generally activity conforms to a dark (active) cycle and a light (inactive) cycle. Rhythms can be entrained in the laboratory following 2 days exposure to 12 hours of light followed by 12 hours of darkness. Measurements have been made at 10, 20, and 30°C with peak frequency and magnitude approximated on an hourly basis. Thermograms have been interpreted using computer-assisted correlations. Optimal design characteristics of a conduction-type calorimeter for such biological measurements have been modeled (NIH GM22679; Hatch NJ00915; Hatch NJ00410).

TU-AM-F8 NEUTRALIZATION AND PROTECTION BIOASSAYS FOR FOOT-AND-MOUTH DISEASE VIRUS. R. Trautman, and C. E. Bennett,* Plum Island Animal Disease Center, Greenport New York 11944

The in vivo protection and the in vitro neutralization tests in suckling mice are shown to be equivalent measures of antibody concentration. Parameters of the assays deduced are: The linear portion of the virus endpoint vs. serum endpoint function for both assays had unit slope for bovine IgM and 2-3 for IgG antibodies. The higher serum concentration required in the mouse protection test for equivalent results to the neutralization test was accounted for mainly by the simple dilution of serum by the mouse. The period between administering the serum and the virus influences the mouse protection test adversely if less than about 6 h, but had no subsequent influence for up to 120 h.

TU-AM-F9 Non-Empirical MODPOT/VRDDO Quantum Chemical Calculations on Drugs and Biomolecules. J.J. KAUFMAN, H. J.T. PRESTON and H.E. POPKIE, JHU Sch. of Med.** Quantum chemical calculations have been run on a variety of drugs and biomolecules with our recently developed MODPOT/VRDDO procedure. This incorporates two desirable options into ab-initio programs: ab-initio effective core model potentials which enable one to treat only the valence electrons explicitly and a charge conserving integral prescreening approximation (VRDDO - variable retention of diatomic differential overlap) especially effective for spatially extended molecules. The results agree to within 0.001-0.002 a.u. with those from completely ab-initio calculations but run from five times faster for one ring systems to better than an order of magnitude for large systems. Results will be presented for the bases of nucleic acids, normal neurotransmitters and their metabolites, carcinogens and their metabolites and drugs.

**Supported in part by NINCDS Contract NO1-NS-5-2320 and in part by NCI Contract NO1-CP-75929

TU-AM-F10 THE INTEGRAL SPECTRUM: FURTHER THEORETICAL AND STATISTICAL CONSIDERATIONS. B.A. Sokol and L.J. DeFelice, Ophthalmology Dept., University of Texas Health Sciences Center, Dallas, Tx. and Anatomy Dept., Emory University, Atlanta, Ga.

Previously a new form of power spectral analysis for noise signals, the integral spectrum I was introduced (Biophys. J. 16:827,1976). In this paper I is shown to be equivalent to the spectral density S; no loss of information occurs, Ss for common noise types are obtained from corresponding Is, assuming infinite data. For finite time length noise data, the mean normalized error of an I point is less than that of a corresponding S point. It is therefore advantageous to use integral spectra in curve fitting routines. The errors of neighboring I points are correlated. This correlation may be expressed as a moving average series. Using the central limit theorem for such a series and the sums of squared residuals from least squares computations a method is presented whereby integral spectra may be used in model discrimination. Computer simulated squid giant axon noise spectra are used to illustrate the method.

Supported in part by NIH GM05278

TU-AM-F11 SCINTILLATION-PROXIMITY ASSAY OF PARTICULATE BINDING PROPERTIES. Hiram E. Hart and Elaine Greenwald* Dept. of Physics, CCNY, New York 10031 and Montefiore Med. Ctr., Bronx, 10467.

A general 6-component method of measuring the statistical distribution of the separation of element pairs will be described. The concept has been applied by employing two different classes of particles in a modification of the usual latex fixation test: a) Tritiated particles (LH) and b) Scintillant particles (L*). Standard liquid scintillation counting equipment was then used to detect the formation of (LH)·(L*) dimers and higher order aggregates. Measurement of antibody, antigen and general serum concentrations has been carried out rather readily, in some systems at concentrations of several picograms/ml. Results will be reported and the possible significance of redundant binding discussed.

TU-AM-F12 THE VECTORIAL GIBBS-DUHEM RELATION.

David B. Shear, Dept. of Biochemistry, Univ. of Missouri, Columbia, Missouri 65201

The Gibbs-Duhem relation expresses a constraint among the variations in the intensive thermodynamic variables that characterize a system, such as temperature, pressure and the chemical potentials of the component species. The usual derivation is based on Euler's theorem on homogeneous functions of the first order as applied to the energy of a system. The relation is often written for the special case of constant temperature and pressure, giving a relation among the variations in the chemical potentials. However, pressure constancy is not a good approximation due to gravity, osmotic effects, etc. Expressions for the chemical potentials may be derived using statistical mechanics and a constant volume lattice model for a liquid. At constant temperature one may then show a relation among the gradients of pressure, gravitational and electrostatic potential, and the chemical potentials of the component species. At any point where there is electromechanical equilibrium, the initial terms independently vanish leaving a relation among the gradients of the chemical potentials alone.

TU-AM-F13 A MATHEMATICAL MODEL FOR MEMBRANE TRANSPORT OF AMINO ACID AND NA IN AND OUT OF VESICLES. A. Babcock,* T. Garvey,* and M. Berman, NIH, Bethesda, Maryland 20014

The model proposed includes an amino acid carrier mechanism capable of Na⁺ cotransport and a passive diffusion component for Na⁺. Analysis of AIB (α-aminoisobutyric acid) uptake kinetics into membrane vesicles prepared from SV3T3 (Simian Virus 40-transformed Balb/c3T3 cells) with varied initial intra- and extra-vesicular concentrations of Na⁺ was carried out. AIB and Na⁺ dissociation constants determined by the model are about 15mM each, which are consistent with parameter values previously reported. A similar analysis of AIB uptake kinetics in vesicles prepared from the parent line, which do not display a prominent overshoot, shows a significantly lower affinity for Na. The change in affinity for Na fully accounts for overshoot observed for intravesicular AIB concentration in vesicles derived from the virally transformed cell line. This suggests that an increase in membrane affinity for Na⁺ may account for the increased amino acid metabolic activity found in SV3T3 cells. The model may provide a useful tool for identifying parameters responsible for differences between malignant and normal cells.

TU-AM-F14 PROTON INVENTORY OF TRANSITION STATE FOR IONIC MIGRATION OF HYDRONIUM ION. Julio F. Mata-Segreda, (Intr. by Carlos de Céspedes). Department of Biochemistry, University of Costa Rica, Ciudad Universitaria "Rodrigo Facio", San José, COSTA RICA.

The proton inventory method was used in the study of the mechanism of ionic migration of hydronium ion. The kinetic parameter used was the equivalent conductance of mixtures of LC1 (L is H or D; D atom fraction n). The conductance of I₃O⁺ at 298 K can be described by the equation:

$$\lambda_n = \lambda_0 (1-n+\phi n)^3 / (1-n+\lambda n)^3$$

where ϕ is the isotopic fractionation factor for a hydrogenic site in the transition state $\phi=0.59 \pm 0.03$, and λ is the fractionation factor of hydronium ion, $\lambda = 0.69$.

The result indicates that three transition state protons and three reactant-state protons contribute to the overall isotope effect. This result favours a hydrodynamic mechanism rather than the classical Grotthuss mechanism.

DNA SYNTHESIS AND REGULATION

TU-AM-G1 DNA MATURATION IN SYNCHRONIZED CHINESE HAMSTER CELLS. M. P. Hagan* and M. M. Elkind, Argonne National Laboratory, Argonne, Illinois 60439.

The elongation of pulse-labeled DNA was followed in synchronized V79 Chinese hamster cells. To observe the elongation, cells were pulse labeled with ³H-thymidine in early S-phase. For approximately 90 min after labeling, the modal molecular weight increased continuously to $\sim 2 \times 10^8$ daltons and remained approximately constant for the following 60 min. Subsequently, a bimodal distribution of molecular weights appeared with a slower sedimenting peak at $\sim 2 \times 10^8$ daltons (97 S) and a rapidly sedimenting peak at ~ 245 S. The area under the 245 S peak increased from 100 to 200 min after labeling while the more slowly sedimenting peak decreased in area. During this period the slower sedimenting peak increased in modal molecular weight to $4-6 \times 10^8$ daltons. Additionally, template DNA, isolated in early to mid S-phase as $4-6 \times 10^8$ dalton species, was observed to give rise discontinuously to a ~ 245 S species of DNA in late S-phase. These data indicate that the DNA synthesized in early S-phase is organized into clusters of replicons which are themselves joined in late S-phase. (Work was supported by the U.S. Dept. of Energy and the U.S. Dept. of the Army.)

TU-AM-G2 EFFECTS OF ETHIDIUM BROMIDE ON DNA SYNTHESIS IN PERMEABLE CHO CELLS. M. Mattern and R. Painter, Laboratory of Radiobiology, University of California, San Francisco, San Francisco, California 94143

CHO cells were made permeable by treatment with 1 percent Tween 80- 0.25 M sucrose and deoxynucleoside triphosphates were incorporated into DNA that was the product of semiconservative replication. The effects of ethidium bromide, which relaxes supercoiling, upon ^3H -dTMP incorporation and upon the size distribution of nascent DNA were studied. Lower concentrations of ethidium bromide stimulated incorporation, whereas higher concentrations were inhibitory. The dependence of ^3H -dTMP incorporation upon ethidium bromide concentration was similar to that of the amount of relaxation of supercoiling. At a concentration of $\sim 2 \mu\text{g/ml}$ of ethidium bromide, when chromosomes are supercoiled least, the amount of ^3H -dTMP incorporation was maximal. A larger fraction of small DNA fragments (12-20S) were synthesized in the presence of ethidium bromide, suggesting that spurious initiations were caused by the relaxation of parts of replicons. The rate of normal DNA synthesis appears to be governed in part by the maintenance and programmed relaxation of supercoiled DNA.

TU-AM-G3 COUPLING OF EXCISION REPAIR TO INHIBITION OF DNA REPLICATION IN NORMAL AND XERODERMA PIGMENTOSUM (XP) HUMAN CELLS, Sang D. Park* and James E. Cleaver, Laboratory of Radiobiology, University of California, San Francisco, California 94143

UV irradiation of normal and XP cells elicits at least three phenomena: 1) rate of DNA synthesis per cell is depressed and recovers. 2) the molecular weight (MW) of newly synthesized DNA drops to a minimum soon after irradiation and recovers exponentially. 3) the low MW of newly synthesized DNA in UV irradiated cells increases to parental size linearly more rapidly than either process (1) or (2). Only process (3) corresponds to "post-replication repair" and this appears to be a minor aspect of the overall response. These results suggest that both DNA damage and breaks involved in excision repair interfere with DNA replication. The major response in normal cells (i.e., 1) is caused by excision breaks that prevent initiation of DNA replication; minor responses (2) and (3) involve transient blocks to DNA chain growth in replicons active in DNA synthesis when irradiated. Normal XP and XP variants have similar rates of post-replication repair but greater initial MW depressions. Work supported by the Department of Energy and SNU-AID.

TU-AM-G4 SIZE OF PUTATIVE GAPS IN POST REPLICATION

REPAIR. R. B. Setlow and S. M. D'Ambrosio*, Brookhaven Nat'l Lab, Upton, NY 11973 and Ohio State Univ., Columbus, OH 43210

The size of pulse labeled DNA in mammalian cells treated with UV or N-acetoxy-AAF (AAAF) is usually smaller than normal and the small DNA is chased into parental size (post replication repair). If the pulse is ^3HdT and the chase is in BrdU, the BrdU regions within the ^3HdT labeled ones may be selectively broken by 313 nm light. If such a DNA is cosedimented in alkali with one given a similar treatment but a ^{14}CdT pulse and no chase, the values of $M(^3\text{H})/M(^{14}\text{C})$ versus 313 nm dose give estimates of the sizes of the putative gaps filled in by BrdU. We used a 254 nm dose of 10 J/m^2 or an AAAF concentration of $7.5 \mu\text{M}$, pulse times of 30-60 min, and chase times of 3-5 h. The apparent sizes of the gaps were much smaller than estimated previously (Lehmann, Life Sci. 15, 2005, 1974). For UV-irradiated V79, XPC, or XP variant cells they were 200-300 nucleotides. The gaps after AAAF treatment of XPC or XP variant cells were about 150 nucleotides. No gaps were detectable in untreated cells or in normal human fibroblasts exposed to AAAF. (Work supported by the U.S. Department of Energy)

TU-AM-G5 MOLECULAR RECOMBINATION AND REPAIR IN "S" AND "G₀" PHASE CHO CELLS. Resnick, M.A.¹, and Moore, P.D.*², Nat. Inst. Res., Mill Hill, London. (Currently: ¹Biochem. Dept., Coll. of Med., E.Tenn.St.U., Johnson City, 37601, and ²Dept. Microbiol., U. of Chicago, Chicago 60637.

The induction by various agents of recombination between homologous chromosomes has been well established in lower eukaryotes. We have attempted to determine if similar events take place in mammalian cells, particularly since recombination between sister chromatids is known to occur. Molecular recombination and the repair of DNA double-strand breaks (DSB) was examined in the "G₀" and S phase of the cell cycle using a t₈ CHO line and techniques of Moore & Holliday (Cell 8 (1976) 573). Mitomycin C (1-2 mg/ml) or ionizing radiation (50 krad) followed by incubation resulted in molecular recombination (hybrid DNA) in S phase cells. Approximately 0.03 to 0.10% of the molecules (M_n 5.6×10^6 Daltons after shearing) had hybrid regions for more than 60% of their length. However, no recombination was detected in "G₀" cells. Since the repair of DSB was observed in both stages with more than 50% of the breaks repaired in 5 hrs., it appears that if DSB repair involves recombination the hybrid regions must be small.

TU-AM-G6 THERMAL EFFECTS ON DNA REPAIR IN CHINESE HAMSTER CELLS. R. Shenkar, Department of Biophysics, Michigan State University, East Lansing, MI 48824

Chinese hamster lung fibroblasts (V-79) were incubated for three days in arginine-deficient medium at 33°C, 37°C, and 41°C. The cells were then treated with hydroxyurea and ultraviolet light. Finally all cells were allowed to incorporate ^3H -Thymidine at 37°C. Cells incubated at 33°C and 41°C prior to ultraviolet light treatment respectively showed about a 50% increase and a 50% decrease in ^3H -Thymidine incorporation than the cells incubated at 37°C prior to ultraviolet light treatment, as determined by autoradiography and measurement of specific activity.

TU-AM-G7 HUMAN CELLS HAVE DIFFERENT PATHWAYS TO PERFORM

EXCISION REPAIR OF THEIR DAMAGED DNA. F. E. Ahmed, and R. B. Setlow, Brookhaven Natl. Lab., Upton, NY 11973. Excision repair after combined treatments of UV and N-acetoxy-2-acetylaminofluorene (AAAF) was studied in repair proficient and repair deficient human fibroblasts (normal, xeroderma pigmentosum [XP] groups C,D,E, XP variants and ataxia telangiectasia). Three methods were used: a) unscheduled DNA synthesis measured radioautographically, b) photolysis of BrdUrd incorporated into parental DNA during repair, and c) sites sensitive to UV endonuclease from *M. luteus*. The three methods gave similar results. Saturation doses of 254 nm (20 Jm⁻²) and AAAF (20 μM) were employed. Two patterns of excision repair due to combined treatments were observed: 1) total repair was additive in normal, XP variant, and ataxia cells, and AAAF did not inhibit repair of UV damage, and 2) total repair was much less than additive usually less than observed for separate treatments and AAAF inhibited dimer excision in XP C, D, and E. We conclude that in the 1st class of cells there are different pathways for repair of UV and AAAF lesions, and in the 2nd class the residual excision enzymes are different from those in normal cells. Supported by US DOE.

TU-AM-G8 DIMER EXCISION AND REPAIR REPLICATION PATCH SIZE IN A *recL* MUTANT OF *E. coli* K-12. R. H. Rothman (Intr. by F. W. Studier), Department of Biology, Brookhaven National Laboratory, Upton, N.Y., 11973.

The *recL*52 mutation was originally isolated in a search for new recombination deficient mutants. Further characterization, however, showed that *recL* plays a negligible role in recombination but plays a major role in post-replication repair and excision repair. The excision repair defect was measured as an inhibition of host-cell reactivation and as a lengthening of the time required to close *uvrA*, *uvrB*-dependent single strand nicks. The present study shows that dimers are excised slowly in a *recL* mutant. This observation is not an artifact of altered rates of DNA degradation since degradation is the same in both *recL*⁺ and *recL*⁻ strains. The repair replication patch size was measured by the bromouracil-313 nm light photolysis technique. In the *recL*⁺ strain the average patch size was found to be about 30 nucleotides in length but in the *recL* mutant, it was greater than 300.

Supported by NIH National Research Service Award GM05643-02 and by The United States Department of Energy.

CHROMATIN II

TU-AM-G9 ROLE OF DNA DEGRADATION IN λ PROPHAGE INDUCTION R.M. Crowl* and R.P. Boyce, Department of Biochemistry and Molecular Biology, University of Florida, Gainesville, Florida 32608.

DNA degradation induced by agents which inhibit DNA synthesis appears to be required for the inactivation of the λ repressor. A λ lysogen of *E. coli* K12 with a *uvrA recB* genotype is inducible by UV, but not by mitomycin C or nalidixic acid. Induction by nalidixic acid is dependent on the *recB* gene product, exonuclease V, which presumably degrades at a stalled replication fork. Induction of λ by mitomycin C is apparently initiated by degradation at a stalled replication fork by exonuclease V or by degradation produced by the *uvr* excision system. DNA degradation produced by UV is not completely eliminated by the *uvrA recB* genotype and is probably due to another exonuclease acting at gaps in the DNA produced by replication of a damaged template. These studies suggest that at least one of three possible modes of DNA degradation is required for induction of λ prophage. (Work supported by NIH Grant GM-19167, and ACS Grant 77-073.)

TU-AM-H1 CHARACTERIZATION OF THE HISTONE CORE COMPLEX FROM CHROMATIN. S. Chung and P. Doty,* Department of Biochemistry and Molecular Biology, Harvard University, Cambridge, Massachusetts 02138

A stable histone complex containing equal molar ratios of H2A, H2B, H3 and H4 has been isolated from chicken erythrocyte chromatin in high salt. This complex has been further characterized by gel electrophoresis, sedimentation velocity, sedimentation equilibrium, and chemical cross-linking studies. In velocity ultracentrifugation, only one single sharp sedimentation boundary has been observed with sedimentation coefficient $S_{20,w} = 3.8 \pm 0.1$. Low speed sedimentation equilibrium studies over a wide range of protein concentrations suggest that the histone complex exists as a weak self-associating system. Analysis of the apparent weight-average molecular weight as a function of concentration indicates that the histone complex in 2 M NaCl, pH 9.0 is in a tetramer \rightleftharpoons octamer equilibrium for which the equilibrium constant has been determined. Evidence of such a tetramer \rightleftharpoons octamer equilibrium in solution is also supported by the results of our chemical cross-linking experiments on the histone core complex.

TU-AM-G10 ENHANCED EFFECTS OF UV ON PROTEIN SYNTHESIS IN *E. COLI* IRRADIATED FROZEN. R. Holladay and R. Bockrath, Indiana University School of Medicine, Indpls., IN 46202

Chloramphenicol-enhanced degradation of DNA (CED) seems to occur in *E. coli* during post-UV incubation regardless of restrictions on protein synthesis, if the cells are irradiated frozen at -79°C (Fong and Bockrath, *Rad. Res.* 72, 134). This could occur because CED is initiated efficiently by photolesions uniquely produced in frozen cells, or because post-UV protein synthesis is more severely inhibited by UV when the cells are irradiated frozen. We have estimated the post-UV protein synthesis in *E. coli* WU36-10 by observing the incorporation of ³H-leucine into cold TCA-insoluble material. The data show UV to have a greater effect on post-UV protein synthesis when the cells are irradiated frozen at -79°C than when irradiated at ambient. Thus CED probably results after irradiation of cells frozen at -79°C because synthesis of an induced inhibitor of DNA degradation is blocked by the irradiation experience. We will discuss our data to indicate an optimal configuration for the induction of post-UV activities requiring *de novo* protein synthesis.

Supported by N.I.H. grant GM 21788.

TU-AM-H2 NUCLEOSOMES AND NUCLEOSOME VARIANTS. R.D. Camerini-Otero, R. H. Simon,* and G. Felsenfeld, Section on Human Biochemical Genetics and Laboratory of Molecular Biology, NIAMDD, NIH, Bethesda, Maryland 20014.

We reported some time ago (Camerini-Otero et al., 1976 *Cell* 8: 333; Sollner-Webb et al., 1976, *Cell* 9: 179; Camerini-Otero and Felsenfeld, 1977, *Nucl. Acids Res.* 4: 1159) that the arginine-rich histones, H3 and H4, play a unique role in the organization of DNA in chromatin. We have recently shown (Camerini-Otero et al. 1977, *Cold Spr. Harb. Symp. on Quant. Biology*, 42: in press) that an octamer of these histones is able to fold a DNA chain about 140 base pairs in length into a hydrodynamically compact structure. We show here that this structure is in fact very similar to a canonical nucleosome formed by such a DNA chain and an octamer of the four histones H2A, H2B, H3 and H4. A second nucleosome variant, also formed *in vitro*, contains the four histones but has a disulfide linkage between the residues of position 110 on the H3 molecules. If, as has been proposed, the nucleosome has a dyad axis, then the disulfide bridge must lie on this axis. The possible biological roles of these two structures will be discussed.

TU-AM-H3 CIRCULAR DICHROISM OF VARYING SIZE MONONUCLEOSOMES. M.K. Cowman and G.D. Fasman, Grad. Dept. Biochem. Brandeis University, Waltham, Massachusetts 02154.

Mononucleosomes of varying DNA length and H1, H5 contents have been isolated from micrococcal nuclease digests of chicken erythrocyte nuclei. The CD spectrum, $[\theta]_{283}^{283} = 4000$, above 250 nm of a mononucleosome preparation with a DNA length of 200 base pairs and 70% of the normal H5 content of chromatin (i.e., a nearly complete repeat unit) is identical to the spectrum observed for intact chromatin. Mononucleosomes with shorter DNA lengths and somewhat reduced H1, H5 contents exhibit lower overall ellipticity above 250 nm. The decrease in overall ellipticity is accompanied by a reduction in the $[\theta]_{275}^{275}/[\theta]_{284}^{284}$ ratio and in the appearance of a negative band near 295 nm. Calculated difference spectra between free DNA and any of the isolated mononucleosomes show a single negative band at 275 nm, similar to the Ψ -DNA spectrum. This Ψ contribution is most intense for mononucleosomes with short linker DNA attached to the core particle. Thus the folding of DNA around the histone core leads to the emergence of a Ψ -DNA CD contribution, in which the linker DNA does not participate. Supported by N.I.H. and NSF grants.

TU-AM-H6 NU-BODY SHAPE AND STRUCTURE IN SOLUTION FROM FLOW BIREFRINGENCE MEASUREMENTS. R. E. Harrington, Department of Chemistry, University of Nevada, Reno 89557.

Streaming birefringence and extinction angle measurements have been made on isolated whole and H1 histone-free nu-bodies from chicken erythrocytes in aqueous EDTA solutions. Results have been obtained at relatively low velocity gradients over a range of 0 to 1 M NaCl concentration. Implications of the data in terms of particle asymmetry and salt-dependent structure will be discussed.

TU-AM-H4 HYDRODYNAMIC CONFORMATION OF CHROMATIN IN LOW IONIC STRENGTH SOLVENT. K.S. Schmitz, Dept. Chem., Univ. Mo.-Kansas City, Kansas City, Mo., and B. Ramsay-Shaw*, Dept. Chem., Duke University, Durham, N.C.

Selected fractions of nuclease-digested chromatin were studied by quasielastic light scattering and sedimentation velocity techniques. The Garcia de la Torre-Blaomfield hydrodynamic theory (G-B) was used to analyze f vs. n , where f is the friction factor and n is the number of nucleosome units. We used three bead diameters in the G-B calculations: 110Å for the core particle bead (based on published hydrodynamic studies of the monomer); 25Å (DNA diameter) for the beads contiguous to the core beads; and a third bead diameter in the range 25-40Å for the remaining beads in the linker region. Two model calculations for a helix conformation are reported; a systematic analysis in which the line of centers for the linker beads coincides with that for the core beads, and a model in which the contact beads define an angle of 90° with the core bead center (based on neutron scattering data of mononucleosomes). The primary difference in the two calculations is in the helix pitch and diameter. This research was supported in part by NIH (GM23681, GM24346) and NSF (PCM7622073).

TU-AM-H7 ABSTRACT WITHDRAWN

TU-AM-H5 LOW-SHEAR VISCOSITY STUDIES ON THE THERMAL DENATURATION OF DNA AND MONONUCLEOSOMES. B. Ramanathan*, J.C. Kent* and K.S. Schmitz, Dept. of Chemistry, Univ. of Mo.-Kansas City, Kansas City, Mo. 64110

Mononucleosomes were obtained by nuclease digestion of calf thymus chromatin for 25 minutes at 5°C. The DNA was obtained from two sources; extracted from the mononucleosome pool, and purchased from Sigma Chemical Corp. The latter sample was sonicated and chromatographed on a hydroxylapatite column to obtain duplex DNA. Derivative melting curves were determined by optical absorption methods for all samples. The mononucleosomes exhibit two melting regions, a broad profile between 75-81°C and a sharp region 84-87°C. Gross hydrodynamic conformational changes were studied with a Zimm-Crothers type viscometer with the capacity to record half-revolutions of the cylinder. The mononucleosome exhibits an initial increase in viscosity $\sim 9^\circ$ below the onset of the optical absorbance changes and a time-dependent increase in viscosity in the transition regions. The latter observation, not seen in the DNA samples, proceeds at a rate dependent on the history of the sample (i.e. a hysteresis loop). Supported by NIH (GM24346) and NSF (PCM 7622073).

TU-AM-H8 SUPERSTRUCTURES OF WET CHROMATINS. S. Basu, Div. of Labs and Research, NYS Dept. of Health, Albany, NY 12201

The wet replication technique, using a differentially pumped hydration chamber in a vacuum evaporator (*J. Appl. Phys.* 47, 741-761, 1976), has revealed that the nucleosome-containing strand of wet eukaryotic chromatin (chicken erythrocytes and rat liver) is organized in at least two distinct classes of superstructures. Class 1 structures are typical polynucleosome supercoils in which the nucleosomes are quite visible, contiguous and well packed in helical arrays. About 1.7µm dia. filamentous material, which may be single or double strand of DNA, is seen wrapped around the polynucleosome coil. Class 2 structures represent the classic 12-15µm dia. smooth or irregularly knobby fibrils, which are often twisted upon each other and make 30µm dia. fibers. The nucleosomes are apparently masked in the Class 2 superstructures. Those two classes of chromatin may also be present in chinese hamster metaphase chromosomes. These superstructures are extremely sensitive to their hydrated state because on drying in general they collapse into 'beads-on-a-string' or thin fibrils (support: USPHS Grant 7R01 GM 23727-01).

TU-AM-H9 BIOPHYSICAL STUDIES OF ISOLATED CHROMATIN AND INTACT CELLS AFTER PARTIAL HEPATECTOMY IN RATS.

P. Miller, W. Linden,* and C. Nicolini. Biophysics Div., Temple University Health Sciences Center, Philadelphia, PA 19140.

Chromatin was isolated from rat liver cells at 0, 3, 5, 11, 18 and 24 hrs. following partial hepatectomy. Consistent with findings in chromatin of cultured cells stimulated to proliferate, there was an increase in chromatin molar ellipticity at 276nm and a decrease in thermal stability 3-8 hrs. after surgery, quite before the onset of DNA synthesis. Utilizing laser flow microfluorimetry on the same unfixed liver cell suspensions stained with EB, cells which have the same amount of DNA but vary in the amount of RNA and/or chromatin conformation (G0 and G1) can be distinguished IN SITU. Differences in chromatin binding sites can be enhanced using RNase and preserved even after fixation. Changes in the tertiary and quaternary structure of isolated chromatin, reflected also in the "quintenary" DNA superpacking IN SITU, are then early events in the control of cell proliferation, which directly mimic changes in transcriptional activity. (This work was supported by Grant CA20034 of the National Cancer Institute).

TU-AM-H10 AN IMPROVED ACRIFLAVINE-FEULGEN REAGENT FOR QUANTITATIVE DNA CYTOFLUOROMETRY. J. W. Levinson*, R. G. Langlois*, V. M. Maher*, and J. J. McCormick, Michigan State Univ., E. Lansing, MI 48824 and Lawrence Livermore Lab, Univ of Calif, Livermore, CA 94550.

We have modified the acriflavine-Feulgen histochemical method for the quantitative determination of DNA by performing the staining with acriflavine dissolved in EtOH. Compared to conventional techniques, this method not only decreases non-Feulgen (background) staining in both the nucleus and cytoplasm, but also increases the fluorescent intensity of Feulgen stained nuclei >4-fold. Cells stained by our modified method had a fluorescence maximum of 507nm, which is similar to the 500nm fluorescence maximum obtained with apurinic acid treated in solution by a modification of the acriflavine-Feulgen method. These fluorescence maxima contrast with the 510nm to 625nm fluorescence maxima obtained when cells stained according to conventional protocol. These fluorescence intensities of nuclei of synchronized cells stained by the modified method were proportional to DNA content. We conclude that our method is more satisfactory for quantitating DNA *in situ* by cytofluorometry than the usual methods. Supported by DHEW Grants CA 21247 and 21253.

TU-AM-H11 CYTOFLUOROMETRIC AND CYTOCHEMICAL COMPARISONS OF NORMAL AND ABNORMAL HUMAN CELLS. J.E. Gill and L.L. Wheelless, Jr.,* University of Rochester Medical Center, Rochester, New York 14642

Acridine Orange (AO) staining of exfoliated cells from epithelial tissues facilitates discrimination between normal and abnormal (i.e. malignant and premalignant) cells: abnormal cells develop highly elevated nuclear fluorescence. To determine the cytochemical basis for this discrimination, clinical specimens containing both normal and abnormal cells were divided into aliquots and stained with AO, Propidium Iodide (PI), or a Feulgen procedure. When AO and Feulgen staining were compared, the abnormal:normal ratio of mean nuclear fluorescence following AO staining was greater than the abnormal:normal ratio of mean nuclear absorbance following Feulgen staining. This finding rules out elevated Feulgen DNA content as the basis for the observed discrimination. When AO and PI staining were compared, the abnormal:normal nuclear fluorescence ratio was highly elevated for both. Also, the fluorescence emission spectra from individual cells indicated DNA as the binding substrate for both. These results support the hypothesis that chromatin in abnormal cells is altered so as to increase accessibility of DNA to intercalating dyes.

TU-AM-H12 BINDING PROCESSES AND EMISSION SPECTRA FOR ACRIDINE ORANGE (AO) STAINING IN THE INTACT CELL.

S. PARODI*, S. LESSIN*, S. FANG*, S. ZIETZ and C. NICOLINI. BIOPHYSICS DIVISION, TEMPLE UNIVERSITY HEALTH SCIENCES CENTER, PHILADELPHIA, PENNSYLVANIA 19140.

We have monitored the spectral emission of cytoplasm and nuclei in AO-stained cells, as functions of total AO concentration and of molar ratio R ($\mu\text{M AO}/\mu\text{M DNA-P}$). A drop of cells, already equilibrated with AO, formed a sealed chamber (16 μm high) between coverslip and slide. The epifluorescence is measured with a Zeiss microscope, 510nm reflector, on line with an Image Analyzer. In the range of 10^{-6} - 10^{-4}M of AO, the differential spectral emission (red vs. green fluorescence) of cytoplasm and nuclei critically depends on the molar ratio R, not from the total dye concentration. Using Melanoma B16 cells, the nucleus and the cytoplasm are both green at $R = 0.1$ to 0.5, respectively, green and red at $R = 1-3$, and both red at $R > 6$. The green emission seems to be related to the AO bound to primary binding sites (with DNA or RNA), while the red to secondary sites (with DNA or RNA). FMF data in the same Melanoma cells corroborate these preliminary conclusions. (Supported by NCI Grants CA18258 and CA20034).

TU-AM-H13 ASYMMETRY OF INTRA-NUCLEAR FUNCTION DURING CELL DIFFERENTIATION. John H. Frenster, Shirley L. Nakatsu† and Michael M. Papaliant† Department of Medicine, Stanford University, Stanford, California 94305.

DNA helix openings can be visualized, measured, and counted during the course of in-vivo cell differentiation within human bone marrow (Nature 248, 334 (1974)). Electron micrographs of individual human bone marrow cells were analyzed for the number and intra-nuclear distribution of DNA helix openings (J. Natl. Cancer Inst. 59, 839 (1977)), and these were correlated with the vector of displacement of the cell nucleus from the cell center within each cell. 122 differentiating granulocyte and erythrocyte precursor cells were analyzed, with 72 % of all cells displaying preferential localization of DNA helix openings in that half of the cell nucleus closest to the cell center. This asymmetry of intra-nuclear function was most intense within those cells mid-way through the course of cell differentiation, and was accompanied by a progressive increase in the nuclear displacement index, measuring the relation between extra-nuclear displacement and intra-nuclear asymmetry, during the course of cell differentiation within each of the cell series. Supported by NIH CA-10174 and CA-13524 and ACS IC-45.

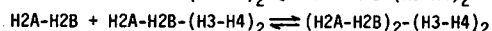
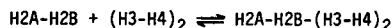
TU-AM-H14 LEFT-HAND DNA SUPERCOILS FORMED BY THE OVERWINDING OF THE HELIX IN RESPONSE TO THE LOWERING OF THE WATER ACTIVITY. E.N. Moudrianakis & T.H. Eickbush.

The Johns Hopkins University, Baltimore, Maryland 21218

We investigated by electron microscopy the effect of water activity and ionic strength on the conformation of the DNA helix. We found that dehydration of the double helix from media of very low ionic strength, and without any proteins, brings about its collapse into a left-hand supercoil with an outer diameter of 90 Å. Both linear and covalently-closed circular DNA molecules form this type of supercoil. The compact state is generated by an overwinding of the DNA helix (increase in turn-angle) which now approximates the C-form DNA. The similarities of this type of DNA compaction to that found in chromatin will be analyzed in terms of our earlier model for chromatin structure, in which we proposed (1) that the binding of histones to DNA lowers the water activity on the helix and thus induces the supercoil. Histone-histone interactions (primarily H3-H4) lock together every two consecutive turns of the supercoil and provide the basis for stability and regulation of the structure. 1. *Molec. Biol. of the Mammalian Genetic Apparatus*, (ed. P. Ts'o) Elsevier/North-Holland, April 1977, pp 301-322.

TU-AM-H15 THE FORMATION OF REVERSIBLE HEXAMERS AND OCTAMERS FROM CALF THYMUS CORE HISTONES. J.E. Godfrey*, T.H. Eickbush and E.N. Moudrianakis, The Johns Hopkins University, Baltimore, Maryland 21218 (Introduced by R.C. Huang).

The histone core complex purified from calf thymus chromatin has been subjected to equilibrium sedimentation analysis. In 2 M NaCl, pH 7.5, 20°C, this complex was found to associate reversibly to form hexamer and octamer species. The data best fit the mode:



At total protein concentrations above 1 mg/ml, octamer is the dominant species present. Moreover, within the concentration range examined (0.1-2.5 mg/ml), monomer species and the H3-H4 dimer are not present in significant concentration. Other modes of association were tested but all gave less satisfactory fits to the data. The possible *in vivo* significance of the reversible hexamer and octamer are briefly considered.

TU-AM-H16 THE HISTONE CORE COMPLEX EXISTS IN SOLUTION AS AN OCTAMER. T.H. Eickbush and E.N. Moudrianakis, The Johns Hopkins University, Baltimore, Maryland 21218.

A protein complex, composed of the four core histones (H2A, H2B, H3 and H4), has been isolated from calf thymus and chick erythrocyte chromatin. No irreversible dissociation or aggregation of this complex occurs in 2 M NaCl, pH 7.5, as determined by column chromatography and sucrose gradient analysis. Various reports have suggested that the histone core complex exists in solution as a "heterotypic tetramer." However, based on gel filtration, sedimentation velocity and sedimentation equilibrium data, we determined the molecular weight of the core complex to be approximately 100,000 daltons. This finding would suggest that the histone octamer (109,000 daltons), postulated to be the fundamental histone unit in chromatin, is also stable in 2 M NaCl, pH 7.5, in the absence of DNA or any protein crosslinking. The effects of various experimental parameters on the stability of this octamer will be discussed in relation to the interactions maintaining this complex in solution.

SYMPOSIUM

CELL-CELL INTERACTIONS IN HIGHER NERVOUS TISSUE

TU-PM-15 CELLULAR INTERACTIONS IN THE DEVELOPMENT OF SYNAPTIC CONNECTIONS IN SIMPLE NERVOUS SYSTEMS
E.R. Macagno, Dept. of Biological Sciences. Columbia University, New York, N.Y. 10027.

The relative roles of genetic and epigenetic factors in the determination of synaptic connectivity are not known. A reasonable hypothesis is that genetic information provides a general framework of instructions which restrict the range of specific developmental pathways available to a neuroblast. Epigenetic factors, such as interactions with other developing neurons, would then further define specific fates, especially which neurons synapse with which others.

To test this hypothesis experimentally we have chosen the following strategy: (1) Work with a cloned organism, hence, maintaining the genetic component constant; (2) Work with a group of neurons which can be individually identified, and for which variations from normal structure and synaptic connectivity can be determined in detail; (3) Scramble the developmental process to modify whether, where and when cellular interactions that presumably affect synaptic connectivity take place. The visual system of isogenic *Daphnia* fits very well with the first two points. The number of neurons is small and the whole system can be reconstructed from serial electron micrographs using computer techniques. In previous work we have not only determined the synaptic connectivity patterns between photoreceptors and second order cells (laminar cells) in detail, but also that at a specific time in development photoreceptor fibers grow into the lamina where they make special membrane contacts with undifferentiated laminar neuroblasts. This interaction appears to signal the beginning of the process that culminates in the synaptic connectivity pattern found in the adult. In order to explore further the role of this interaction we have used a UV microbeam to produce the following modifications of the developmental process: (a) deletion of specific photoreceptors at various developmental stages; (b) rearrangement of the spatial pattern of growth of photoreceptor fibers; (c) rearrangement of the temporal pattern of growth of photoreceptors. Our observations are consistent with a model in which laminar neurons are not individually specified prior to their interaction with growing photoreceptor fibers, but are recruited by incoming photoreceptor fibers with which they later make synaptic contacts. Which cells they synapse with would therefore result from the particular spatial and temporal pattern of interactions which they undergo in development.

TU-PM-25 ROLE OF ION CURRENTS IN CONTROLLING DEVELOPMENT OF NERVE NETWORKS.
L. Jaffe, Purdue University, Lafayette, Ind. 47907

TU-PM-3S OPTICAL MONITORING OF NEURON ACTIVITY. L.B. Cohen, H.V. Davila, A. Grinvald, S. Leshner, W.N. Ross, and B.M. Salzberg. Dept. of Physiology, Yale University School of Medicine, New Haven, CT. 06510

Studies of neuron interactions involved in the control of behavior or the development of the nervous system might be facilitated if it were possible to monitor activity in a large number of neurons simultaneously. Since there are optical signals associated with action potentials and synaptic potentials, it is possible that an optical measuring system could be developed for monitoring activity in many neurons. In contrast to the other methods discussed in this symposium, techniques for optical monitoring of neuron activity are in a relatively primitive stage of development. Thus far we have succeeded in monitoring activity in 14 neurons simultaneously; we hope that the number of monitored neurons can be increased in the near future.

TU-PM-4S 3-D RECONSTRUCTION IN THE ANALYSIS OF NERVE NETS OF ISOGENIC ANIMALS. C. Levinthal and F. Levinthal, Dept. of Biol. Sci., Columbia Univ., N.Y., N.Y. 10027.

Many questions relating to the development and the genetic determination of nerves in an extended network require detailed anatomical information about the shapes of many individual cells as well as their interactions with each other. The basic principles by which such information can be obtained has not changed in the past hundred years. One must still slice and look. However the resolution which can be obtained with serial electron microscopy requires new methods of data handling and reduction in order to make use of the three dimensional information in thousands of thin section micrographs. Both manual and semi-automated methods for interpreting photographic images have been developed which aid in obtaining computer readable data on shape, topology and connectivity of nerve cells.

These methods have been applied to studies of cell shape and topology of identified nerves of small tropical fish which can be grown so that they produce large numbers of genetically identical individuals. Surprisingly large variations were observed in the branching patterns of identified cells in these fish even though they appeared to be identical in all of their external attributes. Preliminary observations suggest that the variations are produced by differences in the amount of crowding in the body cavity of the mother during the early stages of development.

MINISYMPOSIUM

MAGNETO CIRCULAR DICHROIC SPECTROSCOPIES

TU-PM-1M BIOPHYSICAL APPLICATION OF MAGNETIC CIRCULAR DICHROISM: AN INTRODUCTION. John Clark Sutherland, Biology Department, Brookhaven National Laboratory, Upton, New York 11973. Magnetic Circular Dichroism (MCD) is the difference between the absorption of left and right circularly polarized light induced in an isotropic material by an external magnetic field. The MCD anisotropy (the ratio of the MCD to the absorption at a particular wavelength) varies over more than three orders of magnitude depending on the nature of the absorbing chromophore. Thus it is frequently possible to detect the presence and determine the concentration of a chromophore with a high MCD anisotropy in the presence of overlapping absorption bands from other components of a complex biological system. MCD is also useful for detecting the presence of multiple transitions which are unresolved in the absorption spectrum of a chromophore. Proteins containing transition metal ions have been probed extensively by MCD. In contrast to natural Circular Dichroism (CD), MCD is generally insensitive to the chirality of the chromophore or of its environment. Thus the two techniques, which are experimentally similar, provide complementary types of information. The normal method of measuring MCD involves monitoring the intensity of beams of left and right circularly polarized light which have passed through the sample. If the sample contains one or more fluorescent components, its MCD may be determined from the dependence of the amplitude of the fluorescent signal on the polarization of the exciting beam. It is also possible to measure the magnetic field induced circular polarization of fluorescence, phosphorescence and Raman scattered radiation. Current MCD spectrometers cover the spectral region from 130 nm in the vacuum ultraviolet to 5.5 μ in the infrared. (Supported by the Department of Energy and a Research Career Development Award from the National Cancer Institute, NIH).

TU-PM-2M MAGNETIC CIRCULAR DICHROISM SPECTRA OF METALLOPORPHYRINS. Carl Djerassi,^{*} Robert E. Linder, Günter Barth, and Edward Bunnenberg, Chemistry Department, Stanford University, Stanford, California 94305

For molecules with a three fold (or higher) axis of symmetry, magnetic circular dichroism (MCD) spectroscopy measures the magnetic moment of excited electronic states, if the excitation is sufficiently strongly allowed. If the band is only weakly allowed, as is the case for the visible or Q band in metalloporphyrins, vibronic effects can modify the usual procedures. Here coupling to the intense near UV Soret band can even change the sign of the MCD of the vibronic sublevels of the Q band. Evidence for such behavior in three classes of metalloporphyrins is obtained by curve fitting and by comparing the MCD spectra with the first derivative of the absorption spectra.

These vibronic effects are also observed in heme porphyrins even though the spectra are less well resolved. This and certain experimental advantages over absorption spectroscopy (relative freedom from light scattering effects, wide range of intensities in both the visible and near UV spectral regions, and enhanced resolution due to the derivative shape of many bands) lead to such analytical applications as: 1) spin state population analysis in oxidized P-450-LM and 2) spin state population analysis in ligated methemoglobins. More prosaic examples include: 1) determination of uro- and coproporphyrin separately in urine at the 10 μ g/l level; 2) determination of 0.1% oxyhemoglobin in methemoglobin solutions; and 3) determination of myoglobin at levels as low as 0.1-0.2 μ g/ml.

TU-PM-3M NEAR-INFRARED CD AND MCD OF METALLOPROTEINS. P. J. Stephens, Department of Chemistry, University of Southern California, Los Angeles, California 90007.

Near-infrared ($\lambda > 800$ nm) electronic transitions exist in many metalloproteins which contain open-shell transition-metal ions. These transitions can often be of importance in the elucidation of structural and electronic properties of these proteins. They have been little studied, however, since they are frequently weak, beyond the range of available spectrophotometers and overlapped by vibrational transitions of the protein and its aqueous solvent.

We discuss the application of circular dichroism (CD) and magnetic circular dichroism (MCD) spectroscopies to the study of near-infrared transitions of heme, iron-sulfur and copper proteins. The advantages and disadvantages of the near-infrared spectral region relative to the visible-ultraviolet domain and of CD and MCD over absorption spectroscopy will be summarized critically.

DO NOT FOLD ACROSS ABSTRACT

TU-PM-4M NATURAL AND MAGNETIC CIRCULAR DICHROISM OF METALLOENZYMES. B. L. Vallee and B. Holmquist* Biophysics Research Laboratory, Department of Biological Chemistry, Harvard Medical School, Boston, Massachusetts 02115

Circular dichroism (CD) and magnetic circular dichroism (MCD) have greatly aided in the delineation of both structural and functional roles of metals in metalloenzymes and other metalloproteins. MCD is complementary to conventional spectral methods, providing valuable information regarding the presumable nature of the coordination geometry of metals in biological systems. Some Co(II) complex ions, a series of Co(II) substituted metalloenzymes, and non-heme iron and copper proteins have been examined by this means. The MCD spectra of hexa-, penta-, and tetra-coordinate high-spin Co(II) models whose x-ray structure is known exhibit MCD spectra characteristic of these geometries. Based upon comparisons with Co(II) models, the MCD spectra of Co(II) substituted carboxypeptidase, thermolysin and the *B. cereus* neutral protease indicate that the overall geometry of Co(II) at their active sites is tetrahedral. The MCD spectra of both Co(II) alkaline phosphatase and of Co(II) carbonic anhydrase, the latter at alkaline pH, resemble those of penta-coordinate complexes. Inhibitors of carbonic anhydrase and carboxypeptidase generate spectra suggesting changes which are consistent with alterations in coordination geometry. The MCD spectra associated with the iron chromophores of spinach and clostridial ferredoxins, rubredoxin and hemerythrin are each characteristic and distinct and markedly altered by oxido-reduction. Lanthanide substitutions, for example Ca^{2+} in thermolysin, provide yet another application of MCD to probe metal sites. MCD appears to provide a sensitive approach to further characterize the properties and roles of metals in metalloproteins. This work was supported by NIH Grant GM-15003.

TU-PM-5M MAGNETIC CIRCULAR DICHROISM AS A PROBE OF THE SPIN STATES OF HEMEPROTEINS.

Larry Vickery, Department of Physiology, University of California, Irvine.

The ability of hemeproteins to participate in a wide variety of biological processes is due in part to the fact that the electronic properties and chemical reactivity of heme iron can be dramatically modulated by specific interactions with the protein. Consequently many spectroscopic approaches have been used to probe the electronic state of the iron "active center." Of particular interest are methods which can provide information about the iron spin state since the *d*-orbital electron pairing can determine both kinetic and thermodynamic properties of ligand binding and electron affinities. We have studied the visible and near UV spectral region MCD properties of several *b*- and *c*-type hemeproteins [Vickery, Nozawa and Sauer, *J. Am. Chem. Soc.* **98**, 343 and 351 (1976)] and of heme *a* in cytochrome oxidase [Babcock, Vickery and Palmer, *J. Biol. Chem.* **251**, 7907 (1976) and **252**, in press (1977)]. Throughout this wavelength region porphyrin transitions dominate the optical spectra, but for all paramagnetic forms the effect of the iron on the MCD is reflected in the presence of temperature dependent Faraday *C* terms indicating an (iron)spin-(porphyrin)orbit coupling. For ferric heme derivatives the intensity of the Soret band MCD is correlated with the amount of low spin ($S = 1/2$) component present, being much weaker for high spin ($S = 5/2$) species; for ferrous complexes only the high spin ($S = 2$) state gives rise to *C* terms so that it is easily distinguished from diamagnetic low spin ($S = 0$) forms. The MCD technique offers advantages of high sensitivity, applications to both ferric and ferrous redox states, use in unpurified systems and the ability to obtain measurements at physiological as well as cryogenic temperatures. In the case of cytochrome oxidase the method has proved particularly useful for resolving the spectral and functional behavior of the two distinct heme *a* moieties in the enzyme.

TU-PM-6M MAGNETIC CIRCULAR DICHROISM OF NETROPSIN. John Clark Sutherland and John F. Duval, Biology Dept., Brookhaven National Laboratory, Upton, New York 11973.

We report the first measurements of the MCD spectrum of the basic, polypeptide antibiotic netropsin. The MCD shows that the longest wavelength absorption band of Nt (peak at 297 nm) is the sum of at least four components with at least two bands located on each of the 1 methyl pyrrole rings. The MCD spectrum permits a reinterpretation of the natural CD and absorption difference spectrum of the complex which Nt forms with DNA. We conclude that Nt has little effect on the absorption or CD spectra of the DNA and therefore little effect on the secondary structure of the DNA.

(Research supported by the Department of Energy and a Research Career Development Award from the National Cancer Institute, NIH to JCS.)

TU-PM-7M DETERMINATION OF TRYPTOPHAN BY MAGNETIC CIRCULAR DICHROISM. B. Holmquist* and B. L. Vallee, Biophysics Research Laboratory, Department of Biological Chemistry, Harvard Medical School, Boston, Massachusetts 02115.

Magnetic circular dichroism (MCD) offers several advantages for the determination of tryptophan in proteins. The intense positive band near 293 nm uniquely characteristic of tryptophan allows the direct and quantitative measurement of this essential amino acid with high sensitivity and accuracy under conditions which preserve the integrity of the native protein structure and function. Reliable measurement to levels as low as 5 nmoles of this residue are possible. Destruction or modification of the indole ring of tryptophan as occurs with numerous agents employed to assess its role in proteins can be directly monitored by MCD. The application of this spectral method for tryptophan, as employed in several laboratories, provides a clear example of both the analytical and the biochemical value of MCD in the biochemical laboratory. This work was supported by NIH Grant GM-15003.

MUSCLE PROTEINS III

TU-PM-A1 PURIFICATION OF MUSCLE PROTEINS ON IMMOBILIZED CIBACRON BLUE F3GA AFFINITY COLUMNS. A.P. Toste*, R. Crooks, E. Lebowitz, and R. Cooke, Cardiovascular Research Institute, Univ. of Calif. Medical Center, San Francisco, CA 94143

At low ionic strength (e.g. 50mM TES, pH 7), myosin subfragment-1 (S-1) and myosin light chain kinase from skeletal muscle and human platelets bind tightly to affinity columns of Cibacron Blue F3GA immobilized in a 4%-agarose matrix (Blue Sepharose). In all cases, bound protein is released on elution with NaCl gradients (0-1.5M NaCl), whereas ATP and MgATP gradients have no effect on binding. In contrast, G-actin does not bind under any of the conditions tested. Despite strong S-1 binding, ionic conditions favoring both myosin solubility and Blue Sepharose binding have yet to be found. Cibacron Blue F3GA affinity chromatography has proved to be a novel method for purifying kinases and S-1, greatly simplifying conventional purification procedures. Work supported by grants: NSF No. BMS75-14793 and CVRI Fellowship HL07192-01 (A.P.T.).

TU-PM-A2 ON THE NUCLEOTIDE DEPENDENCE OF ACTIN POLYMERIZATION. Wm. J. Perkins* and Ralph G. Yount, Biochemistry Biophysics Program, Washington State University, Pullman, WA 99164

The nucleotide dependence of G-actin to F-actin conversion has been investigated using 8-substituted nucleoside triphosphates and unsplitable ATP analogs. The nucleotides 8-Br-ATP, 8-azido-ATP, 8-azido-cATP all support polymerization of G-actin giving final specific viscosity values about one half those obtained with ATP. Each nucleotide was shown by spectrophotometry and HPLC to be incorporated in the F-actin polymer to the same extent as ATP. Adenylyl imidodiphosphate (AMP-PNP) also supported G- to F-actin conversion. G-actin at low ionic strength in the presence of 5 mM AMP-PNP was unstable with one half of the polymerizability being lost each 3.5 hrs at 0°C. This instability may explain the inability of Manherz et al. (Eur. J. Biochem. 60, 109 (1975)) to duplicate earlier AMP-PNP promoted polymerization studies reported by Cooke and Murdock (Biochemistry 12, 3927 (1973)).

Supported by NIH Grant AM-05195 and by a Grant-in-Aid from the American Heart Association.

TU-PM-A3 THE CONTRACTION OF GLYCERINATED SKELETAL MUSCLE FIBERS AS A FUNCTION OF ATP CONCENTRATION. R. Cooke, and W. Bialek, Dept. of Biochem/Biophys. and the CVRI, University of California, San Francisco, CA 94143.

We have recorded force velocity curves for rabbit fibers over a range of [ATP] from 5 μ M to 1 mM. As [ATP] increases isometric tension increases to a maximum around 50 μ M and then decreases to about 70% of the maximum at 1 mM. In contrast, the maximum velocity of contraction increases linearly as [ATP] is raised, reaching a value of 2-4 lengths/sec at 1 mM. To explain these results, we have developed a theory of the kinetics of cross bridge-nucleotide interaction in a contracting fiber. We conclude that: 1) during isometric contraction ADP bound to an attached cross bridge dissociates with a first order rate constant, k_{46} , of 10 s^{-1} , 2) during an isotonic contraction k_{46} is a function of cross bridge orientation and increases greatly near the end of the power stroke, and 3) following the release of ADP the cross bridge is dissociated by ATP with a rate constant close to that measured for the dissociation of actomyosin in solution. This kinetic model fits the fiber data over the entire range of [ATP]. Work supported by grant from NSF BMS75-14793.

TU-PM-A4 DYNAMICS OF NATIVE MUSCLE THIN FILAMENTS FROM SCALLOP. J. Newman, F. Liu*, and F.D. Carlson, Johns Hopkins Univ., Baltimore, MD 21218

Photon correlation spectroscopic (PCS) measurements on solutions of native thin filaments from adductor muscles of the scallop, *Placopecten magellanicus*, were performed at various concentrations (0.1-2 mg/ml), ionic strengths (0.05 and 0.6 M), temperatures (5-45°C), and scattering angles (15-150°). Under all conditions, the low-angle data ($\leq 30^\circ$) could be analyzed to yield a translational diffusion coefficient, $D_s^0 = (1.28 \pm 0.10) \times 10^{-8} \text{ cm}^2/\text{sec}$, corresponding to a filament length of $1.06 \pm 0.12 \mu$. At the higher temperatures, in the presence of 2mM MgATP, the tropomyosin is completely dissociated from the actin filaments which remain intact (confirmed by centrifuge binding studies) with no change in the low-angle PCS measurements (time constants scaled by temperature/solvent viscosity) indicating a constant length distribution. However, at higher temperatures, the high-angle PCS data show significant departure from the rigid rod model. Similar results were obtained from measurements in 0.6 M salt in which the tropomyosin also dissociates from the actin filaments. Supported by Muscular Dystrophy and NIH.

TU-PM-A5 IONIC PROPERTIES OF PYELOURETERAL PACEMAKER SMOOTH MUSCLE, Monica Mensah-Dwumah* and Christos E. Constantinou, Stanford Univ. Med. Ctr., Stanford, CA 94305.

The contribution of Na, K, and Ca ions to the frequency characteristics of the pyeloureteral pacemaker system of the rabbit were studied in vitro. A comparison of the calyceal and pelviureteral segments was made. It is shown that reduction of the external Na abolishes spontaneous contractility. A minimum concentration of 85 mM Na is necessary for the maintenance of spontaneous contractions. Re-admission of Na restored conditions to those of the control state. Removal of K had a small effect on the frequency and amplitude of contraction. Increased K stimulated a transient increase in the frequency of contractions to levels of four times to those of baseline conditions. A decrease in extracellular Ca abolished the contractibility of pelviureteral segments. An increase in Ca had a slight increase on the effects of both the amplitude and frequency of pacemaker activity. These results evidence that both Na and Ca may be implicated in the genesis of pacemaker activity or at least Ca ions play a role in the regulation of spontaneous activity. (Supported by NIH Grant #AM19366)

TU-PM-A6 ACCELERATION OF CONTRACTILE WAVEFRONT IN THE PERFUSED PYELOURETER OF THE RABBIT. Christos E. Constantinou, Vic Hardgrove* and Monica Mensah-Dwumah.* Stanford Univ. Med. Ctr., Stanford, CA 94305.

Visual observations upon the exposed surface of the renal pelvis indicate the presence of contracting concentric waves originating at the fornix and terminating at the pelviureteral junction. The surface velocity characteristics at four points were made optically using a video system consisting of a camera, monitor and a photocell array. The results show that waves originate peripherally at the calyceal extremity and propagate towards the pelviureteral orifice with increasing velocity. The mean initial velocity at the fornix was 63 mm/sec accelerating to a final velocity of 158 mm/sec. The velocity gradient within the renal pelvis may indicate possible mechanism designed for the expression of the papillae. (Supported by NIH Grant #AM19366)

TU-PM-A9 KINETIC ANALYSIS OF Ca^{2+} BINDING TO TROPONIN C. J. David Johnson, Steve Charlton* and James D. Potter, Pharmacology & Cell Biophysics, Univ. of Cincinnati College of Medicine, Cincinnati, OH 45267 & *Biochemistry, Baylor College of Medicine, Houston, TX 77030

Dansylaziridine (DANZ) binds covalently and selectively to a single amino acid residue of TnC to form TnC-DANZ. TnC-DANZ binds Ca^{2+} , undergoes Ca^{2+} induced C.D. changes and complexes with TnI and TnT as does native TnC. Ca^{2+} binding to the Ca^{2+} - Mg^{2+} sites of TnC produces a small ($\sim 10\%$) decrease in TnC-DANZ fluorescence while Ca^{2+} binding to the Ca^{2+} specific regulatory sites of TnC produces a twofold fluorescence increase and a 10nm blueshift in λ_{max} . Using stopped-flow fluorimetry to follow these fluorescence changes we have determined a kinetic scheme for the Ca^{2+} induced structural changes. Ca^{2+} binds to the Ca^{2+} specific sites of TnC within the 2msec mixing time of the instrument. Removal of Ca^{2+} from these sites occurs with a $t_{1/2} \sim 3\text{msec}$. Removal of Ca^{2+} from the Ca^{2+} - Mg^{2+} sites is much slower ($t_{1/2} \sim 700\text{msec}$). Therefore, the Ca^{2+} exchange rate is very rapid for the Ca^{2+} -specific sites and very slow for the Ca^{2+} - Mg^{2+} sites suggesting that the latter are not directly involved in muscle regulation. JDJ is a Fellow of MDA, JDP is an E.I. of AHA.

TU-PM-A7 FLUORESCENT PROBES STUDIES OF TROPOMYOSIN. R.M. Dowben, C. Ford*, L. Wells*, and T.-I. Lin, UTHSCD, Dallas, Texas 75235.

Sulfhydryl-directed fluorescent probes, dansyl aziridine (DAZ), 4-dimethylamino-4'-maleimido-stilbene (DMAMS), and N-(iodoacetylaminomethyl)-5-naphthylamine-1-sulfonic acid were attached to tropomyosin (TM), in molar ratios of 0.58 to 1.56, to study the microenvironment of reactive sites of TM, polymerization of TM, and binding of TM with actin. The shift in emission max of the dyes attached to TM and solvent perturbation studies suggest that the probes are exposed to the solvent. Viscosity studies indicate that SH modification does not impair polymerization of TM nor the binding of TM with actin. Depolymerization of labeled TM all cause significant spectral and intensity changes which were used to monitor the kinetics and equilibrium of polymerization. On adding actin the fluorescence intensities of DMAMS and DAZ labeled TM increase 30 and 250% respectively, in addition, a new 291 nm excitation peak appears indicating both probes become located in a more hydrophobic environment and close to a Trp residue in actin involving energy transfer. The binding behavior of actin with various labeled TM will be discussed. Support by NIH 16678 and Texas Heart.

TU-PM-A10 PYRENE EXCIMER FLUORESCENCE - A PROBE OF CHAIN SEPARATION IN α -TROPOMYOSIN. S.L. Betcher-Lange* and S.S. Lehrer, Dept. Muscle Res., Boston Biomedical Res. Institute, Boston, MA 02114.

The proximity of the 2 Cys 190 SH's of rabbit skeletal α -tropomyosin (α Tm) suggested that N-(1-pyrene)maleimide-labeled α Tm might show pyrene excimer fluorescence. Labeling at pH 6.0 or pH 7.5 resulted in the formation of two spectroscopically distinguishable products, Pyr_1 - α Tm and Pyr_{11} - α Tm, respectively. The fluorescence spectrum of Pyr_{11} - α Tm suggests that it is the product of a secondary reaction between the initially labeled Cys 190 (Pyr_1 - α Tm) and an adjacent Lys (Wu, C-S.C. et al., Biochemistry 15,3007,1976). Both products show a broad excimer band. The GuHCl-induced unfolding of Pyr_{11} - α Tm was studied at pH 7.5 by measuring both excimer fluorescence at 480 nm and ellipticity at 222 nm. The CD unfolding profiles of Pyr_1 - α Tm and α Tm are identical and have a transition midpoint at 2.1 M GuHCl. In contrast, the transition midpoint for loss of excimer fluorescence occurs at 1.5 M GuHCl. These results indicate that chain separation near Cys 90 takes place prior to the major unfolding transition. (Supp. by NIH(HL-5811, AM-11677), NSF (GB24316) and MDA)

TU-PM-A8 A REACTION INVOLVING PROTEIN SULFHYDRYL GROUPS, BOUND SPIN-LABEL, AND $\text{K}_3\text{Fe}(\text{CN})_6$ AS A PROBE OF SULFHYDRYL PROXIMITY IN MYOSIN AND ACTOMYOSIN. Philip Graceffa* and John C. Seidel, Dept. Muscle Res., Boston Biomed. Res. Inst.; and Dept. Neurol., Harvard Med. Sch., Boston.

The EPR spectrum of myosin labeled with iodoacetamide spin-label (SL-M) shows components corresponding to weakly (W) and strongly (S) immobilized labels. $\text{K}_3\text{Fe}(\text{CN})_6$ treatment of SL-M results in the selective destruction of W, by a chemical reaction involving a protein thiol group, with full retention of S and without loss of ATPase activity. $\text{K}_3\text{Fe}(\text{CN})_6$ destroys the EPR signal of a non-protein-bound spin-label only in the presence of a thiol-containing compound. In the presence of MgADP the S component, attributed to labels bound to the SH-1 thiols of SL-M, is lost on adding $\text{K}_3\text{Fe}(\text{CN})_6$ and this loss of signal can be prevented by blocking the SH-2 thiols, supporting the view (Reisler, E., et al., Biochem. 13, 3837, 1974) that SH-1 is near SH-2. F-actin also promotes the $\text{K}_3\text{Fe}(\text{CN})_6$ -induced loss of S of SL-M. The results indicate that $\text{K}_3\text{Fe}(\text{CN})_6$ can be used to selectively remove the weakly immobilized component of the EPR spectrum of SL-M and to detect the proximity of thiol groups in proteins. (Supported by HL-15391 and HL-5811 from NIH and by a grant from MDA.)

TU-PM-A11 QUENCHING OF FLUORESCENCE LIFETIME STUDIES ON THE ENVIRONMENT AND ACCESSIBILITY OF SULFHYDRYLS IN G- AND F-ACTIN. T. Tao and J. Cho*, Boston Biomedical Res. Institut., Boston, MA 02114, and Dept. of Chemistry, New York University, New York, N.Y. 10003.

G-actin labelled with 1,5-IAEDANS exhibits at least 2 components of fluorescence decay. A two exponential method of moments program fits the decay well, yielding a major component (95%) of decay time 17 ns, and a minor component of 33 ns. Acrylamide quenches the major component preferentially over the minor one (quenching constants 23.1 and $6.5 \times 10^4 \text{ M}^{-1}\text{sec}^{-1}$ respectively). Upon polymerization, a nearly single decay time of 19 ns was found. Addition of acrylamide resolves the decay to the two components again, where both become even less susceptible to quenching (quenching constants of 13.5 and $1.52 \times 10^4 \text{ M}^{-1}\text{sec}^{-1}$ respectively). The data is interpreted as follows: for G-actin, the major -SH group lies in a polar environment that is relatively open to the medium. Upon polymerization to F-actin, the site becomes less polar and less accessible, probably due to the presence of a neighboring actin monomer. The minor -SH group lies in a non-polar and inaccessible site that becomes even more inaccessible in F-actin. (Supported by NIH #R01 AM2163-01)

TU-PM-A12 ³¹P NMR OBSERVATION OF THE STEADY STATE INTERMEDIATE IN MYOSIN HYDROLYSIS OF ATP. E.T.Fossel*, Biophysical Laboratory, Harvard Medical School, Boston, Mass. 02115 (Intr. by R.T. Ingwall)

The steady state hydrolysis of ATP by myosin has been observed by ³¹P Nuclear Magnetic Resonance (NMR). In addition to the ³¹P resonances from ATP and the hydrolysis products, ADP and P_i, a resonance which exhibits characteristics of an intermediate and has a chemical shift of -3.6 ppm (relative to 85% phosphoric acid) is observed. Control experiments such as time course studies and inclusion of a myokinase inhibitor allow the conclusion that the resonance represents the monophosphate portion of the intermediate, Myosin:ADP:P. Characterization of the resonance permit the conclusion that the phosphate is covalently bound to myosin through a serine side chain.

TU-PM-A13 FURTHER EVIDENCE OF ATP UPTAKE BY MUSCLE CELLS. I.H. Chaudry, H. Hirasawa* and A.E. Baue*. Dept. of Surg Yale University School of Medicine, New Haven, CT 06510

To demonstrate whether ATP can penetrate the cell membrane, we have studied the uptake of ³²P- and ¹⁴C-ATP mixture. Rat soleus muscles (30 mg) were incubated for 1 hr at 37°C in 1.0 ml of Krebs-HCO₃ buffer containing 10 mM glucose, 5 mM MgCl₂, 2.5 mM 8-¹⁴C-ATP (0.45 μCi/μmole) and 2.5 mM ³²P-ATP (0.45 μCi/μmole) under 95% O₂: 5% CO₂. Following incubation, muscles were rinsed, blotted, frozen and homogenized. Samples of the muscle extract and incubation medium were subjected to electrophoresis. ³²P and ¹⁴C radioactivity in the individual nucleotide spot was counted. The concentration of adenine nucleotides in medium (μmoles/ml) and tissue (μmole/gm) were calculated from the radioactivity observed in each fraction. Extensive degradation of ¹⁴C-ATP and ³²P-ATP was observed in the presence of muscle. The concentrations of both ¹⁴C-ATP and ³²P-ATP found in the muscle were equal indicating that both entered the cell in the same amount. This provides further evidence that ATP can enter the cells perhaps in an active process. (Supported by USPHS Grant 2 R01 HL19673 03 and Army Contract DAMD-17-76-C-6026).

TU-PM-A14 REACTION OF CARDIAC MYOSIN WITH ATP. L.H. Schliselfeld, Dept. of Biological Chemistry, University of Illinois at the Medical Center, Chicago, IL. 60612

The ATPase activity of beef heart myosin was determined in 15-30 mM NaCl plus KCl and 1.0 mM MgSO₄ at pH 7.4 and 25°. Between 25 and 750 nM ATP the ATPase follows a hyperbolic curve with a K_m of 0.036 μM, which is one-sixth the K_m obtained from skeletal muscle myosin, 0.229 μM. The V_{max} obtained by extrapolation to saturating ATP levels is 0.47 nmoles P_i formed/min/mg protein, which is significantly less than the specific activity measured in 1.0 mM ATP. The specific activity measured in 1.0 mM ATP is constant at 3.0 nmoles P_i/min/mg from pH 5.9 through pH 8.2; then it rises to 5.2 nmoles P_i/min/mg as the pH rises to 9.2. NaCl and EDTA are inhibitors of the Mg²⁺-ATPase. Addition of F-actin to cardiac myosin causes an increase in the ATPase that is a hyperbolic function of the F-actin concentration. The K_m for F-actin is 0.32 μM and the specific activity at saturating levels of F-actin is 35 nmoles P_i/min/mg myosin. At low salt cardiac myosin binds adenylyl imidodiphosphate with a K_D of 0.0581 μM. (Supported by Grants from the Public Health Service No. HL 18179-03 and the Chicago Heart Association).

TU-PM-A15 pH AND CO₂ EFFECTS ON CRAYFISH SLOW MUSCLE.

W. Moody* (Intr. by S. Hagiwara), Los Angeles, CA 90024

Electrophysiological effects of changes in external pH and CO₂ were studied in slow flexor muscle fibers of crayfish (*P. clarkii*). These fibers give only small graded responses when depolarized; steady-state I-V plots (constant current) show an increase in conductance for depolarizations greater than 25-30mV (delayed rectification). Lowering the external pH from 7.4 to 5.6 had little effect on input resistance, rectification, or depolarizing responses. Changing from pH 5.6 HEPES to pH 5.6 HCO₃-100%CO₂ Ringer's caused the rapid appearance of action potential responses to depolarization in all fibers tested; this effect was reversible in pH 5.6 HEPES. I-V plots in the presence of CO₂ showed a marked decrease in the rectification seen; this effect was also seen in fibers bathed in Mn⁺⁺ to block the action potential. The effect of CO₂ was often, but not always, accompanied by an increase in input resistance. These data suggest that CO₂, probably by lowering the internal pH of the fibers, blocks a voltage sensitive K⁺ conductance that normally limits the size of the depolarizing response. (Supported by a postdoctoral fellowship from the Helen Hay Whitney Fdn. and USPHS 09012).

PHOTOSYNTHESIS II

TU-PM-B1 PICOSECOND STUDIES OF COVALENTLY LINKED CHLOROPHYLL DIMERS. M. J. Peillon*, M. Wasielewski, and K. J. Kaufmann, Departments of Chemistry, University of Illinois, Champaign, IL 61801 and Argonne National Laboratories, Argonne, IL 60439.

It has been suggested by several workers that a "special pair" of chlorophyll molecules play a central role in the primary events of photosynthesis. Recently a covalently bound dimer of chlorophyll a has been synthesized. Upon the addition of water or alcohol this dimer folds into a species which exhibits ESR, ENDOR and absorbance spectra reminiscent of the in vivo "special pair". Picosecond absorption spectroscopy and picosecond fluorescence spectroscopy have been employed to study the photochemistry of the covalent dimers on timescales appropriate to primary processes in photosynthesis. Covalently linked chlorophyll a dimers and pyrochlorophyll a dimers have been studied in both their folded and unfolded forms. Results of this study indicate that the environment has a strong effect on the fluorescence lifetime and hence on the electron transfer properties of these dimeric species. This work was supported by the National Science Foundation and the Department of Energy.

TU-PM-B2 FORSTER TRANSFER OF SINGLET EXCITATION ENERGY.

L. L. Shipman, Chemistry Division, Argonne National Laboratory, Argonne, Illinois 60439

The Förster mechanism for migration of singlet excitation has been re-examined and improved in several respects. In addition, Förster transfer parameters have been computed for transfer between chlorophyll *a* molecules over a wide range of Stokes shifts. These parameters have been applied to a kinetic model of the excitation of chlorophyll *a* dimer and the subsequent decay of the excitation by both radiative and nonradiative paths.

This work was performed under the auspices of the Division of Basic Energy Sciences of the U.S. Department of Energy.

TU-PM-B3 PHOTOELECTRON TRANSFER IN PORPHYRINS.

S.G. Ballard^a and D. Mauzerall, Rockefeller Univ. New York, N.Y.

The rate of formation and yields of ions ($P^+ + P^-$) from triplet and ground (T+P) and triplet and triplet (T+T) zinc octaethylporphyrin (P) were measured by conductance changes in various solvents. Analysis of the encounter limited rate of the T+T reaction and of the yield of ions as function of dielectric constant furnishes the distance of electron transfer: 21 ± 1 Å. This is 6 Å larger than the sum of the radii of 2P and is attributed to electron tunneling through solvent. This view of charge transfer on a time scale shorter than dielectric relaxation is supported by independence of dielectric constant of the rate of the T-T reaction. The importance of electron spin states is shown by the smaller yield of uncorrelated ions from the highly exothermic T+T reaction than from the nearly equi-energetic T+P reaction. Confirmation of the spin effects were obtained by observing the increase of ion yield from the T-T reaction as a function of increasing (50 gauss) magnetic field. The kinetics of ion formation and decay are unchanged by the magnetic field, showing that the spin selection effect is on the geminate ion recombination. We predict these effects will be larger and anisotropic in oriented systems.

TU-PM-B4 THEORY OF PROTON HYPERFINE INTERACTIONS IN BACTERIOCHLOROPHYLL CATION AND ANION.

Jane C. Chang and T. P. Das, SUNY, Albany, N. Y. 12222

ESR and ENDOR measurements¹ have shown that bacteriochlorophyll dimer cation ($BChl^+$), is the primary electron donor in reaction center. Continuing our studies in the electronic structures of bacteriochlorophyll derivatives,² we have used the self-consistent charge extended Hückel method including π and δ electrons to study hyperfine interactions in $BChl^+$ a cation and anion the calculated unpaired spin distribution provide proton hyperfine constants in both systems, in good agreement with experiment. The trends of changes in proton hyperfine constants in going from $BChl^+$ cation to anion is explained. The general features in the calculated proton hyperfine interaction in $BChl^+$ a cation and anion are similar to those in bacteriopheophytin (BPh⁺) a cation and anion, as shown also experimentally. Details of electron distributions in $BChl^+$ cation and anion, and comparison with those in BPh⁺ cation and anion will be discussed.

¹G. Feher et al. Ann. NY Acad. Sci. 244, 239 (1975); J.R. Norris et al. ibid. 244, 260 (1975); D.C. Borg et al. J. Am. Chem. Soc. 98, 6889 (1976).

²J.C. Chang, T.P. Das, Biochim. Biophys. Acta, in press.

TU-PM-B5 ¹⁴N HYPERFINE INTERACTIONS IN CATION AND ANION OF BACTERIOPHEOPHYTIN.

Jane C. Chang and T. P. Das,

Department of Physics, SUNY, Albany, N. Y. 12222

We have recently obtained (Bull. Am. Phys. Soc. 22, 277- (1977)) the electronic wave-functions for BPh⁺ a and BPh⁻ a which successfully explained the significant difference experimentally observed in the methyl proton hyperfine constants in rings I and III for BPh⁺ a and their near equality in BPh⁻ a. These wave-functions have now been utilized to analyze the ¹⁴N hyperfine constants a_N . Using a semi-empirical formula (Stone, Maki, J. Chem. Phys. 39, 1635 (1963)) relating the spin populations to a_N , we get for the ¹⁴N of the four rings, in Gauss $a_N(I) = -0.26, 0.03$; $a_N(II) = -0.21, 3.15$; $a_N(III) = -0.36, 0.23$; $a_N(IV) = -0.48, 3.10$, the first and second number in each case referring to the cation and anion respectively. Our results agree with the features of the experimental data which indicate a) that the a_N for the four cation ¹⁴N nuclei (McElroy, Feher, Mauzerall, Biochim. Biophys. Acta 267, 363 (1972); Borg, Forman, Fajer, J. Am. Chem. Soc. 98, 6889 (1976); Hoff, Möbius (to be publ.)) are nearly equal while for the anion (Fajer, Brune, Davis, Forman, Spaulding, Proc. Nat. Acad. Sci. 72, 4956 (1975)) only two are dominant and b) that a_N for the anion are larger than in cation.

TU-PM-B6 ESR STUDY OF ORIENTED PHOTOSYNTHETIC MEMBRANES.

Brian J. Hales, Department of Chemistry, Louisiana State University, Baton Rouge, LA 70803

Membranes oriented on quartz slides have been used to investigate the structure of both the membrane as well as the membrane-bound proteins of photosynthetic bacteria. Nitroxide spin labels have been incorporated into these membranes to monitor their degree of orientation and fluidity under the perturbing effects of irradiation and pH and ionic strength changes. The membrane-bound paramagnetic proteins of the bacterium's electron transport chain have also been studied with low temperature esr spectroscopy in order to determine the orientation of the principal axes of these paramagnetic species in their native membrane. It will be shown that determination of the principal axes is best accomplished through the uses of transverse modulation (where the field of the modulation coils is placed perpendicular to the external magnetic field) and computer simulation. When transverse modulation is used only the anisotropic components of the spectrum are observed facilitating the determination of the principal axis system.

TU-PM-B7 LIGHT TRANSDUCTION BY PIGMENTED BILAYER LIPID MEMBRANES.

H. Ti Tien, Biophysics Department, Michigan State University, East Lansing, Michigan, 48824

Certain photoeffects observed in pigmented bilayer lipid membranes (BLM)⁺ are explained in terms similar to those that take place at semiconductor/electrolyte interfaces. There are two distinct steps in the light transduction: (1) photoexcitation of pigment molecules in and/or adjacent to the BLM to generate electrons and holes via exciton dissociation, and (2) electrons and holes effect redox reactions across the membrane. The existence of two redox solution interfaces connected by an ultrathin lipid bilayer make exciton-exciton fusion possible, thereby providing a mechanism for generating higher energetic species for water oxidation than are available in the exciting light. The scheme has been applied to the thylakoid membrane of chloroplasts and the purple membrane of *H. halobium*.

1. Photochem. Photobiol., 24, No. 2 (1976).

(Supported by a PHS grant GM-14971)

TU-PM-B8 PHOTO-INDUCED VOLTAGES IN SUSPENSIONS OF CHLOROPLASTS ORIENTED IN A MAGNETIC FIELD. J.F. Becker, N.E. Geacintov, and C.E. Swenberg, Dept. of Chemistry and The Radiation and Solid State Laboratory, New York University, New York, N.Y. 10003.

The photovoltage of suspensions of magnetically oriented spinach chloroplasts using polarized light has been measured. The magnitude of this photoemf depends on the polarization of the light and on its direction of propagation with respect to the membrane planes. The photoemf is qualitatively interpreted in terms of the Demer effect, and its magnitude depends on a nonhomogeneous generation of positive and negative charges, and is thus a function of the absorption coefficient. The photoemf arises because of an inhomogeneous absorption of light within a chloroplast particle which is due to the non-random orientation of chlorophyll molecules in the membranes. This gives rise to an inhomogeneous distribution of positive and negative charges along the direction defined by the propagation vector of the light (which is parallel to the vector joining the two electrodes). An emf arises due to the diffusion of these charges, but only when the mobility of the two charges carriers is unequal. This work demonstrates the existence of a Demer-like solid state effect in a biological system. (Supported by NSF Grant PCM76-14359 and in part by USERDA)

TU-PM-B9 Cation Effects on Chlorophyll a Fluorescence at Low Temperature. D. WONG, H. MERKEL, and

GOVINDJEE, Univ. of Ill. Urbana-Champaign. -- Studies on chlorophyll a fluorescence at 77°K in sucrose-washed chloroplasts have shown that the addition of low concentrations (<10 mM) of monovalent cations decrease the ratios of fluorescence at 685 nm (F685) and 695 nm (F695) to that at 730 nm (F730), and that subsequent addition of divalent cations increase these ratios (E.L. Gross and S.C. Hess, Arch. Biochem. Biophys., 159, 832-836, 1973). These intensity changes have previously been ascribed to alterations in fluorescence yields. We have measured the fluorescence lifetimes τ (F685), τ (F695), and τ (F730) at 77°K upon excitation at 633 nm. Our results show that 10 mM NaCl has no effect on τ (F685) and τ (F695) but slightly increases τ (F730). Subsequent addition of 10 mM MgCl₂ increases τ (F685) and τ (F695) by 30-50% with no significant change in τ (F730). Together with the results from parallel measurements of the fluorescence transients of F690 and F730 at 77°K, we conclude that cations affect the rate constants of radiationless processes in the singlet excited chlorophyll a molecules. These changes, however, do not exclude the existence of excitation energy transfer from system II to I.

TU-PM-B10 PROBES OF LIGHT-INDUCED ENERGISATION OF INTACT CHLOROPLASTS. J. D. Mills, R. E. Slovacek and G. Hind Brookhaven National Laboratory, Biology Department, Upton, New York 11973.

The outer envelope of isolated intact chloroplasts presents a barrier to the direct measurement of the Δ pH gradient developed across the enclosed thylakoids. This information is important in resolving the controversial bioenergetics of *in vivo* photosynthesis. It will be shown that both intrinsic (chlorophyll a fluorescence, light scattering) and extrinsic (9-aminoacridine fluorescence) optical probes may be used to monitor the light-induced energisation of isolated intact chloroplasts. Although only semi-quantitative at best, the results indicate that under aerobic conditions, photophosphorylation can be powered by non-cyclic, pseudocyclic and cyclic coupled electron transport. Appropriate use of electron transport acceptors and inhibitors allows selection of conditions under which any one of these three types of electron transport predominates. It is concluded that all three electron transport systems contribute to the energisation of the thylakoid which results in ATP synthesis during the most active periods of CO₂ fixation *in vivo*. (Research supported by U.S.D.O.E.)

TU-PM-B11 PROTON UTILIZATION PATHWAYS IN THE ATP COUPLING MECHANISM OF SPINACH THYLAKOID MEMBRANES, D.P. O'Keefe*, and R.A. Dilley, Dept. of Biol. Sciences, Purdue Univ., W. Lafayette, IN 47907

We have proposed that protons may be used by the ATP coupling mechanism without obligate deposition in the inner osmotic space (BBA 449:95,1976). We have attempted to determine the rate limiting steps occurring in ATP synthesis driven by protons from endogenous buffering groups compared to protons from exogenous permeant buffers. Using the initial kinetics of acid-base phosphorylation, we have found that utilization of protons from a permeant buffer or from the endogenous buffer share a common rate limiting step. By comparing rates of phosphorylation and amounts of proton uptake under conditions of varying steady state electron transport rates, we have found that permeant buffers will increase the threshold amount of H⁺ uptake necessary to initiate phosphorylation, by an amount proportional to the amount of internal exogenous buffer, as expected from the chemiosmotic hypothesis. These results also could reflect proton equilibration of intramembranous protons with the inner osmotic space under steady state conditions.

TU-PM-B12 GLUCOSE INHIBITION OF CHLOROPLAST DEVELOPMENT F. D. Schwelitz, P. Cisneros,* J. Jagielo,* and K. Butterfield.* Dayton, Ohio 45469

The inhibition of chloroplast development observed in cells greening in an ethanol-containing medium appears to differ from that in cells greening in a glucose-containing medium. Addition of ammonium sulfate to the medium brings immediate relief from chloroplast inhibition in cells greening in the presence of ethanol but not glucose. Cells greening in a glucose-medium show an inhibition in development of photosystem II but not photosystem I. Comparison of cells greening in a glucose medium with those greening in the presence of chloramphenicol show many similarities in their inhibition of chloroplast development when the ultrastructure and other aspects of the two cell types are studied. These studies suggest that *Euglena* may have a mechanism similar to catabolite repression in bacteria and that cAMP may be involved in such a system. (Supported by NIH grant GM 22611).

NEUROBIOLOGY II

TU-PM-C1 INCREASE IN DESENSITIZATION RATE OF THE ACETYLCHOLINE RECEPTOR BY DRUGS. R. Anwyl* and T. Narahashi. Northwestern Univ. Med. Sch., Chicago, IL 60611.

Desensitization of extrajunctional acetylcholine (ACh) receptors of denervated rat soleus muscle as evoked by repetitive iontophoretic applications of ACh at 5-10 Hz occurred in three exponential phases, with half-times of 0.05-0.1 sec, 0.5-1.5 sec and 1-100 sec. Increasing the dose of ACh, or perfusing cytochalasin B or chlorpromazine increased the rate of desensitization solely by accelerating its slowest phase. Triton X-100 accelerated both the intermediate and slowest phases. The half-time of desensitization was decreased 50% by 0.0005% Triton X-100, 1×10^{-5} M cytochalasin B or 1×10^{-6} M chlorpromazine. Cytochalasin B, chlorpromazine or altering the ACh dose did not alter the half-time of recovery from desensitization (4.3 sec). Triton X-100 slowed recovery 2-3 fold. On the basis of the cyclical kinetic scheme of desensitization (Katz & Thesleff, 1957), it is suggested that the above agents increase desensitization rate by binding preferentially to the desensitized state of the receptor. Supported by NIH grant 14145.

TU-PM-C2 KINETICS OF RECOVERY FROM CILIARY ARREST MEASURE EPITHELIAL CELL COUPLING William Reed* and Peter Satir, AECOM, N.Y., N.Y. 10461 and UC, Berkeley, Cal. 94720

In the presence of 10^{-2} M Ca^{2+} , local laser micro-injury of the lateral cell ciliated epithelium along a single gill filament of the lamellibranch mussel *Elliptio* induces temporary cessation of active ciliary beat for distances up to 1.5 mm to either side of the stimulus. As activity returns, cells farther from the lesion reactivate earlier than cells closer to the lesion so that recovery spreads from the periphery backwards toward the point of stimulation. The variation of recovery time with distance from the lesion has three distinct forms which are qualitatively similar to the variation of potential with distance along a one-dimensional cable of varying length and under varying stimulus conditions. We suggest that the time of recovery for a particular distance from the lesion is proportional to the change in membrane potential arising at that position due to the electrotonic spread of a lesion-induced depolarization. The time course of recovery may then be used to determine the space constant of the epithelium which functions as a measure of coupling between lateral cells. Supported by HL22560

TU-PM-C3 ELECTRIC FIELD INDUCED REDISTRIBUTION OF ACETYLCHOLINE SENSITIVITY IN XENOPUS EMBRYONIC MUSCLE CELL MEMBRANE. N. Orida* and M.-m. Poo, Dept. of Physiology, Univ. of California, Irvine, CA 92717.

Distribution of acetylcholine (ACh) sensitivity on the surface of spherical, 2-day old cultured embryonic muscle cells (av. dia. 35 μm) was mapped and expressed in volts depolarization/nanocoulomb of charge ejected from the ACh pipette. In control cultures, ACh sensitivity, uniform around the cell perimeter, was 10.8 ± 2.2 s.e. V/nC ($N=27$). When a steady electric field of 10V/cm was applied along the culture substratum for 1.5 hr, an asymmetry of ACh sensitivity was observed. For 14 cells mapped in 3 separate experiments, higher sensitivity (20.3 ± 3.5 s.e. V/nC) was consistently observed on the pole of the cell facing the cathode of the field, while a lower sensitivity (5.0 ± 1.2 s.e. V/nC) was observed on the opposite pole facing the anode. We also observed field-induced asymmetric sensitivity to iontophoretically applied carbachol, a non-hydrolyzable ACh analog. No asymmetric sensitivity was observed when the cultures were pre-incubated with concanavalin A prior to the application of the field. These results are consistent with the notion that redistribution of ACh sensitivity is due to the electrophoretic redistribution of ACh receptors in the membrane plane.

TU-PM-C4 SHAPE ANALYSIS OF ACETYLCHOLINE RECEPTOR BY NEUTRON SCATTERING. D. Wise, A. Karlin*, and B. Schoenborn, Dept. of Neurology, Coll. of Physicians and Surgeons, Columbia Univ., N.Y., N.Y. 10032, and Dept. of Biology, Brookhaven Natl. Lab., Upton, N.Y. 11973

Acetylcholine receptor (AChR) from *Torpedo californica* electric tissue in 0.2% Triton X-100, 50 mM NaCl, 10 mM NaPO_4 (pH 7.0), 1 mM EDTA, 3 mM NaN_3 , and either H_2O or D_2O , was reduced with dithiothreitol to convert all AChR to the monomer form. Neutron scattering data were collected on mixtures containing 0.5 to 2 mg AChR per ml in 0% to 100% D_2O . The analysis indicates that AChR monomer has a radius of gyration (R_g) of 44 ± 7 Å in buffer adjusted to the contrast-match point of Triton X-100 ($16 \pm 2\%$ D_2O). If the AChR monomer were a compact sphere, it would have a R_g of 32 Å. The angular dependence of the scattering intensity is consistent with either a prolate (2.5:1) or oblate (4:1) ellipsoidal shape for the AChR-detergent complex. From the contrast-match point of the complex ($32 \pm 2\%$ D_2O), we calculate that 180 ± 35 Triton X-100 molecules are bound per AChR monomer. (Supported by NIH, NSF, and ERDA. D.W. is a MDA Postdoctoral Fellow.)

TU-PM-C5 HOLOGRAPHIC VISUALIZATION OF THE NERVE IMPULSE. M. Sharnoff, Dept. Physics, Univ. Delaware, Newark, DE 19711 and R. W. Henry and D. M. J. Bellezza, Dept. Physics, Bucknell Univ., Lewisburg, Penna. 17837.

Segmental ganglia of the leech *Hirudo medicinalis* were excised and selected somatosensory T, P, and N cells were impaled with a glass microelectrode containing 4 M KAc. These cells were rhythmically stimulated by depolarizing intracellular current pulses ca 3 nA in amplitude and ca 20 msec long. Their action potentials (AP) were monitored by a high impedance amplifier connected to the microelectrode. The preparation was illuminated by pulsed laser light at 6471 Å and the scattered light was transmitted via magnifying optics to a holographic plate illuminated also with a plane reference wave. Double exposure holograms were recorded with one exposure occurring several msec prior to an AP in the impaled cell and the other at a predetermined point in the AP waveform. Between exposures the reference wave was shifted 180° in phase. Images reconstructed from such holograms are differential images and show the electrically active, stimulated cell brightly silhouetted against the dimmer background of quiescent neighbors. These silhouettes are not present in images obtained from control holograms made without stimulus.

TU-PM-C6 TESTING A RADIAL MODEL FOR POSITIONAL INFORMATION IN THE DEVELOPMENT OF FROG RETINOTECTAL SPECIFICITY. K.Tosney*, S.Hoskins*, R.K.Hunt, MBL, WoodsHole, MA, and Biophysics Dept., Johns Hopkins Univ., Balto., MD 21218

French et al (Science 193:969) have used (r,θ)-coding with two operative rules to elegantly explain data on cell patterning in limb morphogenesis from cockroach to newt. The model is compatible with published data on locus-specific differentiation in *Xenopus* retina (for retinotectal patterns) and with the retina's radial growth mechanics. We here refute the model for *Xenopus* retina, based on electrophysiologic analysis of retinotectal patterns, following embryonic surgeries built around ablation of a 'non-Cartesian half' (posterodorsal 40-60%; PD) of st. 32 right eyebuds. Predictions of the model were not upheld in four separate protocols involving the residual anteroventral (AV) fragment, including leaving it to round-up alone (Predict pattern duplication with mirror-symmetry about an AV-line 45°-off vertical; Obtain normal maps and "Cartesian" duplications about horizontal or vertical meridian) and fusion with a grafted PD-fragment from a left eye (Predict duplications; Obtain normal map). The data argue against radial coding or for different operative rules. (Support by NIH NS-12606; HD-07098).

TU-PM-C7 NEUROPLASTICITY IN XENOPUS. S.Fraser, R.K.Hunt, Biophysics Dept., Johns Hopkins Univ., Balto., MD 21218

Tadpole stages are characterized by annular growth of the retina and optic fiber innervation of the contralateral midbrain tectum (e.g., right eye to left tectum, RE-LT). Larval left-eye removal (St. 56) induces an anomalous ipsilateral (RE-RT) projection in addition to the normal RE-LT map. Electrophysiologic recording showed the RE-RT map was confined to peripheral retina (perhaps to cells added after St. 56) and was topographic but inappropriately ordered: lateral, central and medial regions of the tectum received input in turn from temporal, ventral and nasal retina. Normal rostrocaudal ordering was subjugated to this abnormal mediolateral ordering. Surgical interruption of intertectal visual relay, single unit characterization of the RE-RT visual input, and histologic reconstruction of optic pathways all implicated direct innervation of RT by RE optic fibers. Peripheral retinal fibers thus map differently when alone (RE-RT) or in competition with central retinal fibers (RE-LT). Controls in which all optic fibers were deflected ipsilaterally gave normal maps, ruling out R-L differences and further implicating the presence of central fibers as the causative factor. (Supported by NS-12606 from NIH)

TU-PM-C8 FRACTIONATION OF SIGNALS FOR RETINOTECTAL PATTERNING IN XENOPUS. B.Kosofsky*, C.F. Ide, R.K. Hunt, Biophysics Dept., Johns Hopkins Univ., Balti., MD 21218

Hunt & Frank (Science 189:563) described a surgical recombination of embryonic eye fragments (St.32), in which a dominant fragment A (anterior half of right eye) reprogrammed a slave fragment P (posterior half of left eye) to become its 'mirror image' twinned pattern. We have now isolated fragment combinations which show discrete subfeatures of reprogramming. Normal retinotectal patterns predominate (assayed electrophysiologically after metamorphosis) when the anterior half of St.32 right eye is recombined with dorsal half of another St.32 right eye; chimeric eyes for the Oxford (1-nucleolate) marker confirm the dorsal fragment survives and has been reprogrammed by the anterior fragment into its posterior complement. Conversely, smaller A or P fragments, allowed to round-up alone to form intact eyes, assemble mirror-symmetrical duplicate patterns; but when the two interact, each suppresses duplication in the other over about 30 hrs with no changes in pattern orientation. Thus reprogramming signals may involve discrete components of pattern duplication and pattern orientation. (Supported by NIH NS-12606 and NSF BMS-75-18998).

TU-PM-C9 POSITIONAL SIGNALLING IN CHIMERIC XENOPUS RETINAE. C.F.Ide and R.K.Hunt, (Intr. by M.G.Larrabee) Jenkins Dept. of Biophysics, The Johns Hopkins U., Baltimore Md. 21218

Positional signalling at the retinal margin was studied by grafting previously-specified areas of retina for other areas, e.g., small group of 20 to 50 ventral pole cells for posterior pole cells (donor graft marked by Oxford 1 nucleolate marker/pigmented, host by 2 nucleolate/albino marker). Grafted tissues grow out radially as contiguous pie-slice 'polyclones'. Orthotopic (replacement) pole and center strip grafts give normal maps; heterotopic pole grafts retain their donor position identity, mapping as partial duplicate pie slices in the host map; but occasionally invert their rostral-caudal or medio-lateral ordering on the tectum according to host position. Similarly, exchanging dorso-ventral meridional 1/3 strip from left to right eye (short axis inverted) reprograms donor polyclones along Cartesian axes, via local interactions with host tissues. Positional values are then propagated radially during subsequent growth. Factors involved in reprogramming "polyclones" may also account for "global" re-polarizations seen in recombinant half eyes. Support by NIH (HD-0798; NS-12606).

TU-PM-C10 VOLTAGE-CLAMP STUDIES OF A POTASSIUM MEDIATED HYPERPOLARIZING ACTION POTENTIAL IN NEMATODE PHARYNGEAL MUSCLE. L. Byerly and M.O. Masuda*, Dept. of Physiology, U.C.L.A., Medical School, Los Angeles, Calif. 90024.

Del Castillo and collaborators recorded hyperpolarizing action potentials from the pharyngeal muscle of *Ascaris lumbricoides* and concluded they were produced by an increased permeability to potassium (J. Gen. Physiol. 50:603, 1967). Using voltage-clamp methods, we have found that this potassium current is an inverted analogue of the usual sodium current of muscle and nerve; it is activated by hyperpolarizing steps, inactivates and is released from inactivation by depolarization. Little outward current flows while the active membrane is held at a depolarized level, but the step back to the resting level (-40 mV) elicits a large transient current. The direction of this current reverses at E_K . The time constants for both inactivation and release from inactivation are 40-100 msec. Release from inactivation occurs at potentials more positive than -10 mV, and threshold for activation is about -15 mV; these potential levels are independent of E_K . This current is not blocked by TEA, 4AP, Ba⁺⁺ or Cs⁺. Supported by USPHS Grant NS09012, USPHS Fellowship 1F32 NS05479-01, and CNPq (Brazil).

TU-PM-C11 BLOOD-BRAIN, BLOOD-VITREOUS HUMOR AND PLACENTAL BARRIER MODIFICATION DUE TO MICROWAVE EXPOSURE.

A. H. Frey and E. Coren*, Randomline, Inc., Huntingdon Valley, Pennsylvania, 19006

In a series of studies, Frey, Feld, and Frey (1975), Albert (1976), and Oscar and Hawkins (1977) have found that there is modification of the blood-brain barrier when an animal is exposed to low-intensity microwave energy. Fluorescent dye, radioisotopes, and horseradish peroxidase were used as tracers in these studies. It was found that barrier opening occurs with average power densities between 0.01 and 10 mW/cm². Modulated energy is more effective than continuous wave energy. We have extended these studies with experiments on the blood-vitreous humor barrier of the eye and the placental barrier to gain additional insight into the mechanisms underlying this phenomenon. We shall present data showing a modification of the blood-vitreous humor barrier and lack of modification of the placental barrier under exposure to the energy.

TU-PM-C12 ACCOMODATION IN LOCUS COERULEUS. T. Usdin*, T. Svensson*, Intr. by F. Carlson, Dept. Pharmacology, Goteborg Sweden.

The locus coeruleus (LC) consists almost entirely of tonically active noradrenergic (NA) cell bodies, which are decelerated by α -receptor agonists (NA and clonidine (Clon)) and accelerated by some blocking agents (yohimbine (Yoh) and piperoxane) but not by others, (phenoxybenzamine (Phb) and prazosin (Prz)) leading to two classifications for their receptors. Tricyclic antidepressants imipramine (Imi) and desipramine (Dmi) decelerate LC unit firing perhaps by increasing synaptically available transmitter. Imi has been reported to initially decrease NA turnover but increase it after chronic treatment. We report, from intracellular recordings in rats that Phb and Prz do not affect the deceleration of LC unit firing by Imi, Dmi, or Clon and that Yoh reversed their inhibition and partially blocked the effects of Imi and Clon. The LC units of rats treated chronically with Imi (30mg/kg/12 hr:ip) had 1/2 the firing rate of controls (1.3 ± 2 vs 2.6 ± 2) and decreased sensitivity. Interpretations include adaptation in the α -receptor or blocking by high doses of Imi or its metabolite Dmi. It may provide insight into the 10 day delay for clinical efficacy for the tricyclics.

TU-PM-D2 STEREOCHEMICAL STUDIES OF DNA FOLDING AND DNA SUPERCOILS: STRUCTURAL ASPECTS OF THE UNWINDING AND WINDING OF DOUBLE-HELICAL DNA. Chun-che Tsai, S-C. Kao† and David C. Lash*, Department of Chemistry, Kent State University, Kent, Ohio 44242

Structural and geometrical analyses, with the stereochemical information deduced from the existing X-ray diffraction data of DNA fibers and nucleic acid components, have been applied to investigate the stereochemistry of the folding of double-stranded DNA. A stereochemical scheme for the unwinding or winding of double-helical DNA has been proposed. The stereochemical features and principles that have emerged from these studies will be described at the meeting. These include the stacking pattern between adjacent base-pairs (i.e., the angle between adjacent base-pair planes, the angular twist between adjacent base-pairs, the orientation and position of base-pair with respect to adjacent base-pairs), the orientation and position of base-pairs with respect to the helix axis, the sugar puckering pattern, and a detailed sequence of conformational changes leading to the unwinding or winding of double-helical DNA.

TU-PM-D3 THEORETICAL CALCULATIONS OF CONFORMATIONAL PREFERENCES IN DINUCLEOSIDE MONOPHOSPHATES. IMPLICATIONS FOR RECOGNITION BY EXONUCLEASES. Ravindra Tewari and Steven S. Danyluk, Division of Biol. and Med. Research, Argonne National Laboratory, Argonne, IL 60439

A detailed theoretical study by the PCILO method of conformational preferences for dinucleoside monophosphates UpU and ApA reveals a close similarity between overall UpU and ApA conformations. Specific preferences about the key conformational bonds are C4'-C5' ($\psi = 60^\circ$), C5'-O5' ($\phi = 180^\circ$), P-O3' ($\omega = 310^\circ$), O3'-C3' ($\phi = 210^\circ$), C1'-N ($\chi = 20^\circ$), P-O5' ($\omega = 110^\circ$), for nucleotidyl units with C3'-endo ribose pucker. Except for the P-O5' torsion angle, the values conform to the most frequently observed patterns in structural data for monomers and polynucleotides. An analysis of possible intra-molecular interactions indicates hydrogen bonding between the 3'-OH group and O2 (in uracil) or N3 (in adenine) of bases at the 5' terminal as the source of stabilization for the unique $\omega = 110^\circ$ preference. This new possibility also provides a unique mechanism for stabilization at 3' terminals of polynucleotides. An interaction of this type may be of significance in conferring recognition properties for specific exonucleases. (Work supported by the U.S. DOE.)

NUCLEIC ACID STRUCTURES

TU-PM-D1 THE STRUCTURE OF THE BARIUM SALT OF DNA. C. Auer*, J.H. Venable, Jr., and L.S. Lerman, Dept. of Molecular Biology, Vanderbilt University, Nashville, TN 37235, and Dept. of Biological Sciences, S.U.N.Y. Albany, Albany, NY 12222.

Oriented, crystalline fibers of the barium salt of DNA were prepared and examined by X-ray diffraction. At relative humidities below 75%, Ba⁺⁺-DNA is in the monoclinic A structure. Although the unit cells for Ba⁺⁺-ADNA and Na⁺-ADNA are identical, intensity differences exist which are attributable to a major contribution of the Ba⁺⁺ ions to the diffraction. Patterson maps suggest that the Ba⁺⁺ ions are arranged in a regular helical array. The positions of the Ba⁺⁺ ions in the A-DNA structure have been determined using a least squares refinement ($r=8.2 \text{ \AA}$, $\theta=61.3^\circ$, $z=6.9 \text{ \AA}$). Ba⁺⁺ binding sites are located between three non-chain oxygen atoms of adjacent phosphate groups. Ba⁺⁺ - O bond distances average 2.8 \AA . The structure of the binding site is very similar to cation-binding sites of related molecules. At relative humidities above 75%, Ba⁺⁺-DNA is observed only in the B conformation. These results, coupled with results of similar studies of Ca⁺⁺-DNA, Mg⁺⁺-DNA, and Mn⁺⁺-DNA, suggest a specific role for cations in the B to A conformational transition of DNA.

TU-PM-D4 INVESTIGATION OF GLYCOSYL TORSION ANGLES IN MODEL PYRIMIDINE NUCLEOSIDES: VARIATION IN SPIN-LATTICE RELAXATION TIMES. Alice M. Wyrwicz,¹ Malcolm MacCoss*, and Steven S. Danyluk, Div. of Biol. and Med. Res., Argonne National Laboratory, Argonne, IL 60439

Proton and ¹³C spin lattice relaxation times, T₁, were measured for a series of uridine anhydro cyclonucleosides in which the uracil ring is rigidly fused to the sugar moiety. Since the glycosyl torsion angle is rigidly fixed in the latter compound, a means is available for correlation of relaxation behavior with χ_{CN} .

Analysis of the data shows that the ratio T₁H₆/T₁H₁' varies with χ_{CN} in a highly specific manner. This observation and its relevance to the study of the conformation about the N₁-C₁' bond in naturally occurring pyrimidine nucleosides/tides will be discussed. (Work supported by the U.S. DOE.)

¹Present address: Dept. of Chemistry, University of Illinois at Chicago Circle, Chicago, IL 60680

TU-PM-D5 REACTIONS OF HYDROXYL RADICALS WITH DIHYDRO-PYRIMIDINE BASES: AN ESR-SPIN TRAPPING STUDY, S. N. Rustgi, National Cancer Institute, Bethesda, MD 20014

The reactions of OH radicals with dihydro derivatives of uracil, 1-methyluracil, 6-methyluracil, 1-ethyluracil, 5-methylcytosine, thymine and orotic acid in aqueous solutions have been investigated by the ESR-spin trapping technique. OH radicals were generated by the UV photolysis of H_2O_2 and t-nitrosobutane was used as the spin-trapping reagent. Predominant reaction in all cases was the abstraction of the H atoms attached to the C(6) position. To a lesser extent H abstraction took place from the methyl groups attached to the N(1), C(5) and C(6) positions. For dihydro-1-ethyluracil, H atoms were abstracted from both the carbons of the ethyl group. The radicals formed by H abstraction from the C(5) or C(6) positions of the dihydropyrimidines are equivalent to those formed by H addition to the C(5)-C(6) double bonds of the corresponding pyrimidines. Hence the present results are helpful in distinguishing between the spin-trapped radicals formed by H or OH addition to the C(5)-C(6) double bond of pyrimidines in gamma-irradiated aqueous solutions.

TU-PM-D6 RING-CURRENT EFFECTS ON ^{13}C -NMR OF PURINE. D.M. Cheng*, L.S. Kan, and P.O.P. Ts'o. (Intr. by S.A. Lesko) Div. of Biophysics, J. Hopkins U., Balt., MD 21205

The ring-current magnetic anisotropic effect on ^{13}C atoms in purine has been quantitatively investigated. All ^{13}C resonances were assigned by comparison of the ^{13}C - 1H coupling patterns among purine, 8-deuterio-, and 6,8-di-deuteriopurine. All ^{13}C resonances are shifted upfield in concentration range from 0 to 1.01 molal, 25°C. The $\Delta\delta$ dimerization shifts(d) obtained by the extrapolation method of Chan et al. (JACS 86, 4182) are 0.79, 1.69, 1.23, 1.08, and 0.77 ppm for C_2, C_4, C_5, C_6 and C_8 , respectively. These $\Delta\delta$'s are larger than those of 1H NMR of H_2, H_6 , and H_8 (0.57, 0.77, and 0.55 ppm, respectively). All $\Delta\delta_d$ of carbon resonances can be accommodated by a dimer model with vertical distance of $3.0 \pm 0.2 \text{ \AA}$ based on calculation of Glessner-Prettre et al. (Biopolymers, 15, 2277). The $\Delta\delta_d$ for proton resonances, however, are 0.2 ppm larger than those expected for the same model. Thus, high resolution ^{13}C -NMR can provide geometric information of base-stacking. (Supported by NIH GM-16066 and NSF PCM-74-23423).

TU-PM-D7 CONFORMATIONAL AND BINDING STUDIES OF DEOXYRIBO-OLIGONUCLEOSIDE METHYL PHOSPHONATES. L.S. Kan, P.S. Miller*, J. Yano*, and P.O.P. Ts'o. Div. of Biophysics, Johns Hopkins University, Baltimore, MD 21205

To understand electrostatic interaction, backbone restriction, and biological effects of oligonucleotides, nonionic deoxyribodinucleoside methyl phosphonates, dAOP (O)(CH₃)OdA (or dApdA), dApT, TpdA, TpT, and dAp₂ were studied. Each dimer consists of two diastereoisomers. The bases of dApdA₁ (I) are more stacked than in dApdA₂ (II) (UV hypochromicity: 11% for I, 7% for II). CD data and NMR resonances of base, C_{1'}, and CH₃P protons indicate that the bases of I are oriented in an oblique manner while those of II are oriented in a parallel manner. Both I and II form 2U:1A complexes with poly U (Tm: 15.4° for I; 19.8° for II, 7°C for dApdA). The increased stacking in I and the lower stability of I-poly U complexes may result from restricted rotation about ω' in the dimer caused by the axial methylphosphonyl group. This rotational restriction may influence interaction of longer oligomers with polynucleotides: dAp₂dA and dAp₃dA effectively bind to poly U (Tm 33° and 43°), while Tp₈ binds to poly(dA) (two Tm's exhibited: 20° and 45°) but not to poly A. These compounds exert a specific influence on living cells in culture. (Supported by NIH and NSF)

TU-PM-D8 MICROWAVE RELAXATION EFFECTS OF NUCLEIC ACIDS AND NUCLEOTIDES. Anne K. Krey,¹ Dept. of Microwave Res., Walter Reed Army Inst. of Research, Washington, DC 20012

Calf thymus DNA shows a gradual decrease in permittivity (approaching ϵ' of its aqueous solvent) in the range from 0.5 to 50 MHz (Mandel, N. Y. Acad. Sci. Conf. Electr. Prop. Biol. Polymers, Water, and Membranes, 1977). A dielectric dispersion was likewise observed in the same frequency range for t-RNA and also for most of the mono-nucleotides of both nucleic acids. Of the nucleotides, AMP and dAMP showed no dispersion, while relaxation effects increased progressively for CMP/dCMP, GMP/dGMP, and UMP/TMP with a specificity which is characteristic for the dipole moments of the respective nucleotide bases. Removal of bases increased the observed relaxations of nucleotides as did subsequent deletion of sugars so that phosphates alone showed the largest dispersion effects. Nucleotide dispersions also increased upon addition of phosphates or decreased when a phosphate group was removed. These findings suggest that configurational parameters of mononucleotides determine DNA's and RNA's relaxation effects and, that in doing so, the nucleotides' conformational properties may also be involved. (Pres. address: Div. Research Grants, NIH, Bethesda, Md)

TU-PM-D9 THE LOW FREQUENCY VIBRATIONS OF CALF-THYMUS AND SALMON SPERM DNA. G. Ascarelli* and C. P. Beetz Jr., Purdue University, West Lafayette, Indiana 47907

The low frequency ($20 \text{ cm}^{-1} < f < 400 \text{ cm}^{-1}$) vibrational spectra of calf-thymus DNA and salmon sperm DNA have been measured as a function of temperature ($300^\circ \text{K} \rightarrow 7^\circ \text{K}$), hydration (6% \rightarrow 95% relative humidity) and NaCl concentration. The spectra show a broad absorption centered at 200 cm^{-1} which has a shoulder on the low frequency side whose position depends upon NaCl concentration. Definite line structure and broad shoulders appear above 200 cm^{-1} . These features become more pronounced at low temperatures. At low temperature for identical NaCl concentration, the spectra of calf-thymus and salmon sperm DNA films exhibit differences in the 200 cm^{-1} region despite the fact that they were equilibrated at room temperature in air having the same r.h. Calf-thymus and salmon sperm DNA have almost equal G-C base pair content, 44% and 42%, respectively. The difference of optical absorption must therefore be a result of their different base sequence rather than the concentration of each base. This result is not unexpected since the normal modes of polynucleotides must depend upon the interaction of the different monomers.

TU-PM-D10 THE LOW FREQUENCY VIBRATIONS OF POLY I-POLY C DUPLEXES, 5'CMP, 5'IMP, CYTIDINE AND INOSINE. C. P. Beetz, Jr. and G. Ascarelli*, Physics Department, Purdue University, West Lafayette, Indiana 47907

The optical absorption ($30 \text{ cm}^{-1} < f < 400 \text{ cm}^{-1}$) of Poly I Poly C films has been measured as a function of temperature ($300^\circ \text{K} \rightarrow 12^\circ \text{K}$), hydration (0% \rightarrow 95% relative humidity) and NaCl concentration. The spectra has a broad absorption at $\sim 200 \text{ cm}^{-1}$ with a shoulder at the lower frequency side $\sim 50 \text{ cm}^{-1}$ and two distinct lines at $\sim 316 \text{ cm}^{-1}$ and 374 cm^{-1} . The high frequency features ($> 100 \text{ cm}^{-1}$) are also observed in polycrystalline powders of the nucleotides 5'CMP and 5'IMP. The similarity of the nucleotide and polynucleotide spectra indicates that the phosphodiester linkage and hydrogen bond formation giving rise to the polynucleotide and double helical duplex respectively have little effect on the vibrations at frequencies $> 100 \text{ cm}^{-1}$. The shoulder at 50 cm^{-1} is tentatively associated with the formation of the double helical polynucleotide. The broad nucleotide and polynucleotide absorption is contrasted with the sharp line spectra of polycrystalline powders of the nucleosides cytidine and inosine. The difference is associated with the phosphate-counterion-hydration complex that is only present in the nucleotides and polynucleotides.

TU-PM-D11A Comparison of Theoretical Experimental DNA and Denaturation Profiles. R.A. WHITE and D.L. VIZARD, Univ. of Texas System Cancer Center.*--A comparison of experimental high resolution thermal denaturation of DNA of known sequence is made with theoretical melting curves. The Fixman¹ modification of Poland's² method is used to compute theoretical DNA denaturation curves. It is found that while it is possible to generate theoretical curves in fair agreement with experimental data for a simple sequence such as poly(dAT), the detailed denaturation profile for a more complex DNA sequence such as found in ϕ x-174 bacteriophage cannot be reproduced. The effects of varying the fitting parameters including the loop entropy function is discussed.

¹ Fixman, F., and J.J. Freire, To be published in *Biopolymers* (1978).

² Poland, D. (1974), *Biopolymers* 13:1859-1871.

* Supported by grants, CA-11430 and GM23067, from N.C.I.

TU-PM-D14 SEDIMENTATION ARTEFACTS IN ALKALINE SUCROSE GRADIENTS. J. T. Lett, P. K. Keng*, and C. Sun*, Colorado State University, Fort Collins, Colorado 80523

In 1970 it was proposed that the DNA structure in the mammalian chromosome was based upon structural subunits. That interpretation was challenged on the grounds that the molecular species sedimenting in alkaline sucrose gradients were artefacts of anomalous sedimentation at certain rotor speeds, explicable by the theory of Zimm. Since then, we have made comprehensive investigations of the sedimentation of mammalian DNA in alkaline sucrose gradients in swinging-bucket and zonal rotors, and have identified artefacts of various types. From these investigations it appears that, while Zimm's theory may be correct, most of the publications that report "anomalous" sedimentation, or purport to confirm Zimm's equations, actually describe simpler kinds of artefacts.

Our objectives now are: to alert researchers to the experimental difficulties involved in alkaline sucrose gradient sedimentation by presenting a synopsis of "speed-dependent" artefacts prior to formal publication; to show that once these artefacts are understood or circumvented, the method of alkaline sucrose gradient sedimentation is a powerful tool for detecting very small amounts of damage in chromosomal DNA.

TU-PM-D12 A SPECTRAL AND THERMODYNAMIC ANALYSIS OF HIGH RESOLUTION MELTING OF SHORT, HOMOGENEOUS DNA'S.

R. D. Blake & Paul V. Haydock*, Dept. of Biochemistry, Univ. of Maine, Orono, Me. 04473.

High resolution optical melting curves of DNA are obtained directly from the difference in absorbance between two identical solutions at a small constant temperature difference, ΔT^* ; and monitored continuously with increasing temperature in a ratio recording spectrophotometer. Analysis of 1) second derivative profiles, 2) the spectral dispersion, and 3) hysteresis on cooling, provide means of resolving hyperfine detail during melting of short, homogeneous DNA's. Melting proceeds by discrete subtransitions corresponding to the "concerted" dissociation of ~500 base pair (bp) segments. (The number of bp is determined from profiles at the isosbestic wavelength for the A-T bp [282 nm] and the instantaneous G-C composition). Melting of λ (CI₈₅-S₂) DNA exhibits 35±4 subtransitions of between 100 and 1000 bp. While the size is initially ~500 bp, it later increases due to the extenuating effects of neighboring loop segments. In a 0.012M Na⁺ buffer the apparent unit enthalpy is 5 kcal/(mole of base pairs) and decreases with segment size. (MAES, Proj. #315; NIH, GM 22827)

PROTEIN INTERACTIONS

TU-PM-D13 THE FLEXIBLE DNA DOUBLE HELIX. W.K. Olson, Department of Chemistry, Douglass College, Rutgers University, New Brunswick, N.J. 08903

A scheme has been devised to treat the spatial arrangements and properties of double helical DNA in terms of the constituent atoms and bonds of the system. Heretofore the behavior of DNA in solution has been interpreted in terms of various artificial theoretical models including the rigid rod, wormlike coil, and ideal Gaussian. In this work the flexibility of the DNA double helix is taken to arise solely from minor perturbations of the backbone rotation angles within the DNA-B family of conformations. Computations of the radii of gyration based upon this conformational scheme are consistent with experimentally measured quantities over a wide range of molecular weights. These rotational constraints are also found to provide a plausible mode of folding in native DNA. The 'rigid' DNA-B backbone modeled here is readily condensed into compact, smoothly-folded regular superhelices that fit the known dimensions of chromatin nucleosomes.

TU-PM-E1 DYNAMICAL BASIS OF MACROMOLECULE ASSOCIATION AND TISSUE RECOGNITION. R. Lumry, Chemistry Dept., University of Minnesota, Minneapolis, MN 55455

The broad conformer fluctuation spectra of proteins are characterized by both structural & temporal descriptions, the latter apparently the more important in ligand binding & catalytic processes. Preservation of folded form as among hemoglobin species is essential to preservation of the dynamical properties which support the sophisticated details of oxygen binding. Homotropic & heterotropic linkage are possible because of complementary & anticomplementary dynamical matching at protein-protein interfaces, but stable association also depends as much on successful matching as on the existence of complementary bonding situations. Association for dynamical purposes, e.g. linkage & transport through membrane, cannot be strictly complementary but strong association for tissue assembly, immunological phagocytic processes, etc. requires close dynamical complementarity. *A priori*, we might expect large heat-capacity decreases in the latter, but heat capacity measures energy variance and not the relaxation spectrum of the conformer distribution about which almost everything remains to be determined. Supported by USPHS, NHLI Grant 16833.

TU-PM-E2 MAGNETIC OSMOMETRY, DENSITY AND VISCOSITY ON BOVINE ALBUMIN FRAGMENTS "A" AND "B". T. H. Crouch* and D. W. Kupke, Univ. of Virginia, Charlottesville, Va. 22901

Micromolar concentrations of self-associating protein have been studied with the recently developed magnetic-suspension osmometer. The changes in gas volume of a tiny buoy, stably suspended within a solution, are accurately monitored at pressure differences of ~ 0.2 mm H₂O, corresponding to $< 10^{-6}$ M nondiffusible solute. Bovine albumin was split into the known fragments A and B by pepsin digestion, and the fragments were isolated. When recombined, the enzymic-like activity of the native albumin in decomposing a Meisenheimer complex was mostly restored. The osmotic pressures of mixtures of A and B exhibited curves yielding association constants (20°) of 1.3 to $1.8 \mu\text{M}^{-1}$, in agreement with other data. The volume change by density for the association was -80 ml/mol, suggesting that nonpolar contacts predominate. Magnetic viscometry (0.2 ml/sample) revealed a much larger hydrodynamic volume for the re-associated complex and for fragment A than that for the parent albumin. The results suggest that the activity is not dependent upon a domains conformation like that of the native albumin.

(Supported by Nat. Sci. Found. grant BMS-75-01599.)

TU-PM-E3 STUDIES OF THE KINETICS OF POLYMERIZATION OF PROTEIN FROM TOBACCO MOSAIC VIRUS. S. Loga, and C. L. Stevens, Dept. of Life Sciences, University of Pittsburgh, Pittsburgh, PA. 15260

The rate of disappearance of 4S material and the concomitant appearance of 20S material was followed in the pH range 6.9 to 7.1 by sedimentation measurements with the analytical ultracentrifuge. We found that the rate of appearance of 20S material depends upon pH in the interval and that the equilibrium ratio is no more than slightly dependent on pH. This suggests that it is the double disk that constitutes 20S material here and that their formation is via the two-turn helix.

TU-PM-E4 ENTROPY-DRIVEN POLYMERIZATION OF E66 TOBACCO MOSAIC VIRUS PROTEIN, Ragaa A. Shalaby and Max A. Lauffer, University of Pittsburgh, Pittsburgh, PA. 15260.

Protein of mutant E66 TMV has lysine replacing asparagine at position 140 of the type strain, vulgare. Thus, E66 protein should have one more positive or one less net negative charge at pH 6 to 7. To investigate the effect of charge, a comparative study of the polymerization of E66 and vulgare proteins at pH 6.0, 6.2, 6.4, 6.6 and 6.8 at ionic strengths, 0.15, 0.10 and 0.05, was made by turbidimetry. Polymerization of E66 protein always proceeded at lower temperature than vulgare. However, in the pH range 6.0-6.4, the extent of polymerization was much lower in E66, especially at the higher ionic strengths. Sedimentation velocity results paralleled those from turbidity measurements in that E66 protein polymerizes at lower temperatures than vulgare. 20S component is more abundant in E66 protein than vulgare under all conditions studied. Osmotic pressure measurements also show that E66 protein is more polymerized than vulgare, especially at lower pH values. H⁺ ion titration of E66 protein under different conditions of temperature and ionic strength is underway.

TU-PM-E5 ENTROPY-DRIVEN POLYMERIZATION OF FLAVUM TOBACCO MOSAIC VIRUS PROTEIN, Ragaa A. Shalaby and Max A. Lauffer, University of Pittsburgh, Pittsburgh, PA. 15260.

Protein of the flavum mutant of TMV has the same number of positive groups as vulgare but aspartic acid at position 19 in vulgare is replaced by alanine, yielding the same net charge as E66 protein. Comparative temperature-OD measurements on both flavum and vulgare proteins, prepared identically, were made at pH 5.8 to 6.6 at ionic strengths of 0.10 and 0.05. Higher ionic strengths caused flavum protein denaturation. Compared to vulgare, flavum protein polymerizes at higher temperatures and exhibits similar effects of pH and ionic strength. At pH 6.0, ionic strength 0.05 and 40°C , s_{20}^w decreases from 3.7 at 3 mg/ml to 2.3 at 0.5 mg/ml. Comparable values were obtained at ionic strength 0.10 at pH 6.0 and 7.0. Sedimentation equilibrium experiments showed that in changing from pH 6.0 to 7.0, the minimum molecular weight near the meniscus decreases from 30,000 to 25,000 at 40° , ionic strength 0.10 and from 42,000 to 35,000 at 10° , ionic strength 0.05. All these results indicate that under similar conditions, flavum protein is in a lower state of aggregation than vulgare.

TU-PM-E6 FLUORESCENCE POLARIZATION OF MACROMOLECULES WITH SEGMENTAL FLEXIBILITY. W. A. Wegener*, V. J. Koester, and R. M. Dowben, Biophys. Grad. Prog., Univ. Texas Health Sci. Cntr., Dallas, Texas 75235.

This project aims particularly to study the segmental flexibility of myosin and immunoglobulins by fluorescence depolarization. We consider the effect one rigid macromolecular subunit has upon another subunit when both are immersed in solution and free to undergo Brownian motion, but are flexibly attached at a common point. Diffusion coefficient expressions are developed for the allowed degrees of freedom, when hydrodynamic interactions between the two subunits can be ignored. A computer simulation is presented that uses Brownian motion based upon these diffusion coefficients to simulate the orientation relaxation of the segments using an ensemble of several thousand identical bodies. The simulation generates time-dependent fluorescence depolarization curves for a fluorophore rigidly attached to one of the subunits. Supported by NIH grant HL-16678.

TU-PM-E7 DYNAMIC LIGHT SCATTERING FROM A SOLUTION OF MICROTUBULES. Jon S. Gethner, Laboratory of Chemical Physics, NIAMD, N.I.H., Bethesda, Md. 20014 and Felicia Gaskin, Depts. of Pathology & Biophysics, Albert Einstein College of Medicine, Bronx, New York 10461

Dilute solutions of microtubules obtained from the temperature-induced self-assembly of porcine and calf-brain tubulin were examined using dynamic light scattering techniques. Tubulin solutions having concentrations from 4.95 mg/ml to 0.24 mg/ml were assembled. The resulting microtubules were found to have a diameter of 240 Å and lengths from 6 to 39 μm . The effective diffusion constant determined from the analysis of correlation functions was found to be directly proportional to the average length of the microtubules rather than inversely proportional to length as would be expected from a solution of rods undergoing Brownian motion. However, the angular dependence of the linewidth of the correlation functions was found to scale with q^2 and have a zero intercept. Since the linewidth for such solutions is apparently not simply related to the translational diffusion constant of the particle, models other than Brownian motion of independent particles must be employed to account for the experimental results. Several models for collective behavior of the rods are discussed.

TU-PM-E8 X-RAY SCATTERING STUDY OF THE BINDING DISTANCE BETWEEN HORSE CYTOCHROME C HEME AND HEAVY MOLECULES. C. S. Borso, Princeton University, Princeton, N.J. 08540 and J. B. Stamatoff, Bell Laboratories, Murray Hill, N.J. 07974.

The distance scale predicted by the proposed Hopfield theory of electron tunneling is of fundamental importance to the understanding of biological electron transfer. A direct measurement of this distance between cytochrome C and other hemoproteins would be an important verification of the theory. Here we report a measurement of the distance from the heme iron in horse cytochrome C to a bound molecule in solution. The method employed involves the usual radius of gyration study combined with chemical modification of the cytochrome and electron density matching of the solvent. The isomorphism between the scattering lengths and the masses is used to develop a scattering parallel-axis theorem and thereby to provide a means of obtaining the distance from the intensity data.

TU-PM-E9 CONFORMATIONAL DYNAMICS IN CYTOCHROME C.

R. Hantgan* UNC Chapel Hill, N.C. and H. Taniuchi* N.I.H. Bethesda, Md. Intr. by Jan Hermans.

The non-covalent complex (1-53)H:(54-104) derived from cytochrome c (Hantgan and Taniuchi, J.B.C. 252: 1367, 1977) exhibits substantial biological activity as well as fluorescence and circular dichroism spectra characteristic of the intact protein. We have used this complementing system to investigate the dynamic nature of protein structure by determining the rate of the exchange reaction: (1-53)H:(54-104)* + (54-104)=(1-53)H:(54-104) + (54-104)* (*denotes a covalently attached radioactive label) as a function of temperature and valence of the heme iron. At 25°, ferric complex, $\Delta H^\ddagger = 44$ kcal/mole, $\Delta S^\ddagger = 65$ cal/deg mole, $\Delta G^\ddagger = 23.5$ kcal/mole. Thus, a dynamic equilibrium of enthalpy-favored folding and entropy-favored unfolding characterizes the tertiary structure of the ferric complex at pH 7, 15-37°. Reduction of the heme iron dramatically decreases the rate of unfolding of the complex. As the x-ray structures of ferric/ferrous cytochrome c are the same (Mandel et al. J.B.C. 252:4619, 1977), this decrease in conformational fluctuations may account for the resistance to proteolysis which is unique to the ferrous form.

TU-PM-E10 STRUCTURAL ANALYSIS OF BLOOD FACTORS (X, IX, AND II). D.D. Solomon,* O.M. Malhotra,* D.W. Kormos and A.G. Walton, Department of Macromolecular Science, Case Western Reserve University and *Department of Pathology, V.A. Hospital, Cleveland, Ohio 44106

The structure of several serine protease blood factor enzymes and their proenzymes has been evaluated by a combination of CD spectroscopy, conformational analysis on fragments and the intact proteins, and comparison with the tertiary structure of chymotrypsin and related enzymes. By these means it is possible to evaluate segmental similarities and differences. In most cases additional residues are accommodated in bends and loops lying on the molecular exterior. In other cases the regions act as sites for interaction with other subunits. As a specific example, prothrombin is found to be a three subunit structure, the structurally unique unit (thrombin) has six regions differing from chymotrypsin, two are the C and N terminal regions, two lie in surface loops, one modifies the chymotrypsinogen cleavage site and one lies adjacent to the active site. Correlation between experimental and theoretical methods allows a fairly detailed model to be derived.

TU-PM-E11 AGGLUTINATION OF ANTIGEN COATED CARRIER PARTICLES BY ANTIBODY. G.K. von Schulthess,*

R.W. DeBlois and G.B. Benedek, Cambridge, MA 02139

Because of its importance in sensitive immunoassay methods,¹ we have measured the evolution of the distribution of n-particle aggregates of latex particles (r=120nm) coated with human serum albumin (antigen) crosslinked by goat anti-human serum albumin antibodies as a function of time, antibody concentration and latex particle concentration using the resistive pulse technique with a 2µm diameter pore produced by the Nuclepore process. Histograms of the n-particle distributions obtained experimentally will be presented for both the regime of light aggregation and heavy aggregation. Comparison between these data and the Smoluchowski coagulation and the Flory-Stockmayer polymerization theories will be presented.

¹G.K. von Schulthess, R.J. Cohen, N. Sakato and G.B. Benedek, *Immunochemistry* 13, 955 (1976).

TU-PM-E12 EFFECT OF TEMPERATURE ON THE "PROCESSING" OF 8S AND 4S ESTRADIOL RECEPTOR FROM HUMAN BREAST CANCER. K.M. Anderson, J. Phelan*, M. Marogil*. Oncology Research Laboratory, Depts. of Biochem. and Med., Rush-Pres.-St. Luke's Med. Center, Chicago, Illinois 60612

Estradiol receptor proteins, extracted from human breast cancer at low ionic strength, appear predominantly as 8S macromolecules, that are converted to 4S species by high salt, freeze-thawing or increased temperature. We examined the effect of increased temperature on transformation of 8 to the 4S species. A quantitative recovery of 8S receptor, labelled at 4° with ³H-estradiol occurred after incubation at 30°, but not at 37°. At 37° prelabelled 8S species degraded while the 4S species were unaffected. If unlabelled cytosol was first incubated at either 30° or 37° and radioactivity added subsequently, no binding to 4 or 8S receptors occurred. A role for proteolytic enzymes in the loss of receptor activity at either temperature could not be shown by the use of PMSF, trypsin inhibitor, NaHSO₃ or TLAK.